

2

NAVAL POSTGRADUATE SCHOOL

Monterey, California

AD-A255 176



S DTIC
ELECTE
SEP 11 1992
A **D** THESIS

COMPUTER MODELING
OF TACTICAL HIGH FREQUENCY
ANTENNAS

by

Bobby G. Gregory Jr.

June 1992

Thesis Advisor:

R. W. Adler

Approved for public release; distribution is unlimited.

92 9 10 070

251450

92-25023



111 P93

UNCLASSIFIED

SECURITY CLASSIFICATION OF THIS PAGE

REPORT DOCUMENTATION PAGE				Form Approved OMB No. 0704-0188		
1a. REPORT SECURITY CLASSIFICATION UNCLASSIFIED			1b. RESTRICTIVE MARKINGS			
2a. SECURITY CLASSIFICATION AUTHORITY			3. DISTRIBUTION/AVAILABILITY OF REPORT Approved for public release; distribution is unlimited.			
2b. DECLASSIFICATION/DOWNGRADING SCHEDULE						
4. PERFORMING ORGANIZATION REPORT NUMBER(S)			5. MONITORING ORGANIZATION REPORT NUMBER(S)			
6a. NAME OF PERFORMING ORGANIZATION Naval Postgraduate School		6b. OFFICE SYMBOL (If applicable)	7a. NAME OF MONITORING ORGANIZATION Naval Postgraduate School			
6c. ADDRESS (City, State, and ZIP Code) Monterey, CA 93943-5000			7b. ADDRESS (City, State, and ZIP Code) Monterey, CA 93943-5000			
8a. NAME OF FUNDING/SPONSORING ORGANIZATION		8b. OFFICE SYMBOL (If applicable)	9. PROCUREMENT INSTRUMENT IDENTIFICATION NUMBER			
8c. ADDRESS (City, State, and ZIP Code)			10. SOURCE OF FUNDING NUMBERS			
			PROGRAM ELEMENT NO.	PROJECT NO.	TASK NO.	WORK UNIT ACCESSION NO.
11. TITLE (Include Security Classification) COMPUTER MODELING OF TACTICAL HIGH FREQUENCY ANTENNAS						
12. PERSONAL AUTHOR(S) GREGORY, Bobby G. Jr.						
13a. TYPE OF REPORT Master's Thesis		13b. TIME COVERED FROM _____ TO _____		14. DATE OF REPORT (Year,Month,Day) June 1992		
15. PAGE COUNT 112						
16. SUPPLEMENTARY NOTATION The views expressed in this thesis are those of the author and do not reflect the official policy or position of the Department of Defense or the U.S. Government.						
17. COSATI CODES			18. SUBJECT TERMS (Continue on reverse if necessary and identify by block number) NEC-3, PAT7, HT-20T, ELPA-302, Horizontal Dipole			
FIELD	GROUP	SUB-GROUP				
19. ABSTRACT (Continue on reverse if necessary and identify by block number) The purpose of this thesis was to compare the performance of three tactical high frequency antennas to be used as possible replacement for the Tactical Data Communications Central (TDCC) antennas. The antennas were modeled using the Numerical Electromagnetics Code, Version 3 (NEC3), and the Eyring Low Profile and Buried Antenna Modeling Program (PAT7) for several different frequencies and ground conditions. The performance was evaluated by comparing gain at the desired takeoff angles, the voltage standing wave ratio of each antenna, and its omni-directional capability. The buried antenna models, the ELPA-302 and horizontal dipole, were most effective when employed over poor ground conditions. The best performance under all conditions tested was demonstrated by the HT-20T. Each of these antennas have tactical advantages and disadvantages and can optimize communications under certain conditions. The selection of the best antenna is situation dependent. An experimental test of these models is recommended to verify the modeling results.						
20. DISTRIBUTION/AVAILABILITY OF ABSTRACT <input checked="" type="checkbox"/> UNCLASSIFIED/UNLIMITED <input type="checkbox"/> SAME AS RPT. <input type="checkbox"/> DTIC USERS			21. ABSTRACT SECURITY CLASSIFICATION UNCLASSIFIED			
22a. NAME OF RESPONSIBLE INDIVIDUAL ADLER, R.W.			22b. TELEPHONE (Include Area Code) (408) 646 - 2352		22c. OFFICE SYMBOL EC/Ab	

DD Form 1473, JUN 86

Previous editions are obsolete.
S/N 0102-LF-014-6603SECURITY CLASSIFICATION OF THIS PAGE
Unclassified

Approved for public release; distribution is unlimited.

COMPUTER MODELING
OF TACTICAL HIGH FREQUENCY
ANTENNAS

by

Bobby G. Gregory, Jr.
Captain, United States Marine Corps
B.S.E.E., University of Colorado, 1985

Submitted in partial fulfillment
of the requirements for the degree of

MASTER OF SCIENCE IN ELECTRICAL ENGINEERING

from the

NAVAL POSTGRADUATE SCHOOL
June 1992

Author:

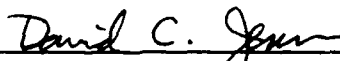


Bobby G. Gregory, Jr.

Approved by:



R. W. Adler, Thesis Advisor



D. C. Jenn, Thesis Co-Advisor



M. A. Morgan, Chairman

Department of Electrical and Computer Engineering

ABSTRACT

The purpose of this thesis was to compare the performance of three tactical high frequency (HF) antennas to be used as possible replacement for the antenna system of the Tactical Data Communications Central (TDCC). The antennas were modeled using the Numerical Electromagnetics Code, Version 3 (NEC-3), and the Eyring Low Profile and Buried Antenna Modeling Program (PAT7) for several different frequencies and ground conditions. The performance was evaluated by comparing gain at the desired takeoff angles, the voltage standing wave ratio (VSWR) of each antenna and its omni-directional capability. The buried antenna models, the ELPA-302 and horizontal dipole, were most effective when employed over poor ground conditions. The best performance under all conditions tested was demonstrated by the HT-20T. Each of these antennas have tactical advantages and disadvantages and can optimize communications under certain conditions. The selection of the best antenna is situation dependent. An experimental test of these models is recommended to verify the modeling results.

Accession For	
NTIS CRA&	<input checked="" type="checkbox"/>
DTIC TAB	<input type="checkbox"/>
Unannounced	<input type="checkbox"/>
Justification	
By	
Distribution	
Availability Codes	
Dist	Avail and/or Special
A-1	

DTIC QUALITY INSPECTED 1

TABLE OF CONTENTS

I. INTRODUCTION	1
A. OVERVIEW	1
B. BACKGROUND	1
II. PROBLEM DISCUSSION	3
A. PROBLEM STATEMENT	3
B. ANTENNAS	3
III. MODELING SOFTWARE	8
A. NUMERICAL ELECTROMAGNETICS CODE-3	8
1. STRUCTURE MODELING	9
2. WIRE MODELING	10
B. PAT7 PROGRAM	12
C. TAKEOFF ANGLE CALCULATION	14
IV. MODELING RESULTS	17
A. GENERAL	17
B. HT-20T MODEL	18
C. ELPA-302 MODEL	33
D. HORIZONTAL DIPOLE MODEL	63
V. EXPERIMENTAL VERIFICATION	92

VI. CONCLUSIONS	94
A. MODEL COMPARISON	94
B. RECOMMENDATIONS	94
APPENDIX A. SAMPLE NEC-3 DATA SET	96
APPENDIX B. SAMPLE PAT7 PROGRAM DATA SET	97
LIST OF REFERENCES	98
INITIAL DISTRIBUTION LIST	99

LIST OF FIGURES

Figure 1. The hub-spoke deployment of the TDCC. . . .	4
Figure 2a. HT-20T Antenna.	6
Figure 2b. ELPA-302 Antenna.	6
Figure 2c. Horizontal Dipole Antenna.	6
Figure 3. Skywave Transmission chart developed by Prof. R.A. Helliwell, Stanford University, 1964.	16
Figure 4. HT-20T Antenna.	19
Figure 5. VSWR for HT-20T over good ground.	20
Figure 6. Elevation pattern for HT-20T over good ground for $f=2, 4$, and 8 MHz.	21
Figure 7. Elevation pattern for HT-20T over good ground for $f=12, 20$, and 30 MHz.	22
Figure 8. Elevation pattern for HT-20T over fair ground for $f=2, 4$, and 8 MHz.	23
Figure 9. Elevation pattern for HT-20T over fair ground for $f=12, 20$, and 30 MHz.	24
Figure 10. Elevation pattern for HT-20T over poor ground for $f=2, 4$, and 8 MHz.	25
Figure 11. Elevation pattern for HT-20T over poor ground for $f=12, 20$, and 30 MHz.	26
Figure 12. Azimuth pattern for HT-20T for $f=2$ MHz over good ground, varying takeoff angle(θ).	27

Figure 13. Azimuth pattern for HT-20T for $f=4$ MHz over good ground, varying takeoff angle(θ).	28
Figure 14. Azimuth pattern for HT-20T for $f=8$ MHz over good ground, varying takeoff angle (θ).	29
Figure 15. Azimuth pattern for HT-20T for $f=12$ MHz over good ground, varying takeoff angle (θ).	30
Figure 16. Azimuth pattern for HT-20T for $f=20$ MHz over good ground, varying takeoff angle(θ).	31
Figure 17. Azimuth pattern for HT-20T for $f=30$ MHz over good ground, varying takeoff angle (θ).	32
Figure 18. ELPA-302 Antenna	34
Figure 19. VSWR for ELPA-302 over good ground, varying heights.	36
Figure 20. VSWR for ELPA-302 over poor ground, varying heights.	37
Figure 21. Elevation pattern for ELPA-302 for $f=2$ MHz over good ground.	38
Figure 22. Elevation pattern for ELPA-302 for $f=2$ MHz over fair ground.	39
Figure 23. Elevation pattern for ELPA-302 for $f=2$ MHz over poor ground.	40
Figure 24. Elevation pattern for ELPA-302 for $f=4$ MHz over good ground.	41
Figure 25. Elevation pattern for ELPA-302 for $f=4$ MHz over fair ground.	42

Figure 26. Elevation pattern for ELPA-302 for $f=4$ MHz	
over poor ground.	43
Figure 27. Elevation pattern for ELPA-302 for $f=8$ MHz	
over good ground.	44
Figure 28. Elevation pattern for ELPA-302 for $f=8$ MHz	
over fair ground.	45
Figure 29. Elevation pattern for ELPA-302 for $f=8$ MHz	
over poor ground.	46
Figure 30. Elevation pattern for ELPA-302 for $f=12$ MHz	
over good ground.	47
Figure 31. Elevation pattern for ELPA-302 for $f=12$ MHz	
over fair ground.	48
Figure 32. Elevation pattern for ELPA-302 for $f=12$ MHz	
over poor ground.	49
Figure 33. Elevation pattern for ELPA-302 for $f=20$ MHz	
over good ground.	50
Figure 34. Elevation pattern for ELPA-302 for $f=20$ MHz	
over fair ground.	51
Figure 35. Elevation pattern for ELPA-302 for $f=20$ MHz	
over poor ground.	52
Figure 36. Elevation pattern for ELPA-302 for $f=30$ MHz	
over good ground.	53
Figure 37. Elevation pattern for ELPA-302 for $f=30$ MHz	
over fair ground.	54
Figure 38. Elevation pattern for ELPA-302 for $f=30$ Mhz	
over poor ground.	55

Figure 39. Azimuth pattern for ELPA-302 for $f=4$ MHz, h=0.5m, varying takeoff angle (θ).	56
Figure 40. Azimuth pattern for ELPA-302 for $f=12$ MHz, h=0.5m, varying takeoff angle (θ).	57
Figure 41. Azimuth pattern for ELPA-302 for $f=30$ MHz, h=0.5m, varying takeoff angle (θ).	58
Figure 42. Azimuth pattern for ELPA-302 for $f=4$ MHz, constant takeoff angle (θ), varying heights.	59
Figure 43. Azimuth pattern for ELPA-302 for $f=12$ MHz, constant takeoff angle (θ), varying heights.	60
Figure 44. Azimuth pattern for ELPA-302 for $f=30$ MHz, constant takeoff angle (θ), varying heights.	61
Figure 45. Horizontal Dipole.	64
Figure 46. VSWR for horizontal dipole for varying heights over good ground.	65
Figure 47. VSWR for horizontal dipole for varying heights over poor ground.	66
Figure 48. Elevation pattern for horizontal dipole for $f=2$ MHz over good ground.	67
Figure 49. Elevation pattern for horizontal dipole for $f=2$ MHz over fair ground.	68
Figure 50. Elevation pattern for horizontal dipole for $f=2$ MHz over poor ground.	69
Figure 51. Elevation pattern for horizontal dipole for $f=4$ MHz over good ground.	70
Figure 52. Elevation pattern for horizontal dipole for	

Figure 52. Elevation pattern for horizontal dipole for f=4 MHz over fair ground.	71
Figure 53. Elevation pattern for horizontal dipole for f=4 MHz over poor ground.	72
Figure 54. Elevation pattern for horizontal dipole for f=8 MHz over good ground.	73
Figure 55. Elevation pattern for horizontal dipole for f=8 MHz over fair ground.	74
Figure 56. Elevation pattern for horizontal dipole for f=8 MHz over poor ground.	75
Figure 57. Elevation pattern for horizontal dipole for f=12 MHz over good ground.	76
Figure 58. Elevation pattern for horizontal dipole for f=12 MHz over fair ground.	77
Figure 59. Elevation pattern for horizontal dipole for f=12 MHz over poor ground.	78
Figure 60. Elevation pattern for horizontal dipole for f=20 MHz over good ground.	79
Figure 61. Elevation pattern for horizontal dipole for f=20 MHz over fair ground.	80
Figure 62. Elevation pattern for horizontal dipole for f=20 MHz over poor ground.	81
Figure 63. Elevation pattern for horizontal dipole for f=30 MHz over good ground.	82
Figure 64. Elevation pattern for horizontal dipole for f=30 MHz over fair ground.	83

Figure 65. Elevation pattern for horizontal dipole for f=30 MHz over poor ground.	84
Figure 66. Azimuth pattern for horizontal dipole for f=4 MHz, h= 0.5m, varying takeoff angle (theta). . . .	85
Figure 67. Azimuth pattern for horizontal dipole for f=12 MHz, h= 0.5m, varying takeoff angle (theta). . . .	86
Figure 68. Azimuth pattern for horizontal dipole for f=30 MHz, h= 0.5m, varying takeoff angle (theta). . . .	87
Figure 69. Azimuth pattern for horizontal dipole for f=4 MHz, constant takeoff angle (theta), varying heights.	88
Figure 70. Azimuth pattern for horizontal dipole for f=12 MHz, constant takeoff angle (theta), varying heights.	89
Figure 71. Azimuth pattern for horizontal dipole for f=30 MHz, constant takeoff angle (theta), varying heights.	90

I. INTRODUCTION

A. OVERVIEW

Computer modeling of wire antennas provides an inexpensive and efficient means for predicting the performance of antennas. There are several software packages available which use various numerical methods to predict antenna characteristics. The Numerical Electromagnetics Code, Version 3 - Method of Moments (NEC-3) uses the method of moments for analysis of the electromagnetic response of antennas and other metal structures. NEC-3 is capable of modeling antennas located above ground and buried or near the earth. The Eyring Low Profile and Buried Antenna Modeling Program (PAT7) is based on equations developed in Reference 1 which also uses the method of moments and field integral equation techniques. PAT7 is used primarily to model near-earth or buried antennas. Each program has its advantages and limitations for applications based on antenna geometry and location.

B. BACKGROUND

The Marine Corps Tactical Systems Support Activity (MCTSSA) at Camp Pendleton, California is exploring the possibility of replacing an existing antenna system. Two antennas have been proposed as possible replacements. MCTSSA has requested that a computer model of both antennas be

generated so that a theoretical comparison of characteristics and capabilities can be accomplished. This thesis discusses the computer models used for the comparison, analyzes the results of the models and proposes an additional model for consideration.

II. PROBLEM DISCUSSION

A. PROBLEM STATEMENT

The antenna to be investigated is used for the Tactical Data Communication Central (TDCC) which provides an HF radio communications hub for the centralized computer processing of data for the tactical command and control of Marine Air Wing assets. Operational employment of the TDCC normally dictates that the distant stations are within a 600 mile radius of the hub as illustrated in Figure 1, so the antenna must be omnidirectional. The transmitters operate with one kilowatt of power output. The current system uses an antenna which requires a coupler that has a poor maintenance history. It is desired that the new antenna not require a coupling device to eliminate this problem. The antenna must also be field expedient and require no more than two men to erect it. It must be broadband so that trimming antenna dimensions for each frequency is not required.

B. ANTENNAS

Two antennas which fit the criteria above were chosen for further analysis. The HT-20T, designed by the Antenna Products Corporation, and the ELPA-302, designed by the Eyring Corporation, were decided upon by MCTSSA as antennas that met the requirements above. The HT-20T is a back-to-back sloping,

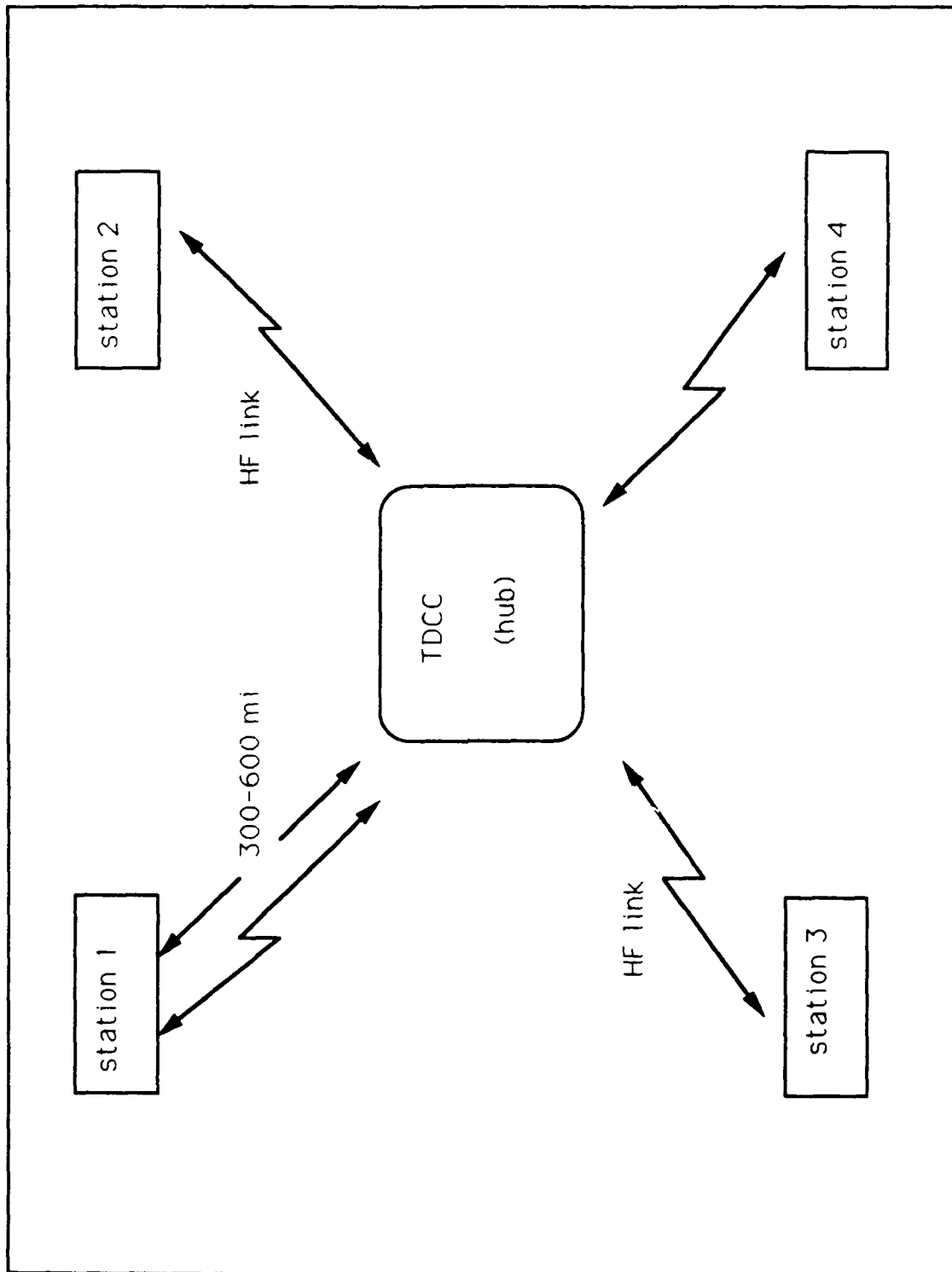


Figure 1. The hub-spoke deployment of the TDCC.

horizontal dipole configuration as shown in Figure 2a. The ELPA-302 is a buried or near-earth horizontal dipole array antenna as shown in Figure 2b.

Additionally, a simple horizontal dipole antenna (Figure 2c) was proposed as a result of this thesis which would satisfy these requirements as well as requirements for manpack radios in the Marine Corps inventory. The reason a horizontal dipole was chosen is that it is a common, field expedient antenna that is familiar to Marine Corps communicators. Its advantages are that it can be erected above ground, as it is now most commonly used, or it can be buried or employed near earth, which has not been a common practice, but is practical. The horizontal dipole is ideally suited for Marine Corps type missions since buried or near earth antennas are more easily concealed, easy to employ, and lightweight.

The length of the horizontal dipole was chosen after considering test results from Eyring, Inc. on the ELPA-302 antenna design. These results showed that when operating at the lowest desirable frequency, 2 MHz, the electrical length of a 91.5 meter buried antenna is approximately 0.75 wavelengths. Above ground, this antenna would be 0.6 wavelengths long. The difference in length is due to the conductivity and permittivity of the soil conditions, which are frequency dependent, that change the electrical length of the buried antenna. The desired power gain for an antenna in

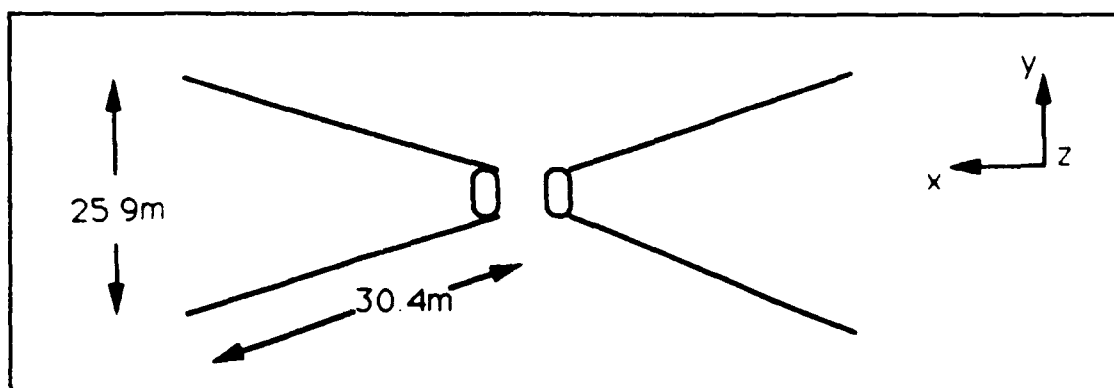


Figure 2a. HT-20T Antenna.

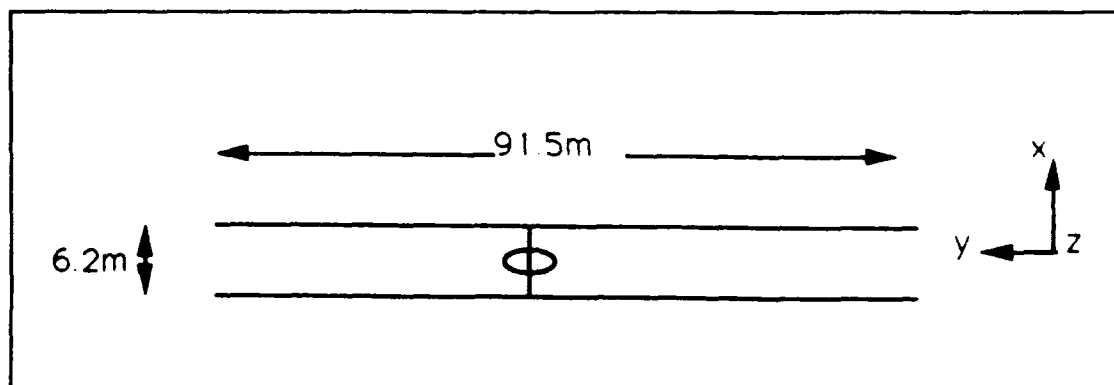


Figure 2b. ELPA-302 Antenna.

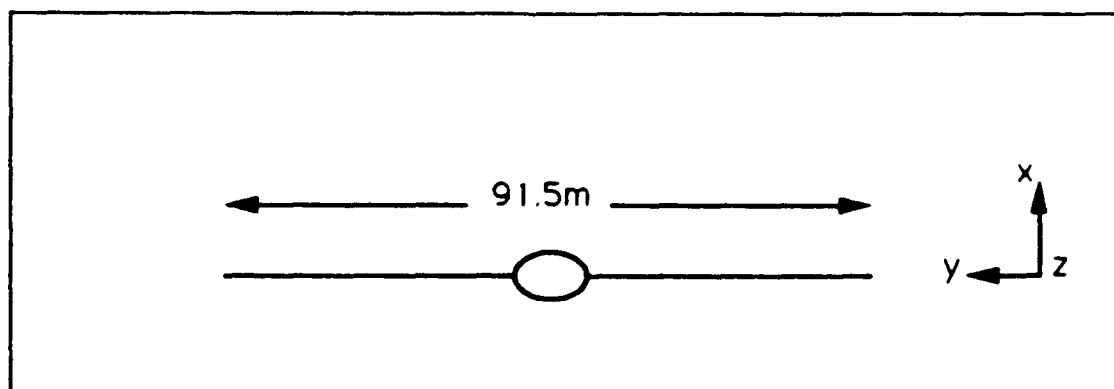


Figure 2c. Horizontal Dipole Antenna.

contact with the soil occurs at an electrical length of one wavelength. As the operating frequency of the antenna increases and additional wavelengths are formed on the element, a higher antenna gain results and produces a higher signal-to-noise ratio. Considering this information and the practical aspects of carrying and burying an antenna, a length of 91.5 meters was chosen as optimum. The input impedance of a buried antenna will be discussed later. [Ref. 2]

Comparisons between normalized radiation power output over good, fair and poorly conducting ground conditions at several heights of employment, required takeoff angles for propagation paths, and a discussion of the results and recommendations are discussed in this thesis.

III. MODELING SOFTWARE

A. NUMERICAL ELECTROMAGNETICS CODE-3

The Numerical Electromagnetics Code-Version 3 (NEC-3) was developed by the Lawrence Livermore National Laboratory located in Livermore, California. NEC-3 is a user-oriented computer code for the analysis of the electromagnetic response of antennas and other metal structures using the numerical solution of integral equations for the currents induced on the structure by sources or incident fields [Ref. 3]. This approach avoids many of the simplifying assumptions required by other solution methods and provides a highly accurate and versatile tool for electromagnetic field analysis.

The code combines an integral equation for smooth surfaces to provide convenient and accurate modeling of a wide range of structures. A model may include nonradiating networks and transmission lines connecting parts of the structure, perfect or imperfect conductors, and lumped element loading. A structure may also be modeled over a ground plane that may be either a perfect or imperfect conductor. NEC-3 also has the capability to model antennas with elements that touch or are buried in the ground using the Sommerfeld method.

The excitation may be either voltage sources on the structures or an incident plane wave of various polarizations.

The output may include induced currents and charges , near electric or magnetic fields, and radiated fields. Hence, the program is suited to either antenna analysis or scattering and Electro-Magnetic Pulse (EMP) studies.

The integral equation approach is best suited to structures with dimensions up to several wavelengths. Although there is no theoretical size limit, the numerical solution requires a matrix equation as the structure size is increased relative to one wavelength. Hence, the modeling of very large structures may require more computer time and file storage than is practical on a specific machine. In such cases, standard high-frequency approximations such as geometrical optics, physical optics, or the geometrical theory of diffraction may be more suitable than the integral equation approach used in NEC.

1. STRUCTURE MODELING

The basic elements for modeling structures in NEC are short straight segments for thin wires and flat patches for surfaces. An antenna and any conducting object in its vicinity that affect its performance must be modeled with strings of segments following the paths of wires and with patches covering closed surfaces. Proper choice of the segments and patches for a model is the most critical step in obtaining accurate results. In this thesis, thin wire modeling by NEC is used.

2. WIRE MODELING

A wire segment is defined by the coordinates of its two end points and its radius. Modeling a wire structure with segments involves both geometrical and electrical factors. Geometrically, the segments should follow the paths of conductors as closely as possible, using a piecewise linear fit on curves. The following are electrical considerations for wire segment modeling:

- The segment length Δ relative to the wavelength λ :
 - Should be less than about 0.1λ in order to get accurate results in most cases.
 - May be somewhat longer than 0.1λ on long wires with no abrupt changes while a shorter segment, 0.05λ or less, may be needed in modeling critical regions of the antenna, such as feed points and connections of multiple segments.
 - For Δ less than 0.001λ should be avoided since the similarity of the constant and cosine components of the current expansion can lead to numerical inaccuracy.
- The wire radius, r , relative to λ is limited by the approximation used in the kernel of the electric field integration equation. The segment radius α relative to both segment length Δ and wavelength λ requires that:
 - α should be less than 0.1λ .
 - α should be less than 0.125Δ .
 - α can be less than 0.5Δ , but this requires the extended thin-wire kernel option by placing the EK card in the input data set. The limits on an EK card are straight-line segments and no multiple connection points.
- Connected segments must have identical coordinates for connected ends. NEC-3 connects two end segments if the separation between the end of the segments is less than 0.001 times the length of the shortest segment.

- Segment intersections other than at their ends do not allow currents to flow from one segment to another.
- Large wire radius changes should be avoided particularly for adjacent segments. If the segment has a large radius, then sharp bends should be avoided as well.
- When modeling a solid structure with a wire grid, a large number of segments should be used.
- A segment is needed at the point where a network connection, a voltage or a current source, is going to be located. Current sources are limited to isolated, very short constant current sources located at the origin. (i.e., excitation of tiny constant current dipole).
- Base fed wires connected to ground should be vertical.
- The segments on either side of the excitation source should be parallel and have the same length and radii.
- Parallel wires should be several radii apart.
- Before modeling a structure, the limit of the number of segments and the number of connection points should be checked for the particular version of NEC.

Once the antenna geometry and ground plane are specified, the type of excitation must be declared. The excitation can be either a voltage source or an incident plane wave of various polarizations.

The wire radius, a , relative to Δ , is limited by approximations used in the kernel of the electric field integral equation. The thin-wire kernel and the extended-wire kernel approximations are used to approximate the current distribution for each wire segment. From these current distributions, far-field radiation patterns are calculated.

NEC-3 requires that for the thin-wire kernel approximation, the segment length to wire radius ratio, Δ/a , must be greater than 8 for errors less than 1% and Δ/a for the extended-wire kernel approximation must be greater than 2 for the same accuracy. Segments with bends in the wire should avoid using small values for Δ/a . The angle of intersection of wires is not restricted in any manner. Segments cannot overlap since the division of current between two overlapping segments is indeterminate. A large radius change between connected segments should be avoided since this will introduce errors in calculations. A segment is required at each point where a network connection or voltage source will be located.

B. PAT7 PROGRAM

The PAT7 program is specifically designed to model the performance of buried or near earth antennas and traveling-wave antennas in the 1 kHz to 100 MHz frequency range. The model is based on the theory developed in Reference 1 which uses the formal solution of Maxwell's equations to calculate the electromagnetic fields and associated distributions of current and charge in bounded regions. The electrical properties and characteristics of the material media in which the antenna is located and its effects on fields and currents are the focus of the analysis. [Ref. 4]

PAT7 tabulates and plots both pattern and feedpoint characteristics for models in real earth environments. Ground

conductivity and dielectric constants as a function of frequency are used to characterize the burial or underlying environment of the antenna. Radiation patterns are described as a function of elevation, azimuth, and polarization. Groundwave patterns are described in terms of field strength at a specific far field distance over real ground conditions.

PAT7 possesses an NxM multi-element array modeling capability. The assumed geometry of the model consists of from 1 to N parallel, linear elements arranged in a subarray. From 1 to M of these subarrays can be combined in-line to form an array.

The program very accurately describes the performance of real antennas when the input model uses measured data in describing the various input parameters used in making calculations. Buried antennas are most effective when they are insulated from their environment. The following are electrical considerations, characteristics, and capabilities the user must be concerned with when modeling with PAT7:

- Desired elevation and azimuth angle of view, in degrees, to obtain desired antenna radiation pattern.
- Transmit frequency
- Soil conductivity and permittivity
- Antenna wire insulation conductivity and permittivity. The complex permittivity of the wire insulation should be 1.2 times less than that of the surrounding ground.
- Antenna element length and height (negative values are used for buried antennas) Height must be less than 0.1λ and cannot be zero because PAT7 does not calculate elements touching the air-ground interface.

- Wire radius must be small compared to antenna length. (Same conditions as NEC-2)
- Conductor radius and insulation radius. (The insulation radius must obviously be larger than the conductor radius.)
- Number and spacing of elements used in array modeling as well as number of and distance between subarrays. Subarrays cannot overlap.
- Main beam steering. (The user can steer the main beam in a desired direction. This is done in practice by controlling the feed signal and using phase sensitive baluns.)
- The actual impedance of the feed element may be used, otherwise a matched, perfect feed element is assumed.
- The desired wave type (ground or skywave) to be computed.
- E-field polarization(vertical, horizontal or mixed).
- Designation whether element is end or center fed.
- Antenna may be either terminated by a user given load impedance or open termination.

A graph of the antenna radiation pattern is then produced. A sample input screen is shown in Appendix B.

C. TAKEOFF ANGLE CALCULATION

The takeoff angle for High Frequency communications is an important characteristic in antenna design. In order to obtain the desired signal strength at the receive station, the maximum power radiated at a specific azimuth and elevation, or takeoff angle, must be calculated so that the signal reflected off the ionosphere to the receive station is optimal. The takeoff angle for the problem discussed in this

thesis was determined using Reference 5 and the skywave transmission chart as shown in Figure 3. The takeoff angle was calculated for two ranges, 300 and 600 miles. A one hop path is considered optimum since signal attenuation and path losses are minimized. For daytime communications, a one hop propagation path was used with a reflection off the 'E' layer at an altitude of 110 km. For nighttime communications, a one hop path reflected off the F_2 layer at an altitude of 300 km was used. Using Figure 3 and the conditions above, for daytime communications, a one hop path requires a takeoff angle of 39 and 20 degrees for the ranges of 300 and 600 miles respectively. For nighttime communications, again using a one hop path, the takeoff angles are determined to be 49 and 28 degrees for the ranges of 300 and 600 miles respectively. These takeoff angles will be used to compare the results of the computer models. [Ref. 5]

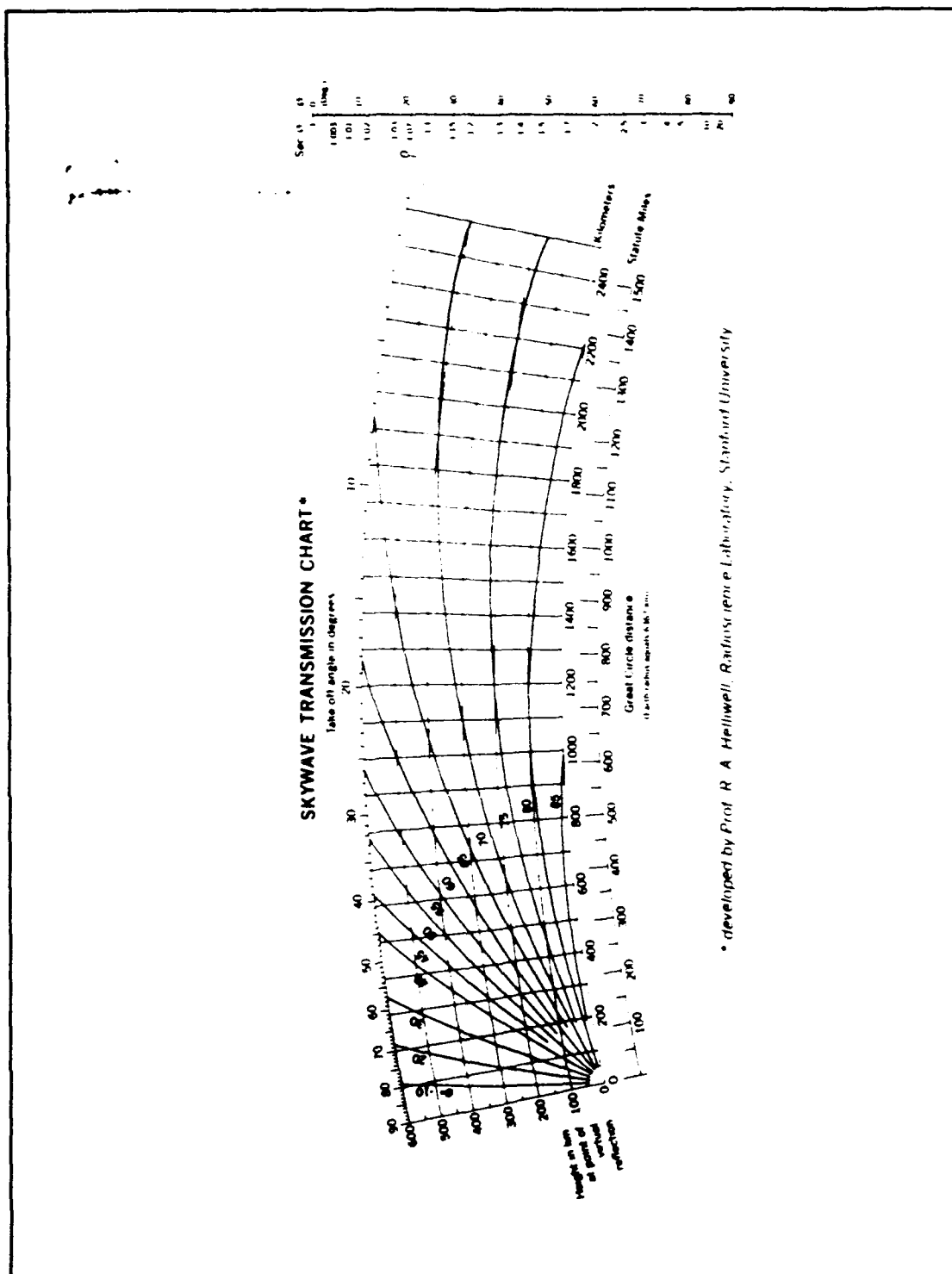


Figure 3. Skywave Transmission chart developed by Prof. R.A. Helliwell, Stanford University, 1964.

IV. MODELING RESULTS

A. GENERAL

In order to make an accurate comparison of the antennas, some common conditions were imposed. Each antenna was modeled over the three types of grounds with different conductivities, σ , and relative permittivities, ϵ_r . The values used for the various ground conditions were: for "good" ground, $\sigma = 0.01$ S/m and $\epsilon_r = 30$; for "fair" ground, $\sigma = 0.005$ S/m and $\epsilon_r = 12$; and for "poor" ground, $\sigma = 0.001$ S/m and $\epsilon_r = 6$ [Ref. 1]. The HT-20T was modeled at the fixed height and dimensions as described in Reference 6. The ELPA-302 and horizontal dipole were modeled for dimensions given in Reference 2 at four different heights to allow for comparisons of non-traditional employment. Radiation patterns were computed for each of the antennas under the various height and ground conditions. Antenna performance was analyzed using the maximum gain achieved at the desired takeoff angles and direction, and each antenna's voltage standing wave ratio (VSWR) over the 2 to 30 MHz frequency spectrum. The transmission line impedance was taken as 50 ohms, a standard value for most radio frequency (RF) applications. The frequencies chosen to make comparisons were 2, 4, 8, 12, 20 and 30 MHz. These frequencies were chosen after analysis showed that these frequencies most

accurately represented the antenna's characteristics over the frequency spectrum.

B. HT-20T MODEL

The HT-20T is a omni-directional, "sloping vee-like", orthogonal dipole antenna designed primarily for High Frequency (HF) skywave propagation. It consists of two dipole antennas mounted mutually perpendicular in azimuth as illustrated in Figure 4. Each element is terminated with a 400 ohm resistor. The center of the antenna is 27 feet above the ground.

The VSWR varies between 1.02 and 1.78 over good ground conditions as illustrated in Figure 5. The VSWR of fair and poor ground is also within these limits but not illustrated because the change in ground conditions had little effect on VSWR in this case. The antenna radiation patterns are illustrated in Figures 6 through 17. Each figure shows the pattern for a fixed ground condition for frequencies under consideration. The antenna is oriented for transmission of the main beam along the positive and negative x-axis. The reference plane from which plots were taken was from the xz-plane and azimuthal plane through the origin. From examination of these antenna radiation patterns, it is evident that the HT-20T is omni-directional and demonstrates good skywave propagation gains at 39 and 49 degree takeoff angles. The radiation patterns show a maximum gain of -2 db at 20 Mhz

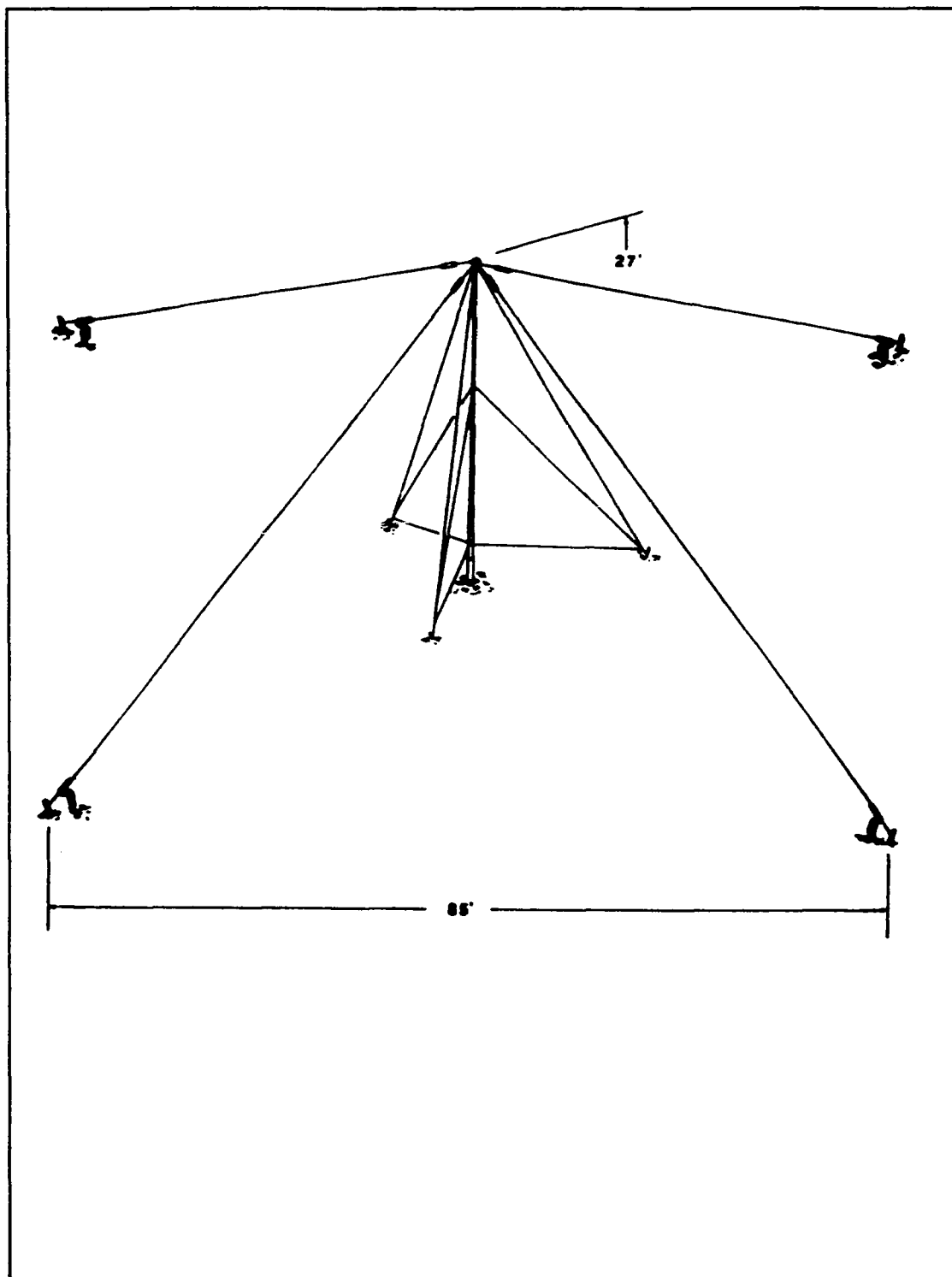


Figure 4. HT-20T Antenna.

HT-20T Antenna

(Good Ground)

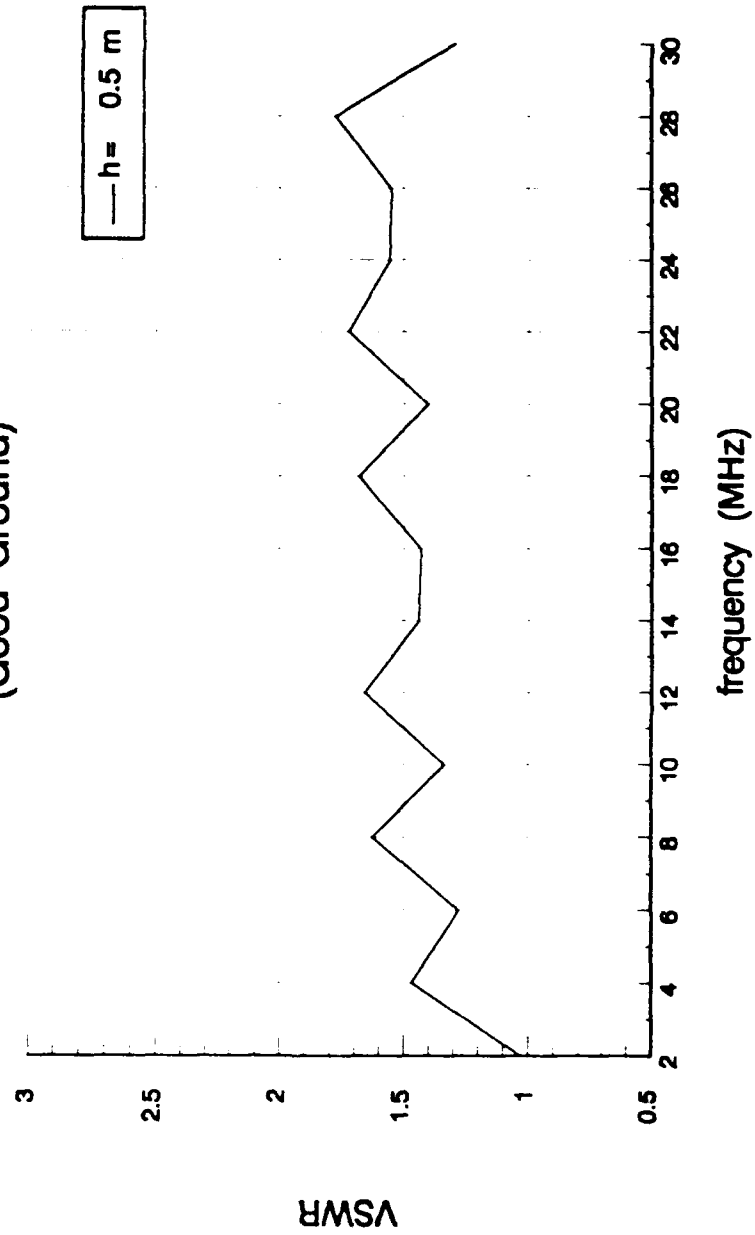


Figure 5. VSWR for HT-20T over good ground.

HT-20T Antenna

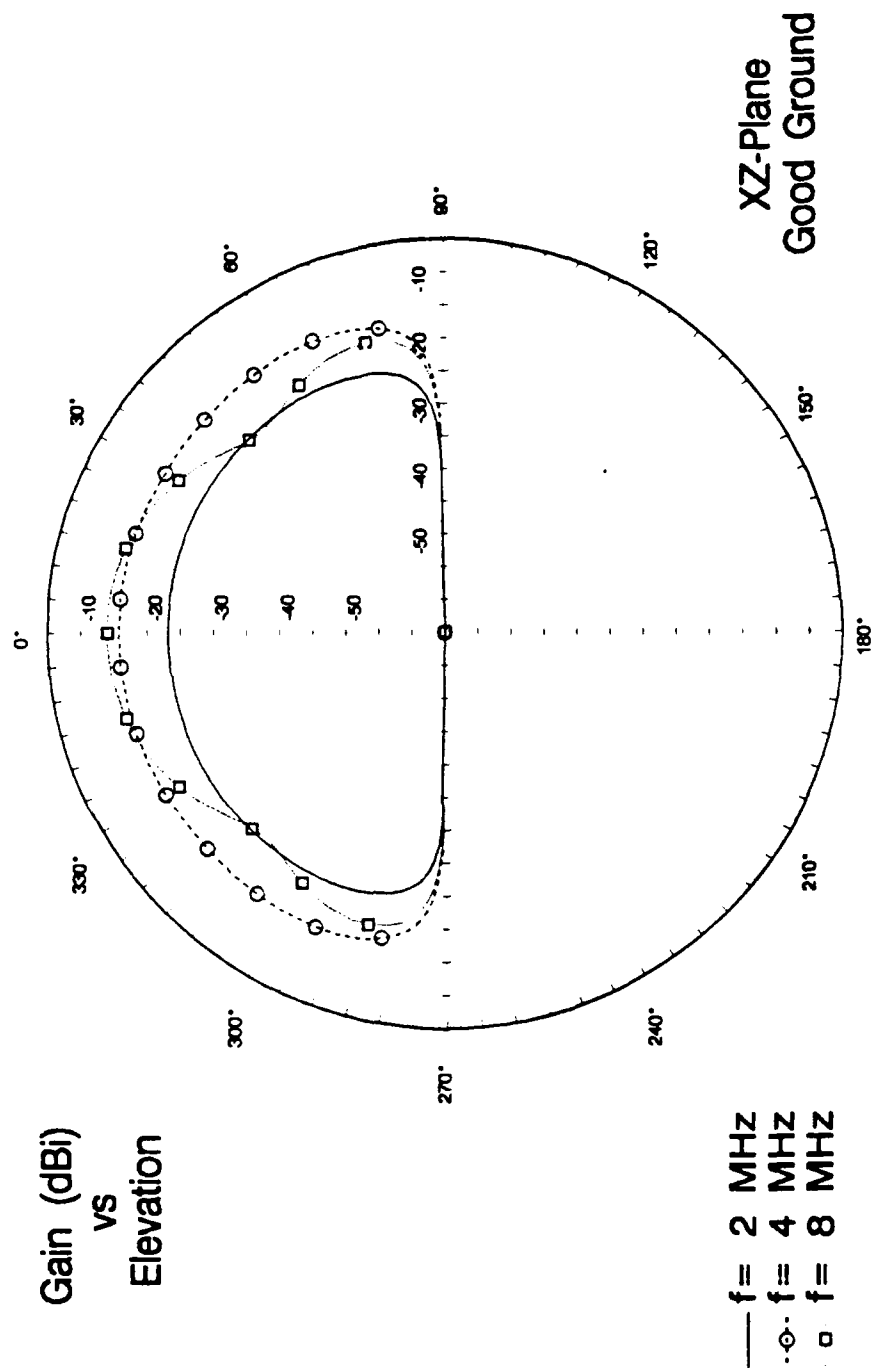


Figure 6. Elevation pattern for HT-20T over good ground for $f=2, 4,$ and 8 MHz.

HT-20T Antenna

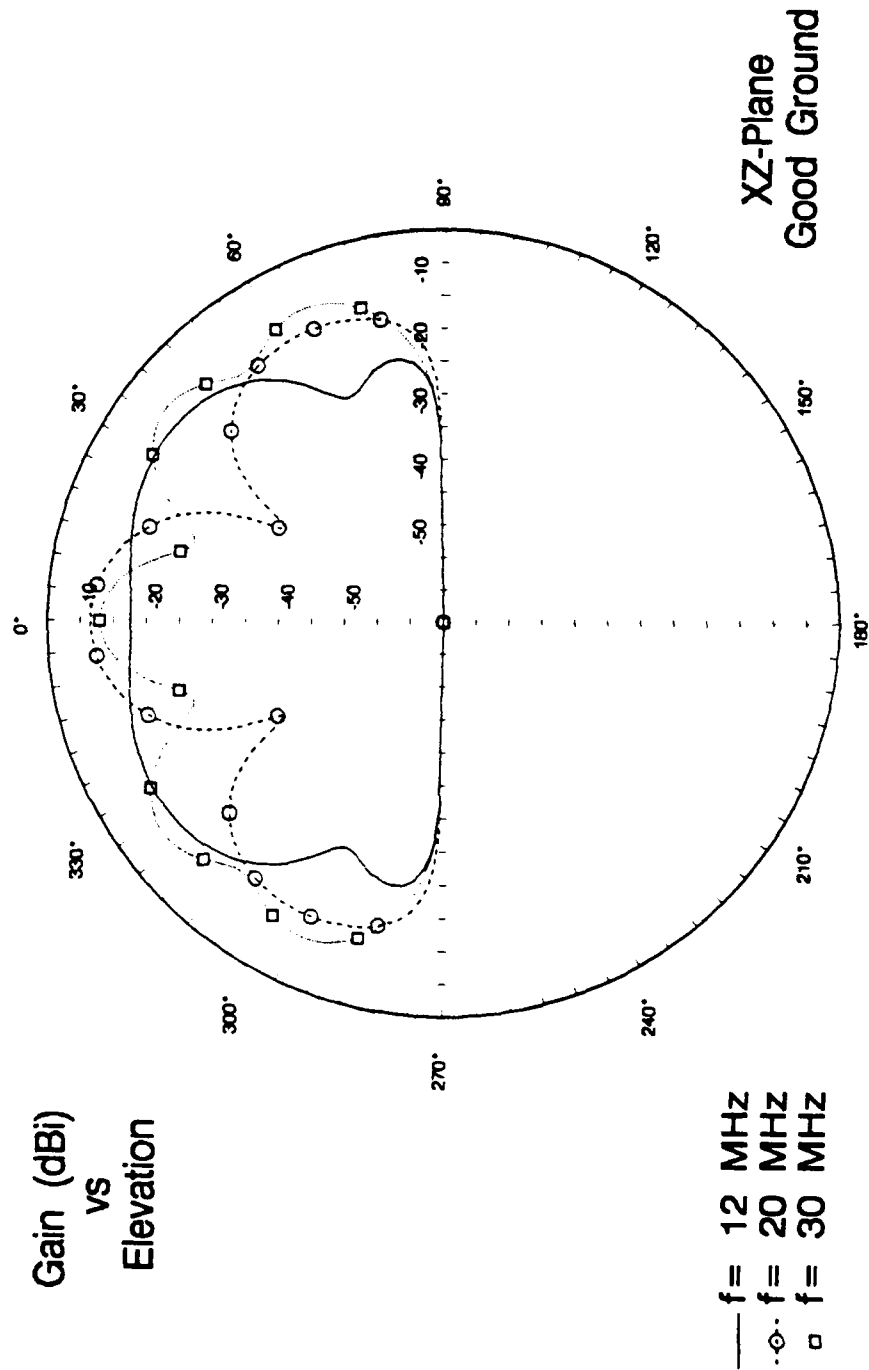


Figure 7. Elevation pattern for HT-20T over good ground for $f=12, 20$, and 30 MHz.

HT-20T Antenna

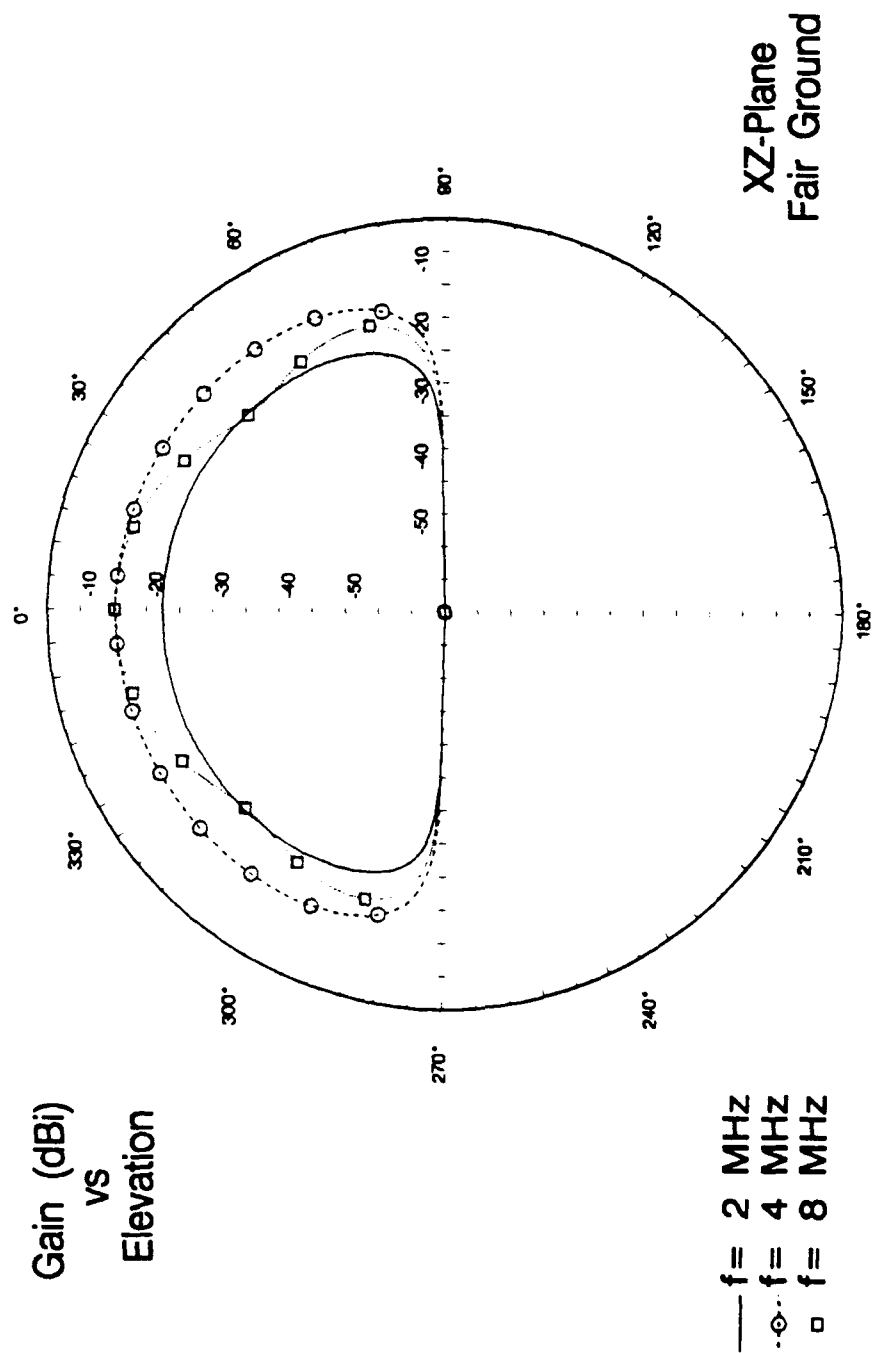


Figure 8. Elevation pattern for HT-20T over fair ground for $f=2, 4$, and 8 MHz.

HT-20T Antenna

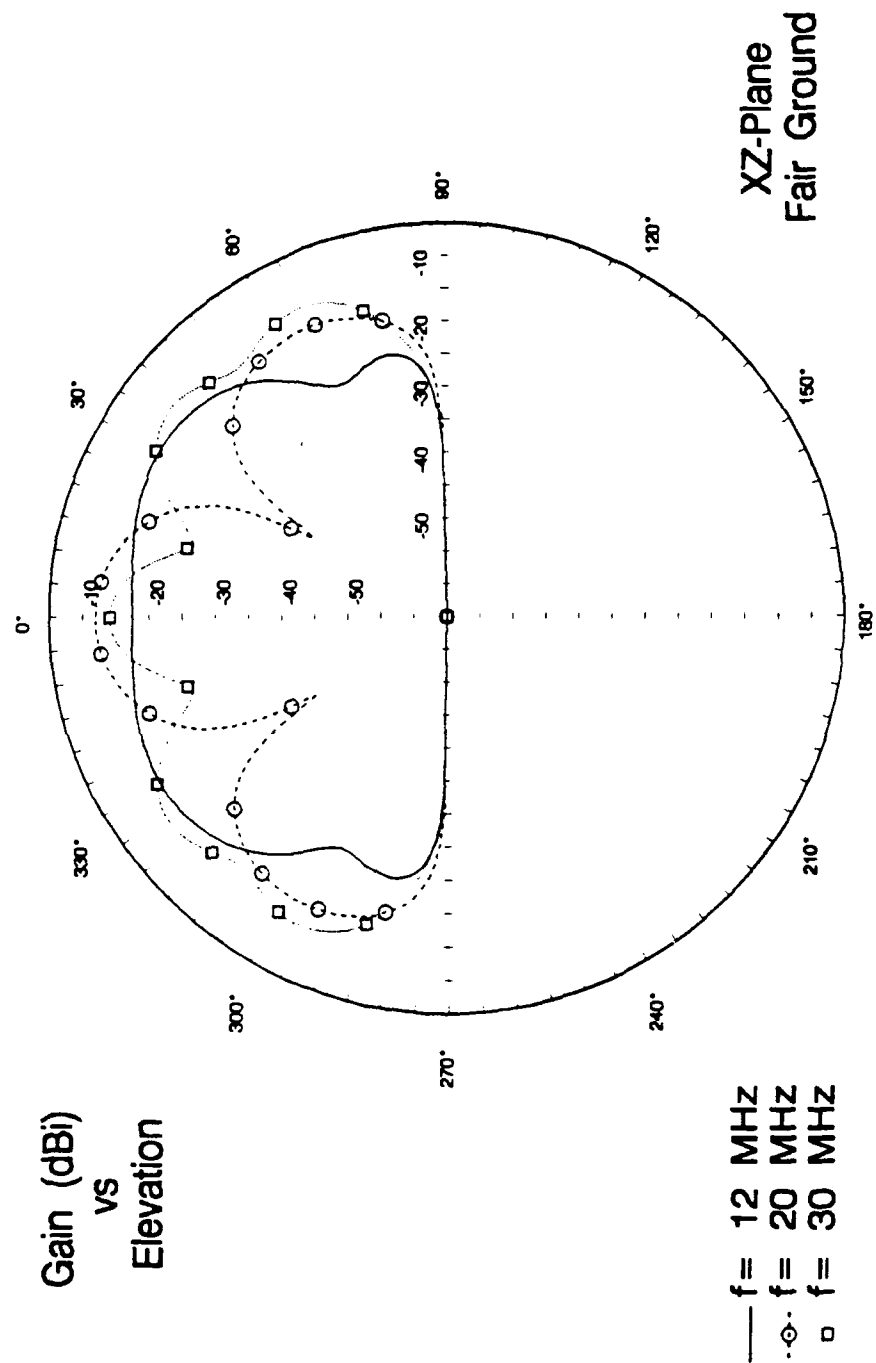


Figure 9. Elevation pattern for HT-20T over fair ground for $f=12, 20$, and 30 MHz.

HT-20T Antenna

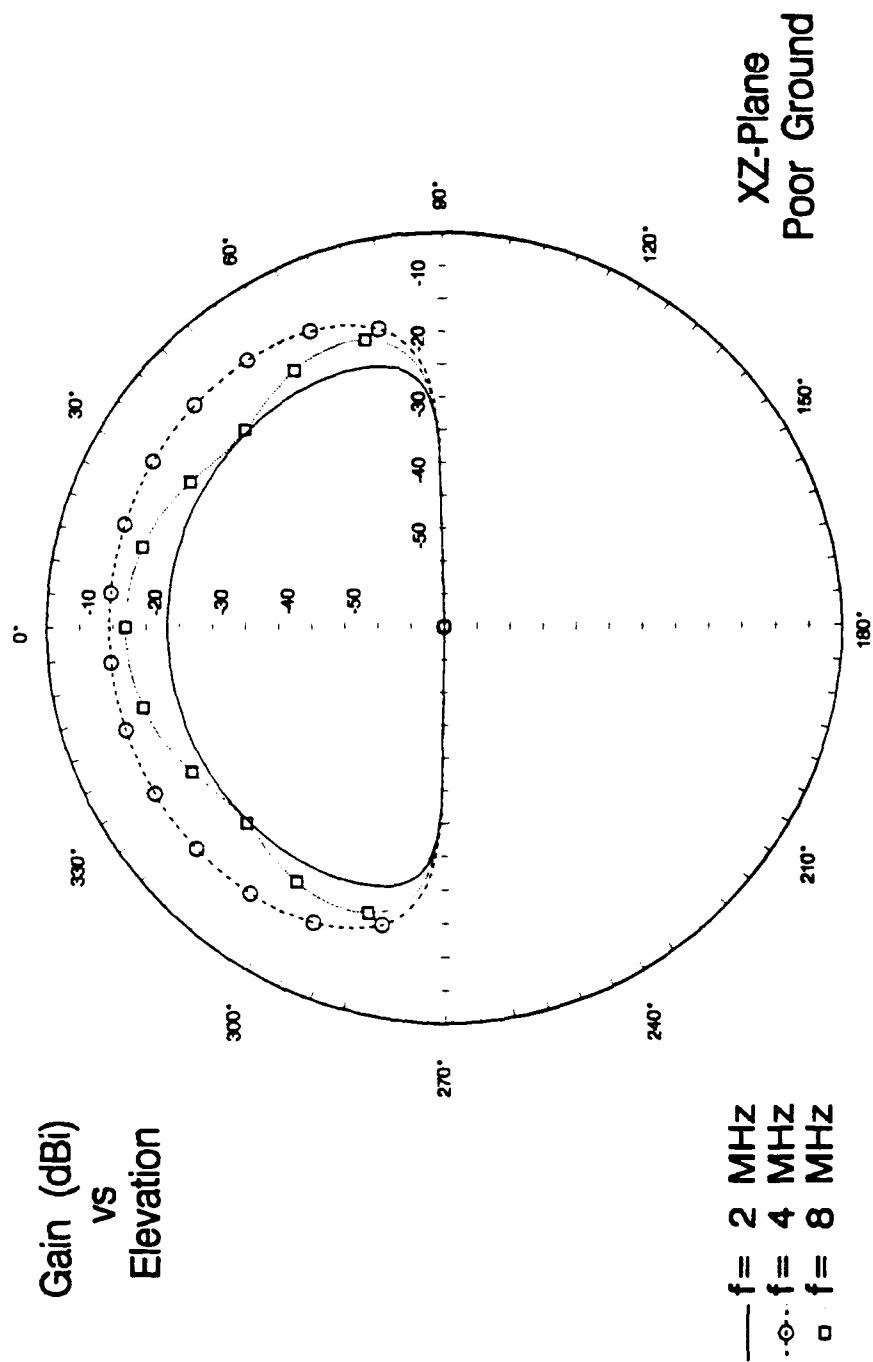


Figure 10. Elevation pattern for HT-20T over poor ground for $f=2, 4$, and 8 MHz.

HT-20T Antenna

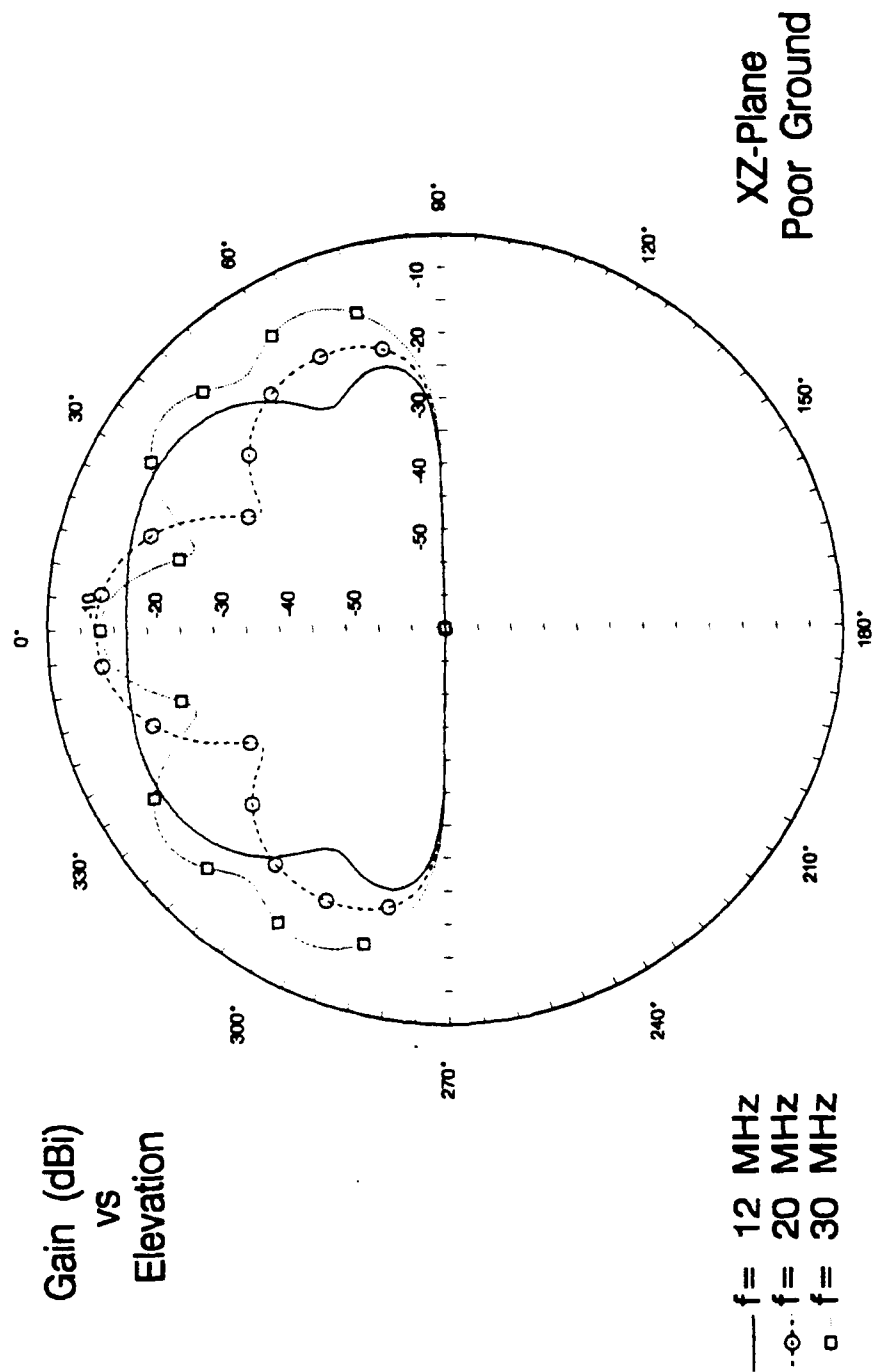


Figure 11. Elevation pattern for HT-20T over poor ground for $f=12, 20, \text{ and } 30$ MHz.

HT-20T Antenna

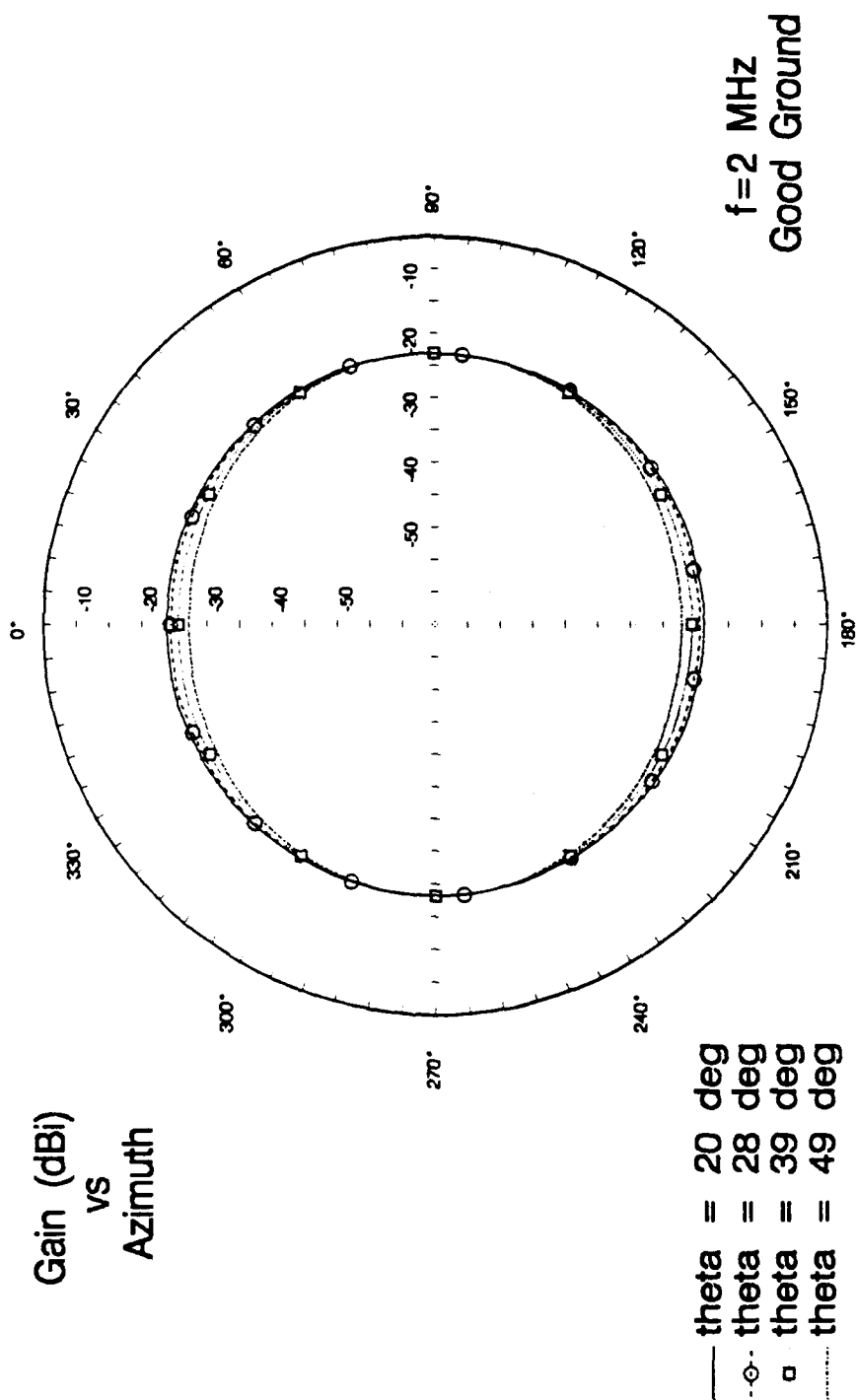


Figure 12. Azimuth pattern for HT-20T for f=2 MHz over good ground, varying takeoff angle(theta).

HT-20T Antenna

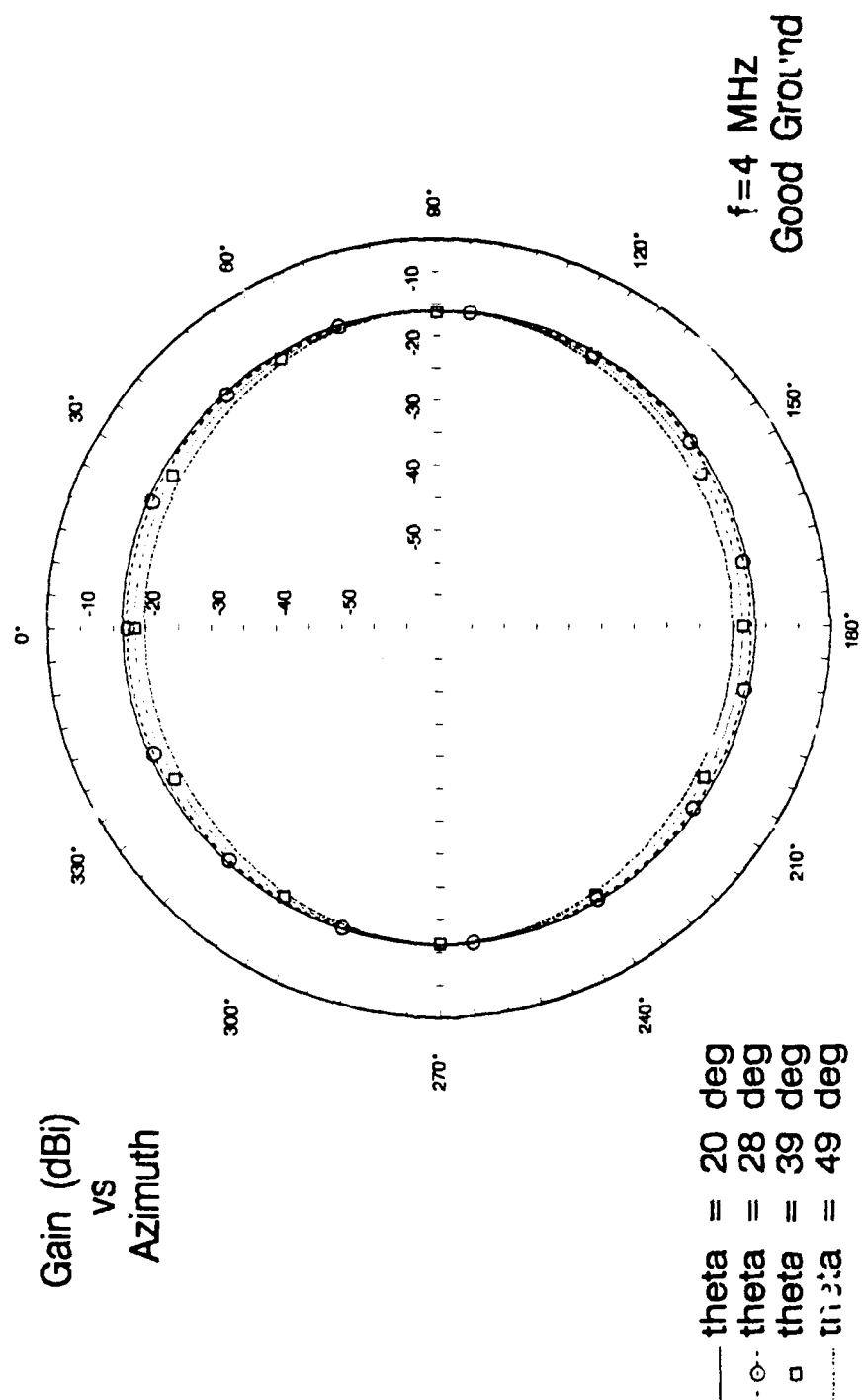


Figure 13. Azimuth pattern for HT-20T for f=4 MHz over good ground, varying takeoff angle(theta).

HT-20T Antenna

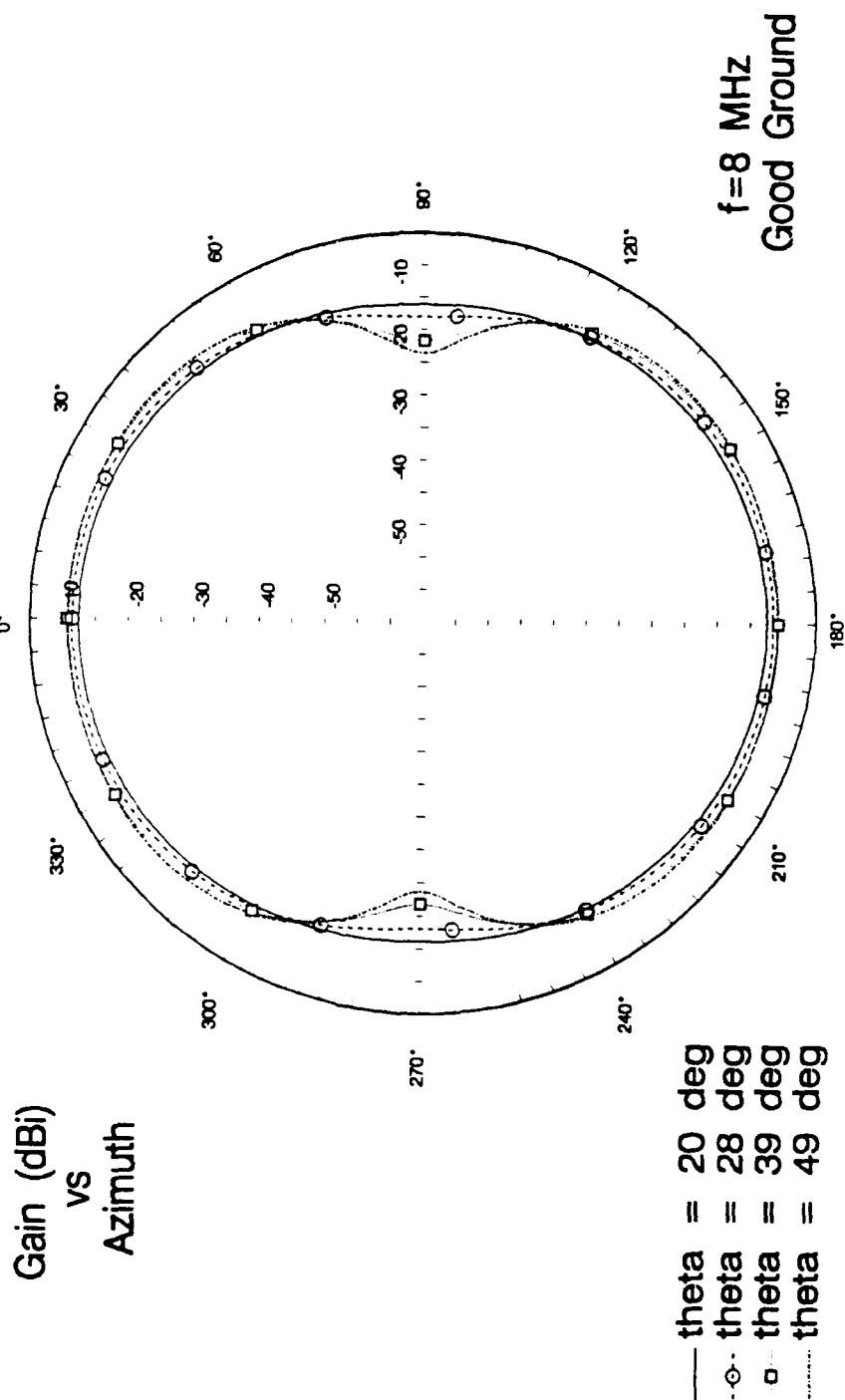


Figure 14. Azimuth pattern for HT-20T for f=8 MHz over good ground, varying takeoff angle (theta).

HT-20T Antenna

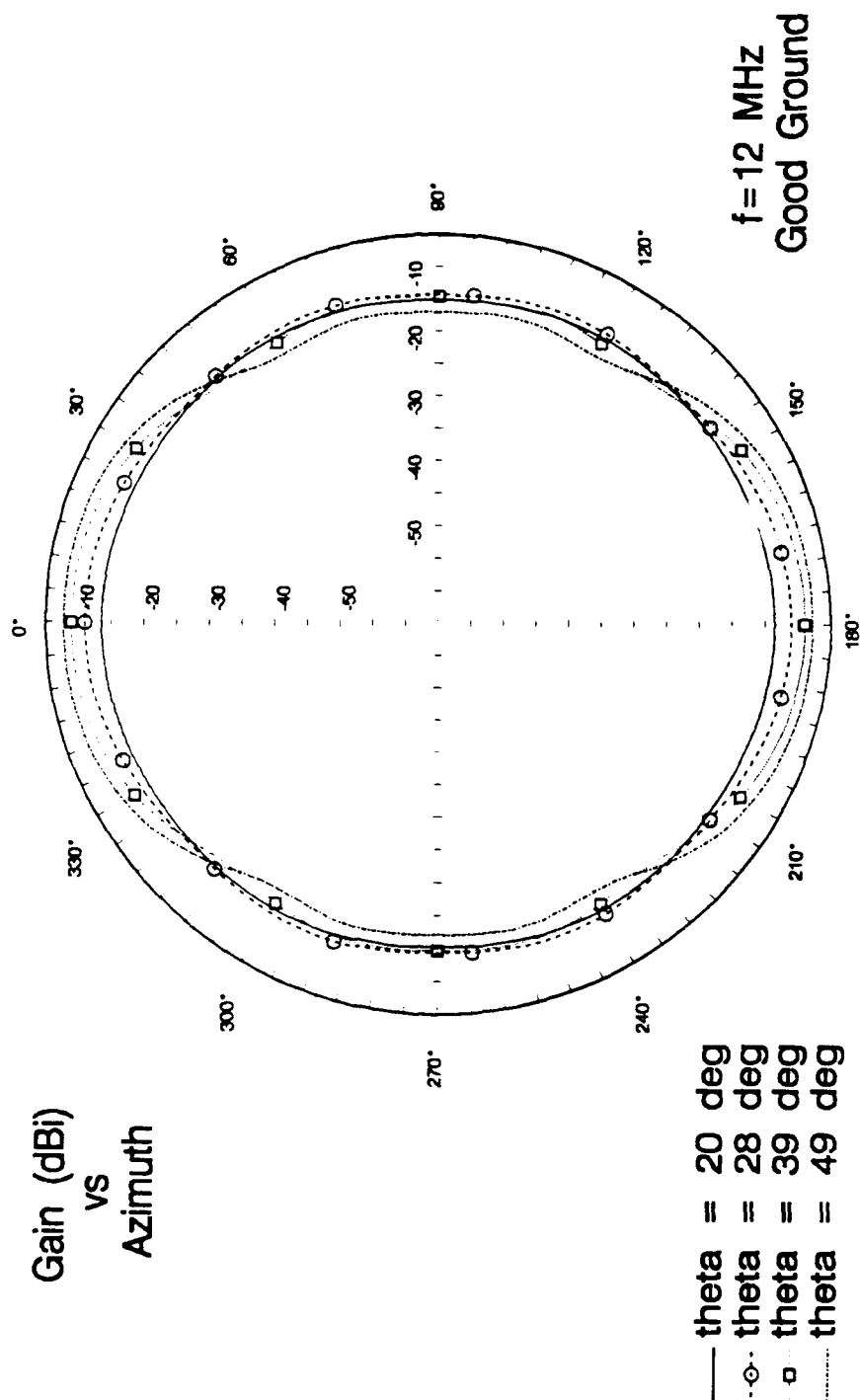


Figure 15. Azimuth pattern for HT-20T for f=12 MHz over good ground, varying takeoff angle (theta).

HT-20T Antenna

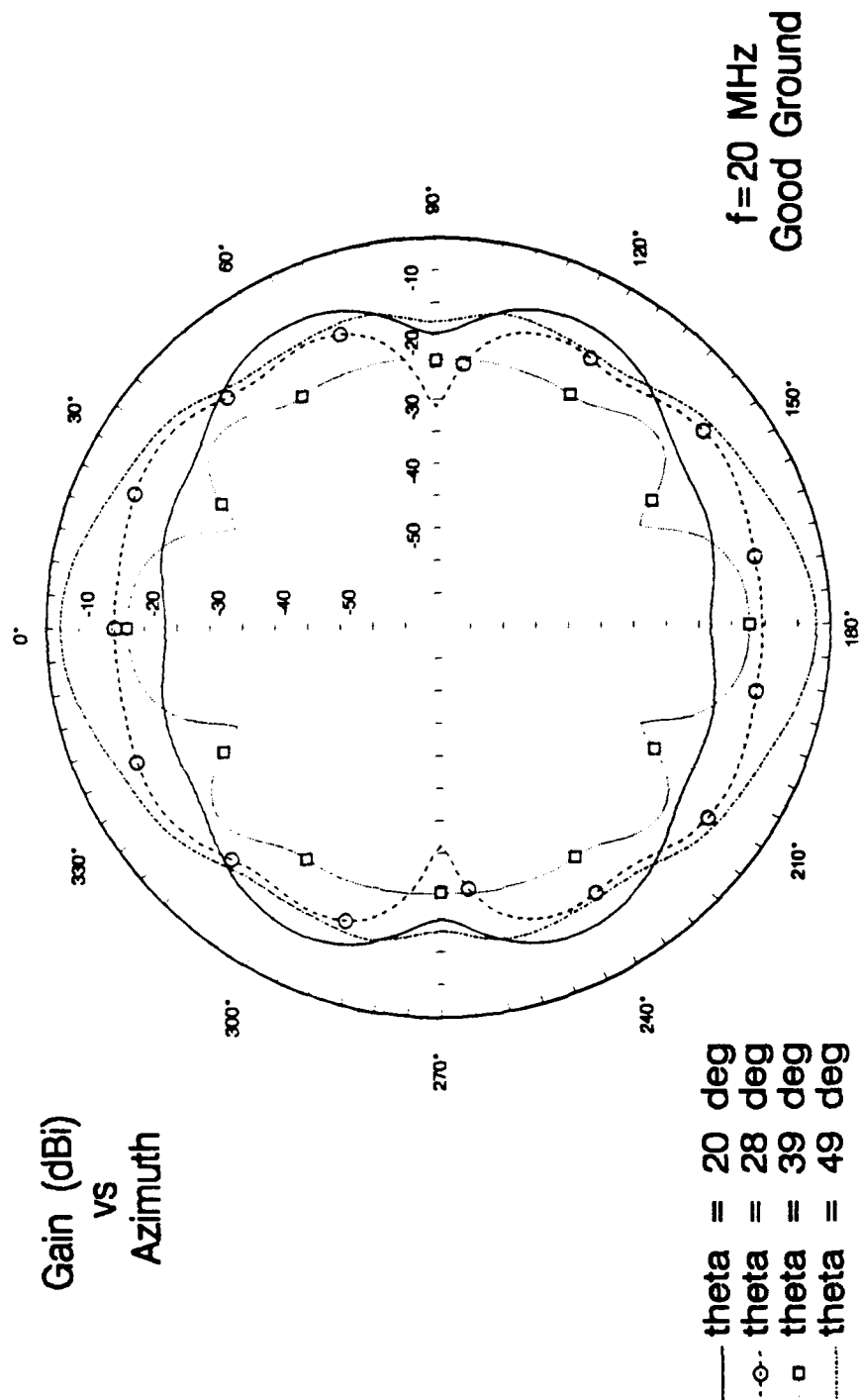


Figure 16. Azimuth pattern for HT-20T for f=20 MHz over good ground, varying takeoff angle(theta).

HT-20T Antenna

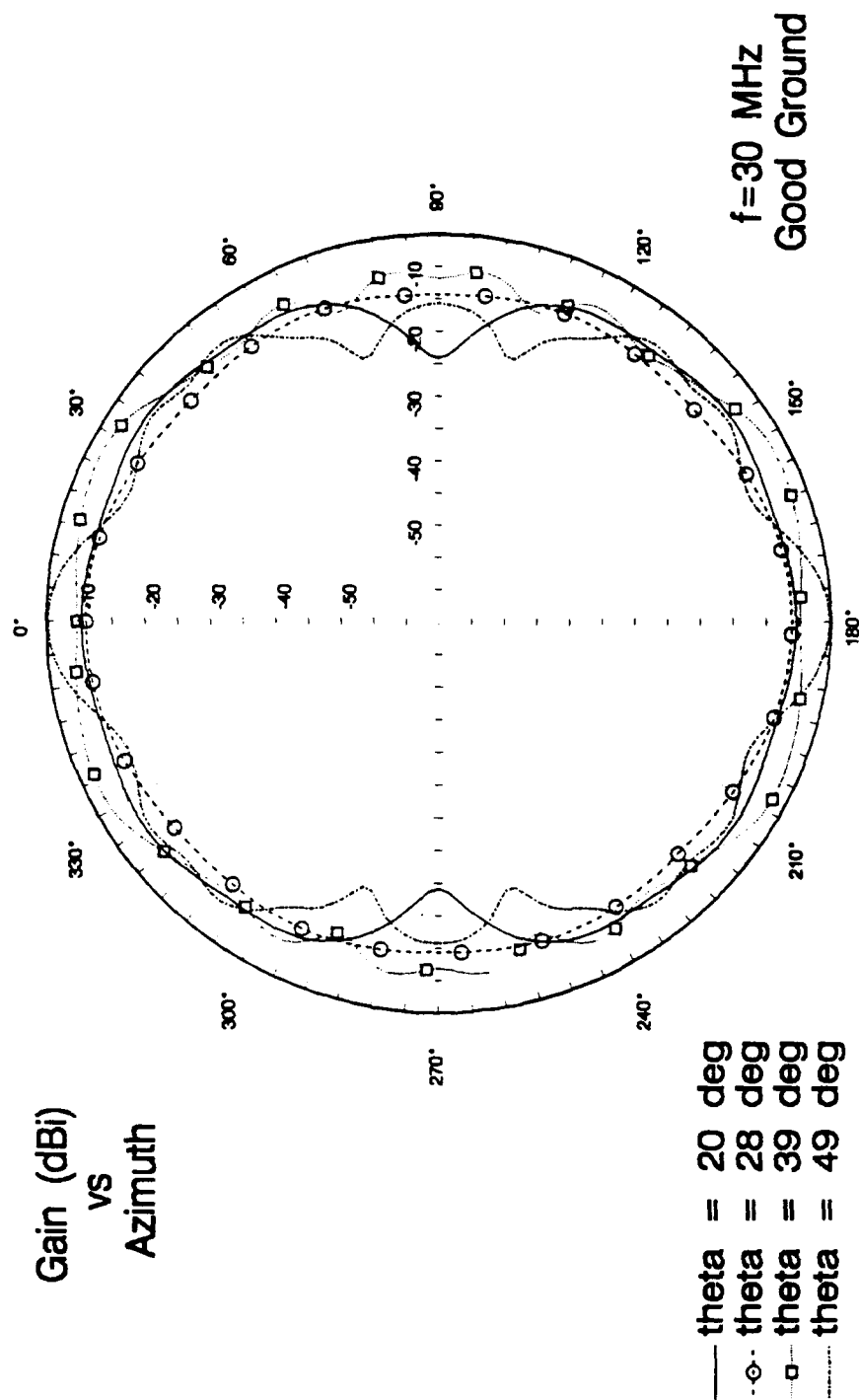


Figure 17. Azimuth pattern for HT-20T for f=30 MHz over good ground, varying takeoff angle (theta).

over good ground.

A change in ground conditions does have some effect on the radiation pattern. As the ground conditions vary from good to poor, peak gain varies 2 to 3 dB at takeoff angles greater than 30 degrees, depending upon frequency. For takeoff angles below 30 degrees, however, there is virtually no change. These results are expected because, although the ground has some effect, the antenna as designed is high enough to minimize ground interactions. The antenna radiation patterns also match those predicted in Reference 6, which validates this model.

C. ELPA-302 MODEL

The ELPA-302 antenna is a broadband HF skywave antenna and is illustrated in Figure 18. It does not require tuning either electronically or by trimming the antenna length. The antenna is fed by an Element Feed Unit (EFU) which acts as a balun and phase controller. By using the EFU, the main antenna beam can be steered in elevation and azimuth. The ELPA-302 can also be terminated so reflections on the radiating elements are reduced or eliminated. The ELPA-302 was modeled in PAT7 using a matched termination to minimize reflections on the antenna and an elevation steering at 34 degrees, the median takeoff angle, to achieve the best possible results. [Ref. 2]

The VSWR for the ELPA-302 was calculated for good and poor

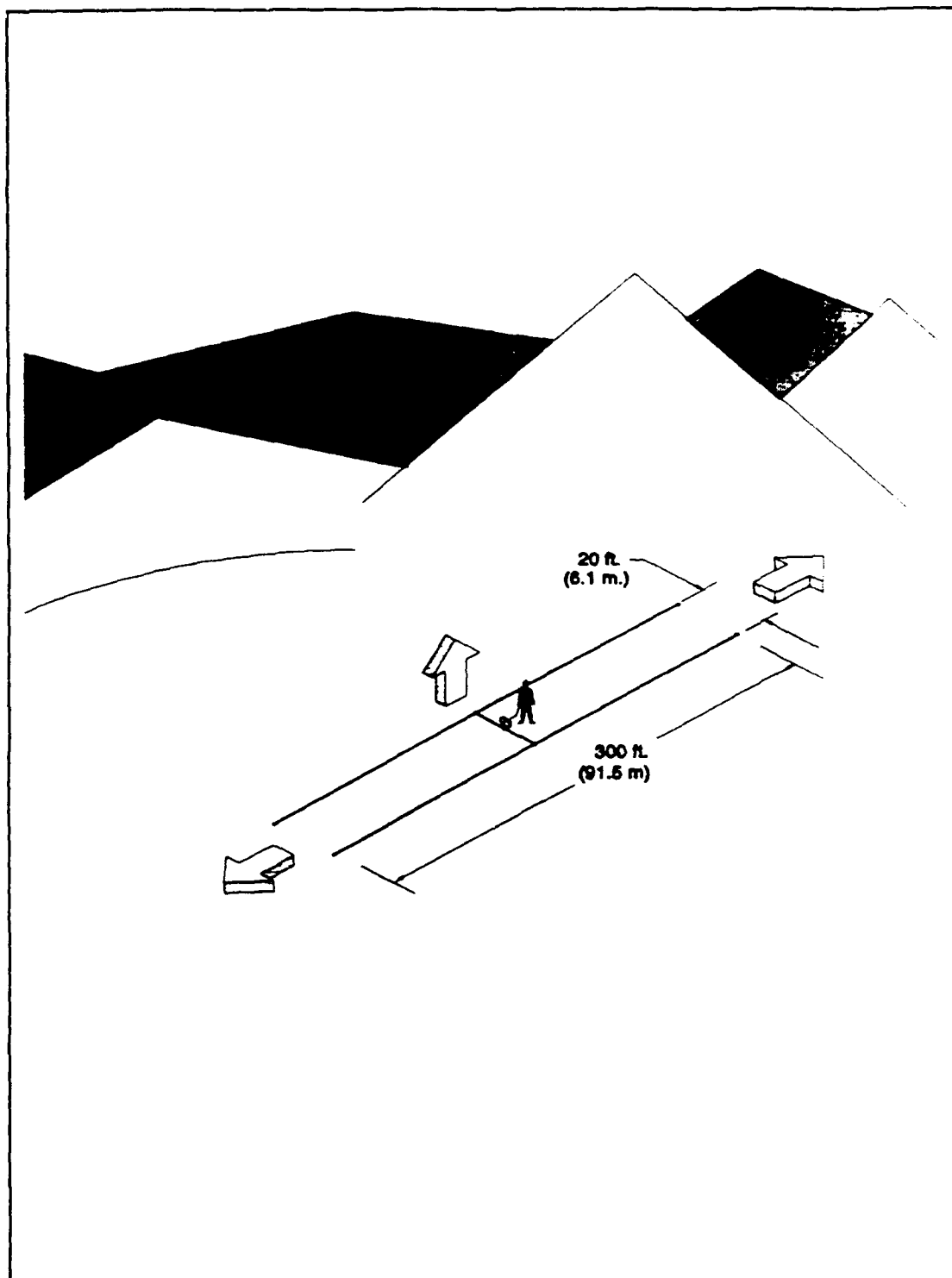


Figure 18. ELPA-302 Antenna

ground conditions at each height as illustrated in Figures 19 and 20. For good ground, the VSWR is somewhat higher for heights above ground. For poor ground, the VSWR is significantly lower for heights below ground. This can be explained by examining the electrical characteristics of the various types of ground. Ground conductivity and permittivity are functions of frequency. The electrical characteristics of poor ground effectively reduce the input impedance of the antenna to a value closer to the 50 ohm transmission line impedance. This results in a reduction in VSWR for poor ground. Good ground does not have this effect because the conductivity and permittivity are higher and do not significantly help the antenna to match the transmission line impedance. Although the VSWR is reduced for the antenna buried in poor ground, the negative consequences are that the gain is also reduced by burying the antenna. [Ref. 3]

The antenna radiation patterns for the ELPA-302 are illustrated in Figures 21 through 44. Each figure shows the pattern for a fixed ground condition for the heights of 0.5 meters, 0.006 meters, -0.5 meters, and -1.0 meters. These heights were chosen because they are the most practical when using the ELPA-302 for the TDCC mission. The patterns are oriented with the main beam along the positive and negative x-axis. The reference plane from which plots were taken was from the xz-plane through the origin. The radiation patterns

ELPA-302 Antenna

(Good Ground)

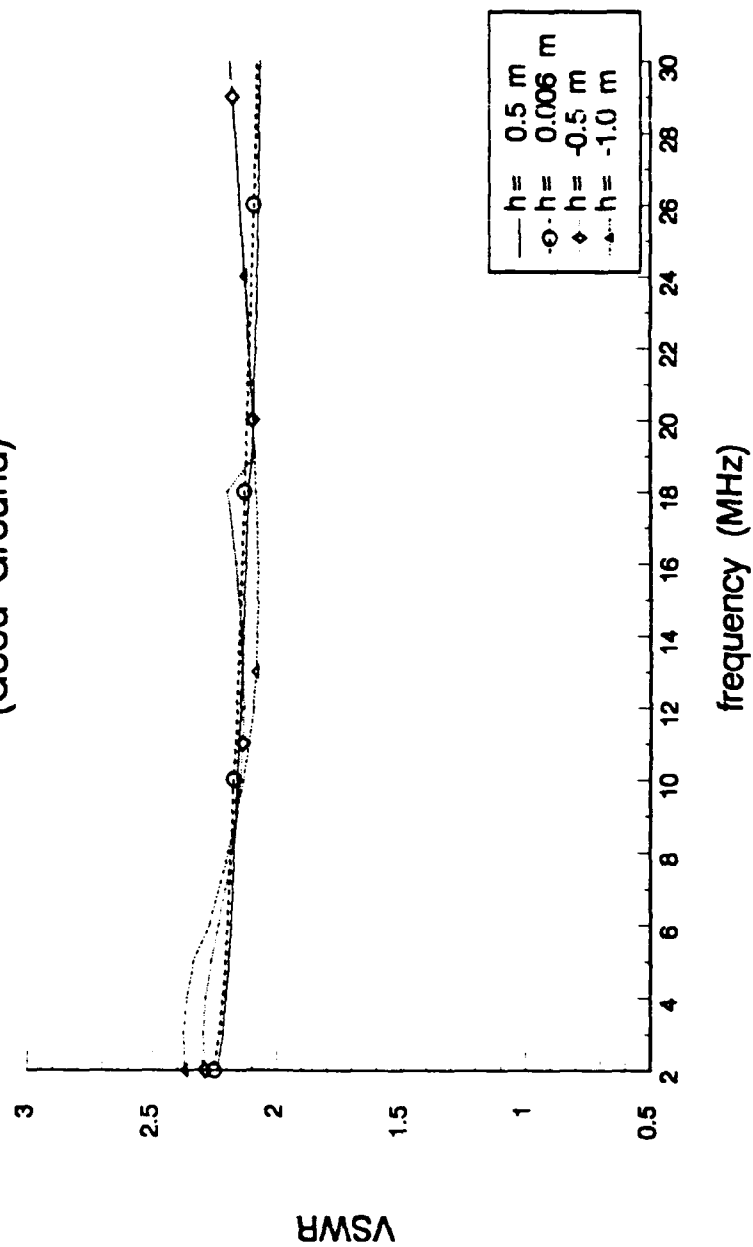


Figure 19. VSWR for ELPA-302 over good ground, varying heights.

ELPA-302 Antenna

(Poor Ground)

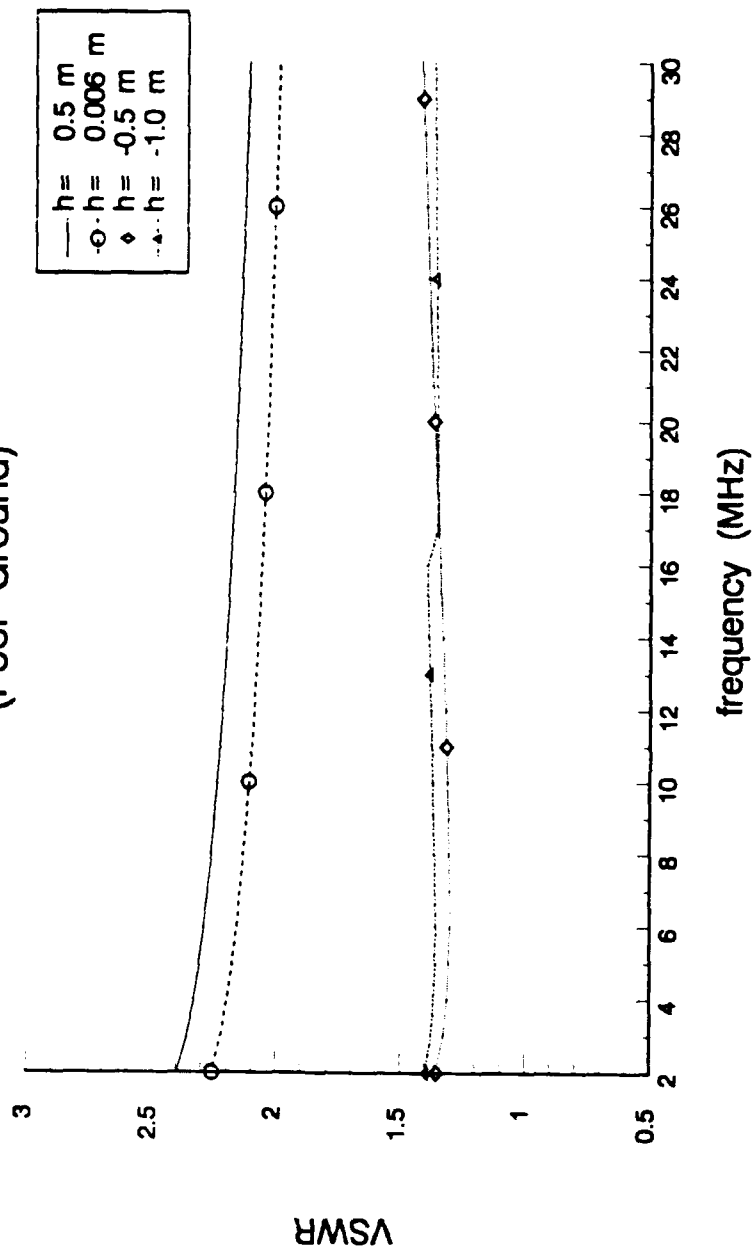


Figure 20. VSWR for ELPA-302 over poor ground, varying heights.

ELPA-302 Antenna

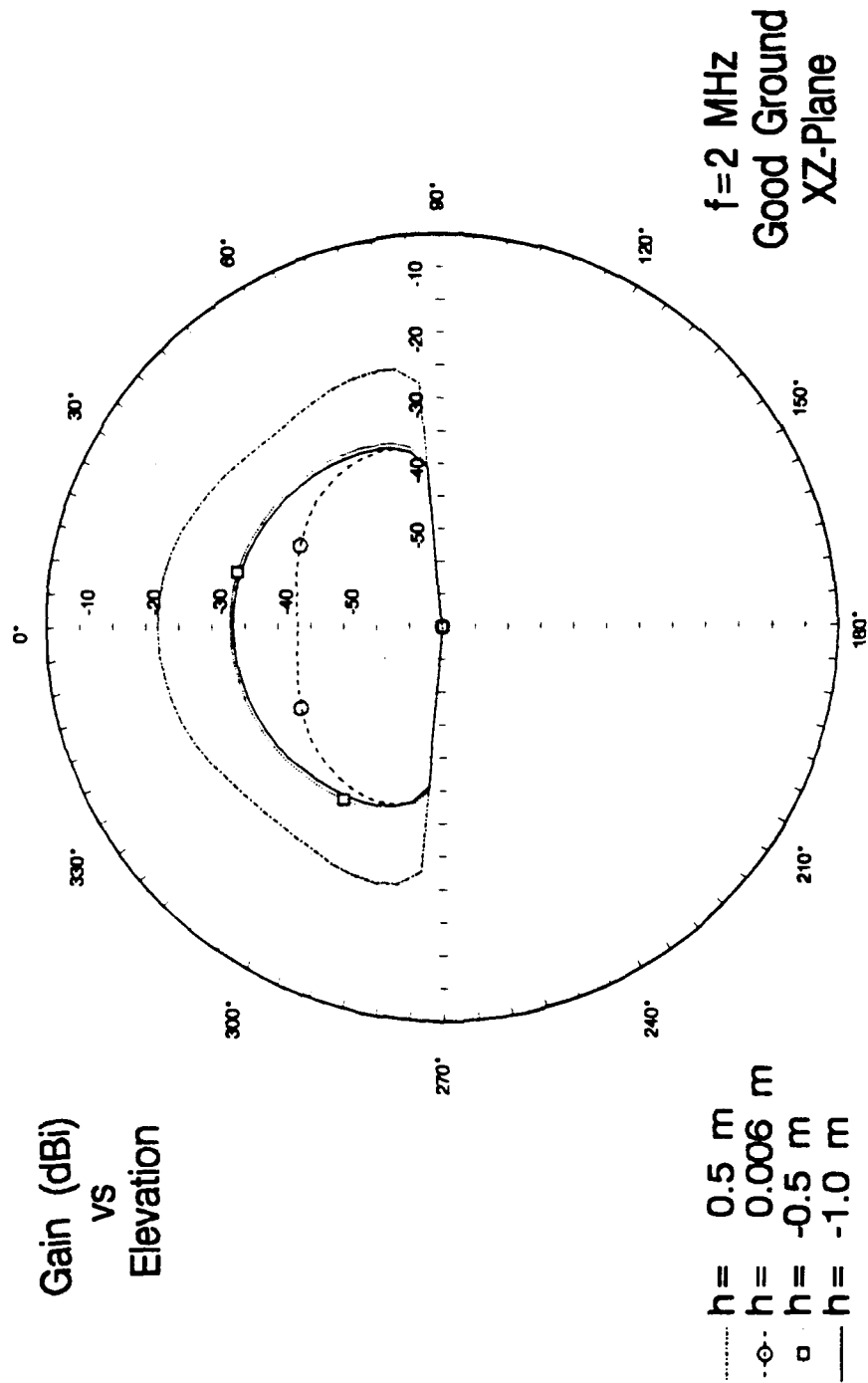


Figure 21. Elevation pattern for ELPA-302 for f=2 MHz over good ground.

ELPA-302 Antenna

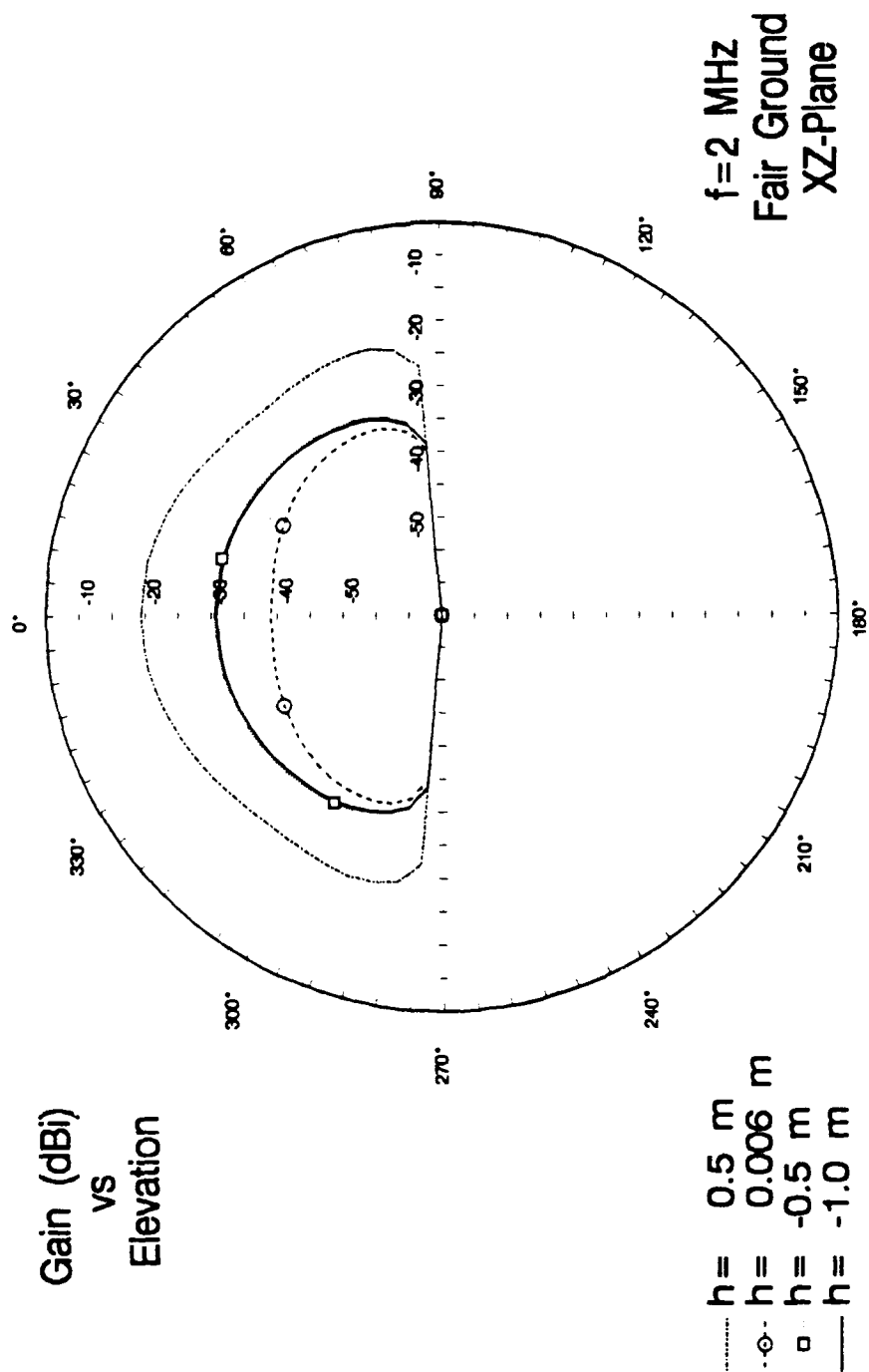


Figure 22. Elevation pattern for ELPA-302 for f=2 MHz over fair ground.

ELPA-302 Antenna

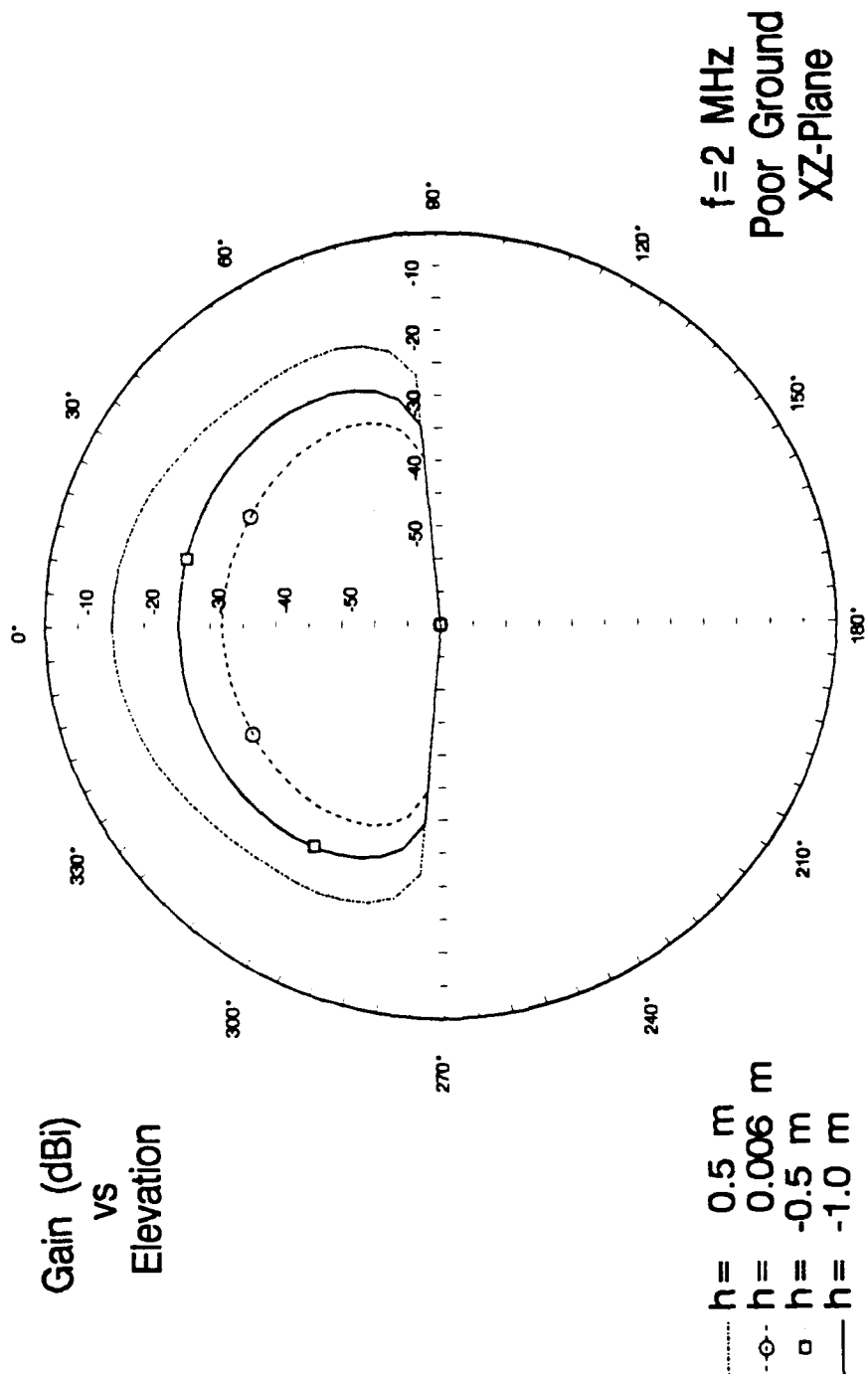


Figure 23. Elevation pattern for ELPA-302 for f=2 MHz over poor ground.

ELPA-302 Antenna

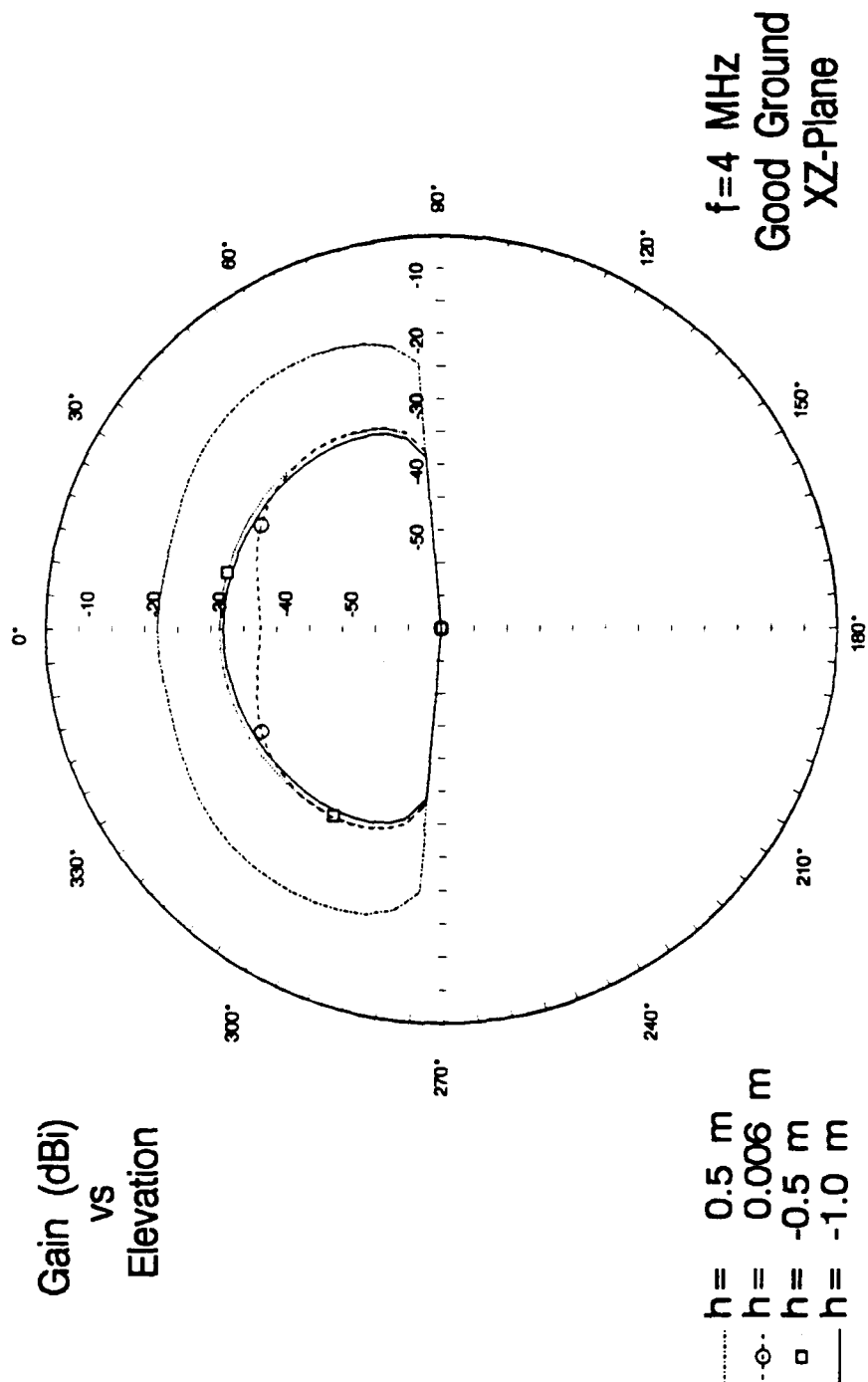


Figure 24. Elevation pattern for ELPA-302 for $f=4$ MHz over good ground.

ELPA-302 Antenna

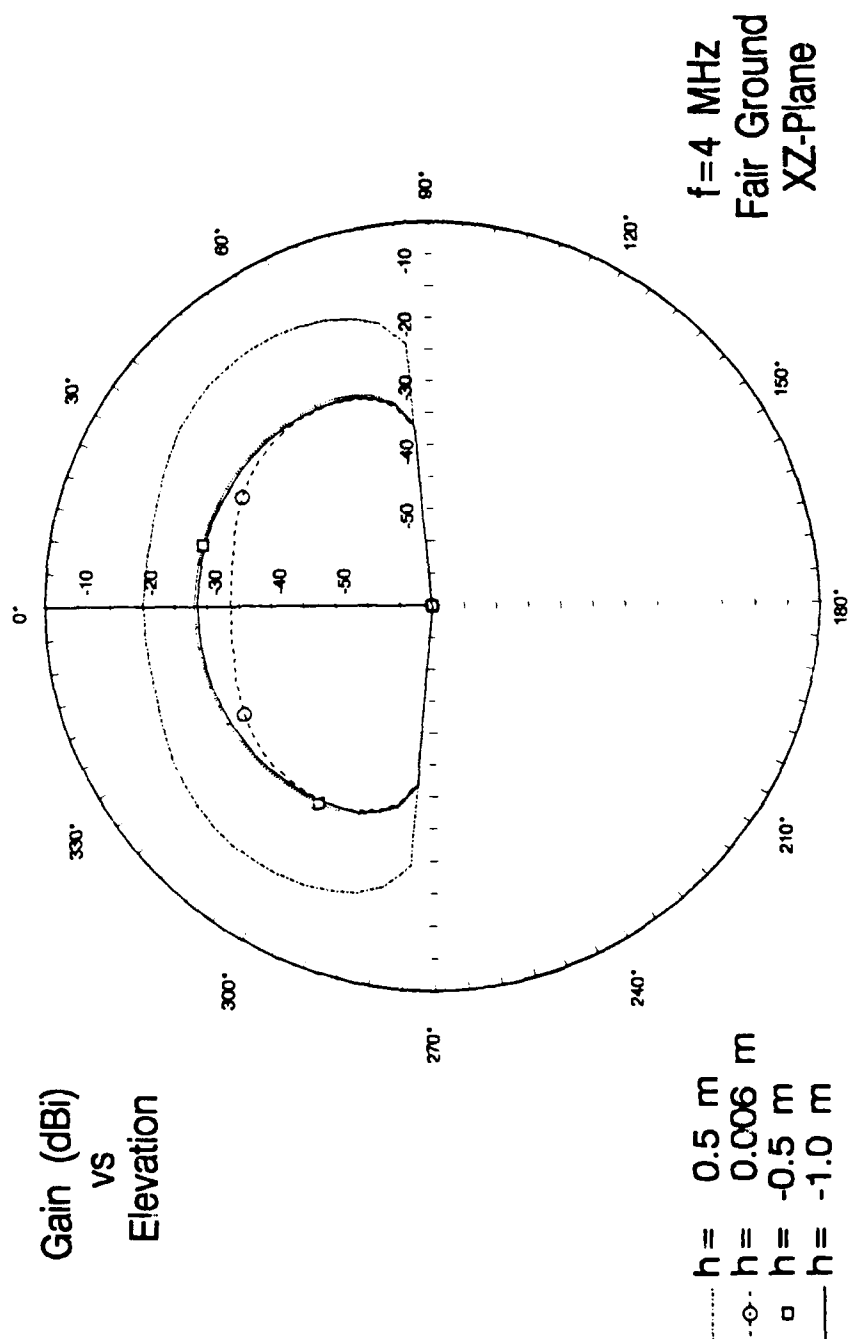


Figure 25. Elevation pattern for ELPA-302 for $f=4$ MHz over fair ground.

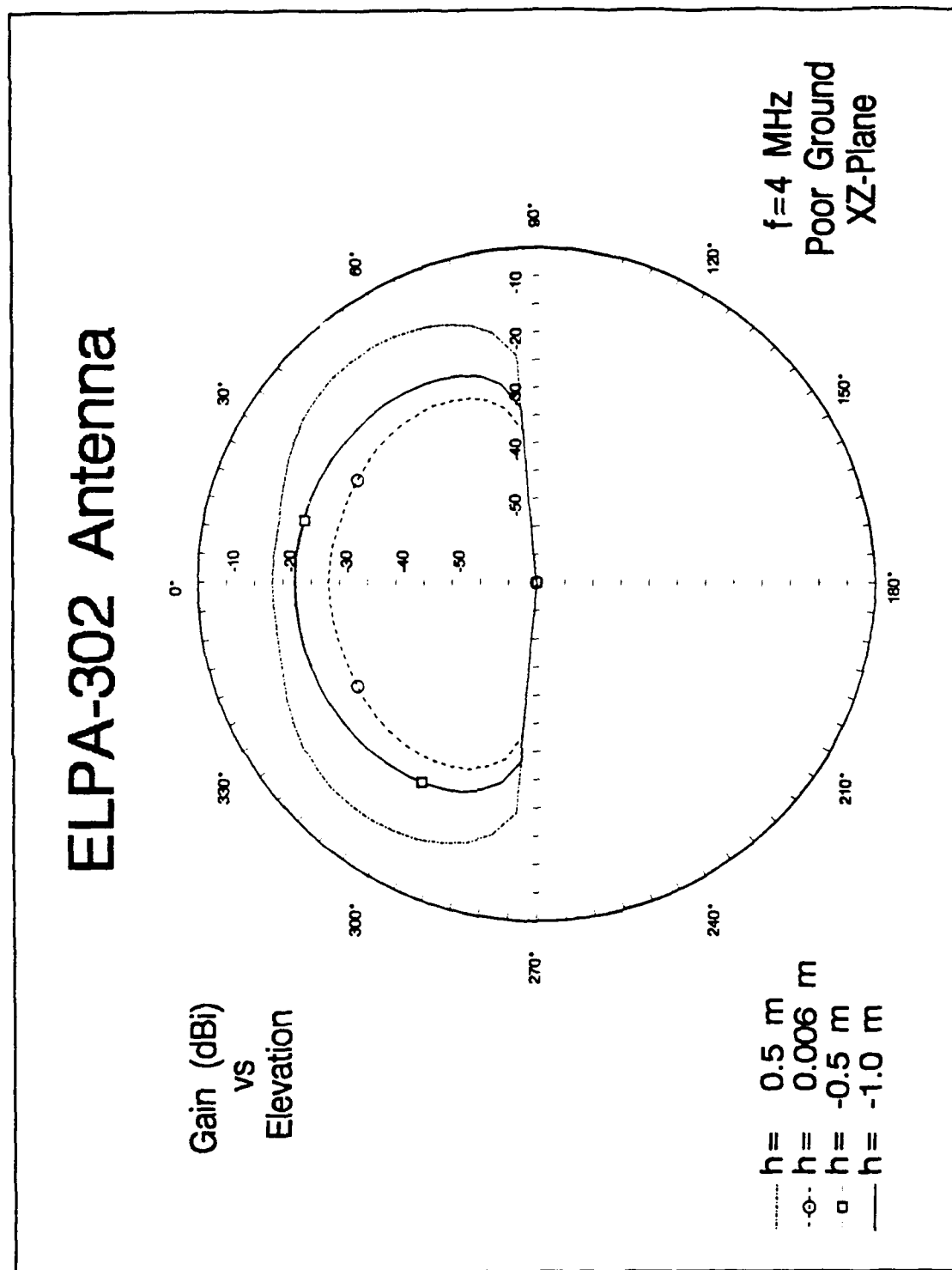


Figure 26. Elevation pattern for ELPA-302 for $f=4$ MHz over poor ground.

ELPA-302 Antenna

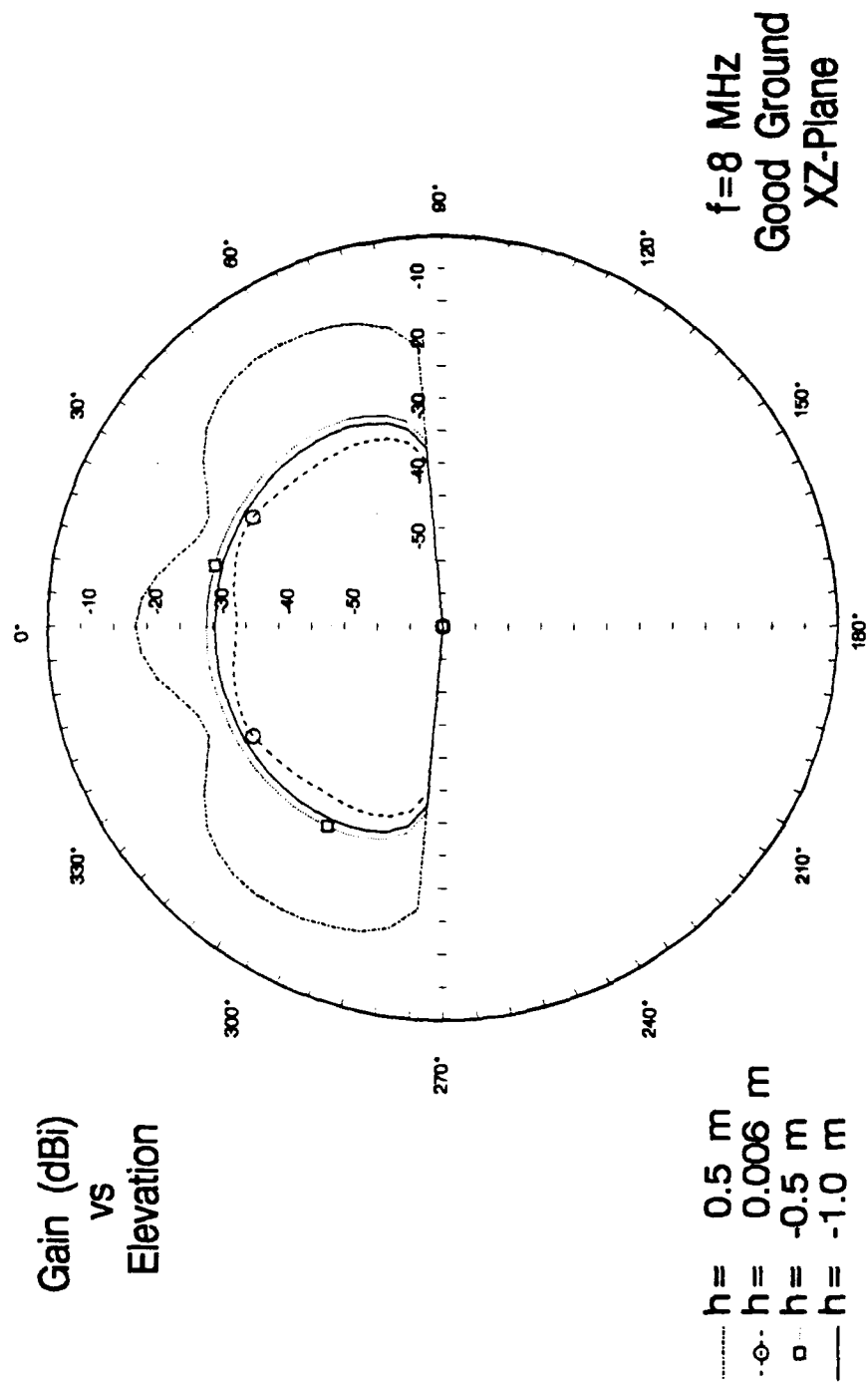


Figure 27. Elevation pattern for ELPA-302 for f=8 MHz over good ground.

ELPA-302 Antenna

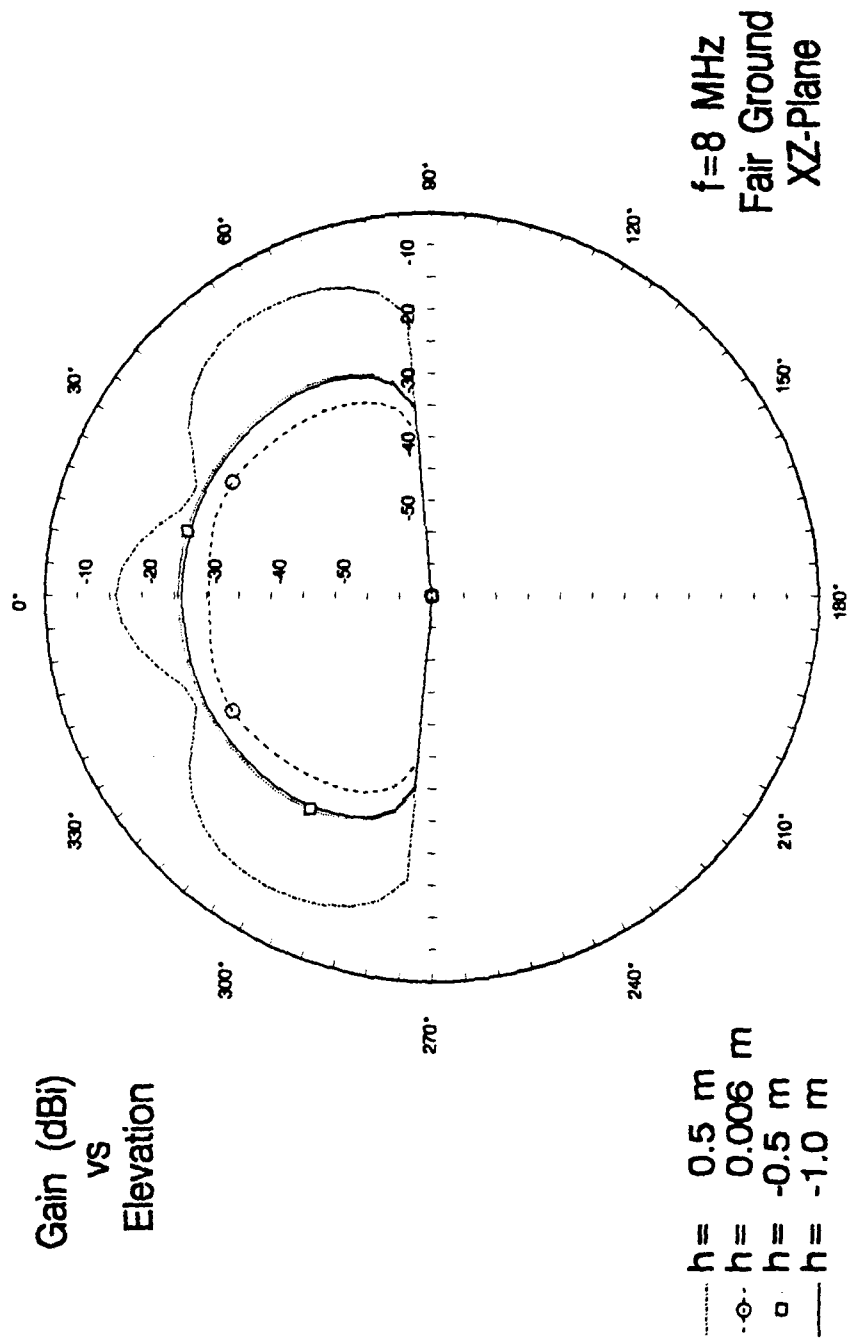


Figure 28. Elevation pattern for ELPA-302 for f=8 MHz over fair ground.

ELPA-302 Antenna

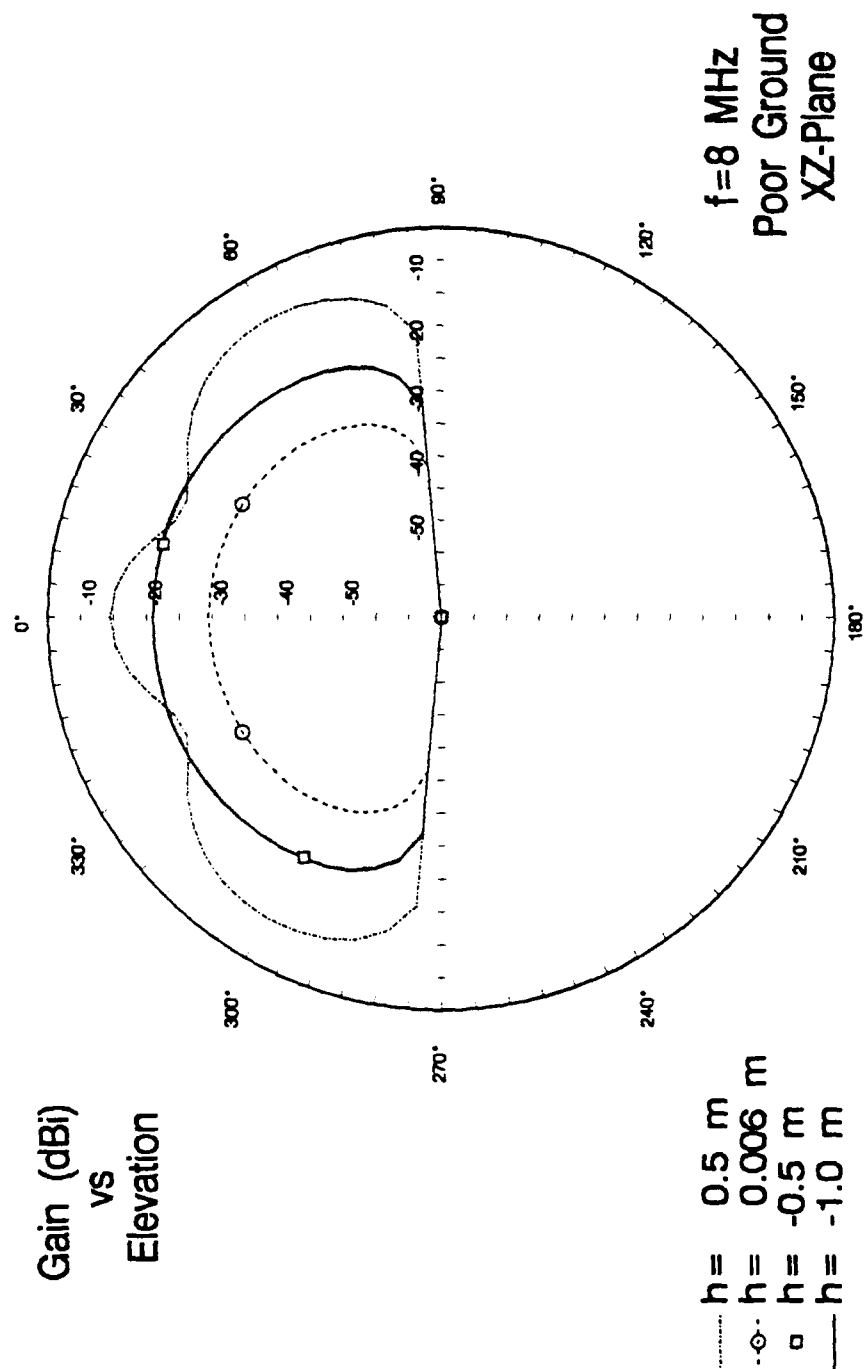


Figure 29. Elevation pattern for ELPA-302 for f=8 MHz over poor ground.

ELPA-302 Antenna

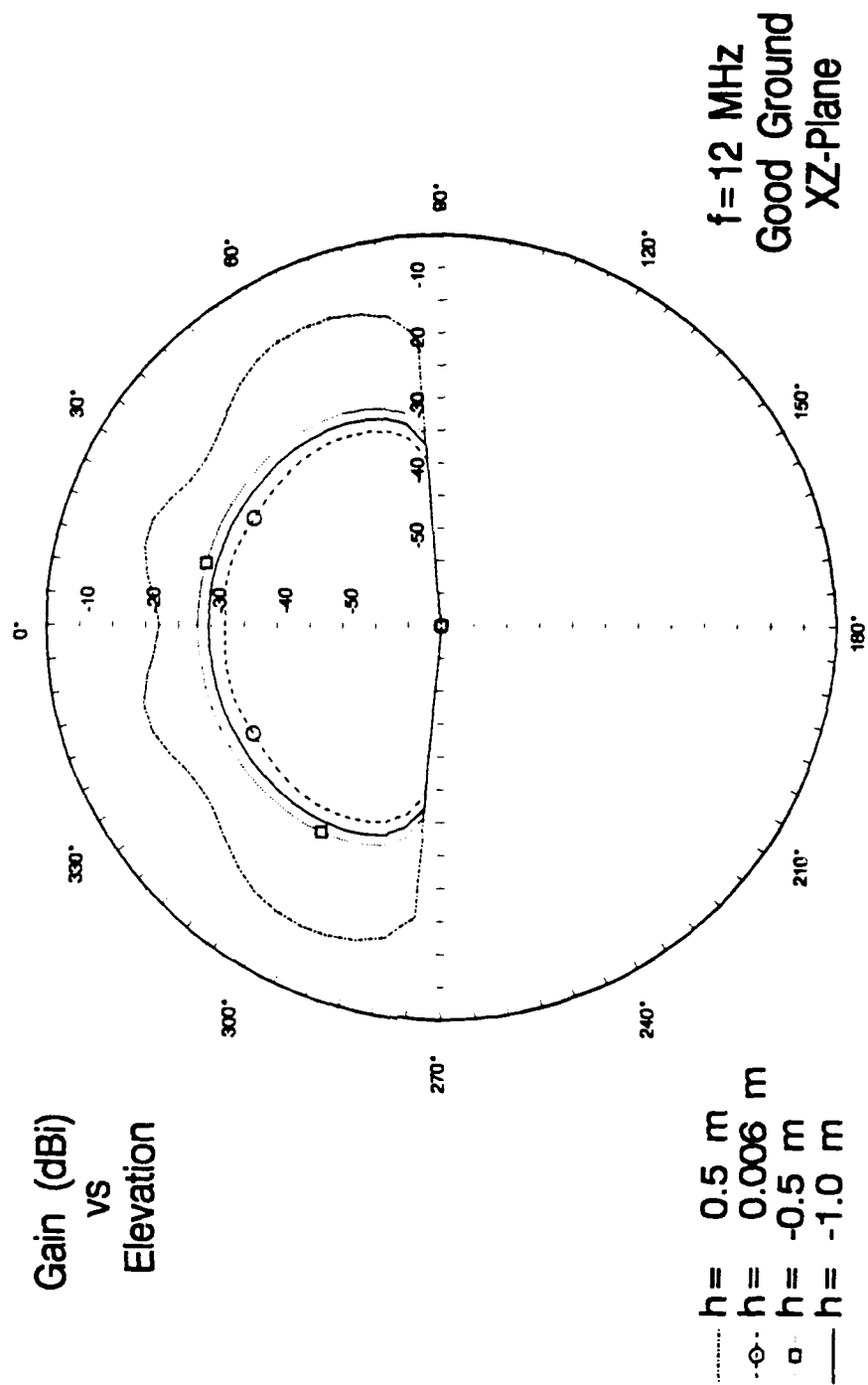


Figure 30. Elevation pattern for ELPA-302 for $f=12$ MHz over good ground.

ELPA-302 Antenna

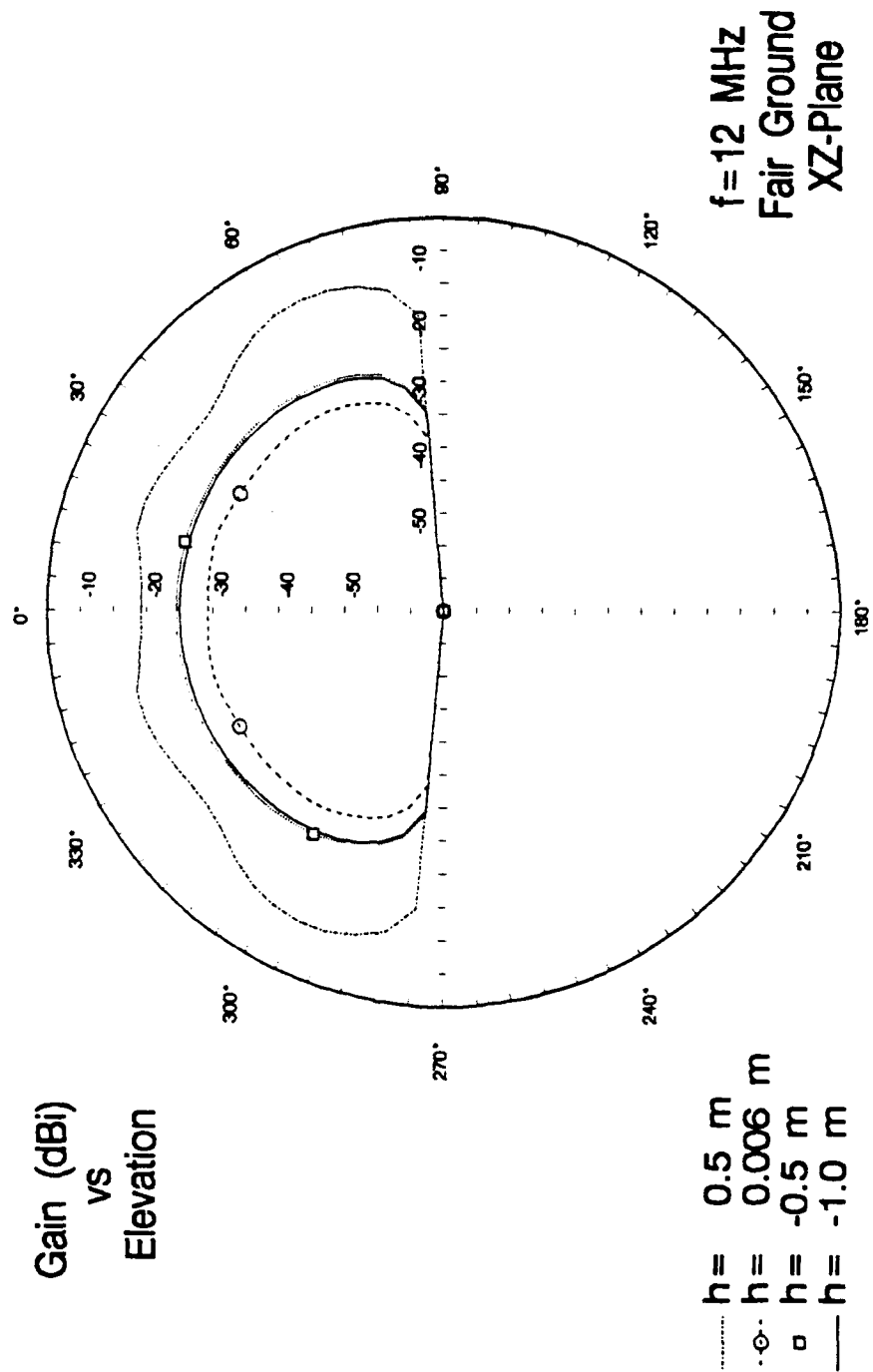


Figure 31. Elevation pattern for ELPA-302 for f=12 MHz over fair ground.

ELPA-302 Antenna

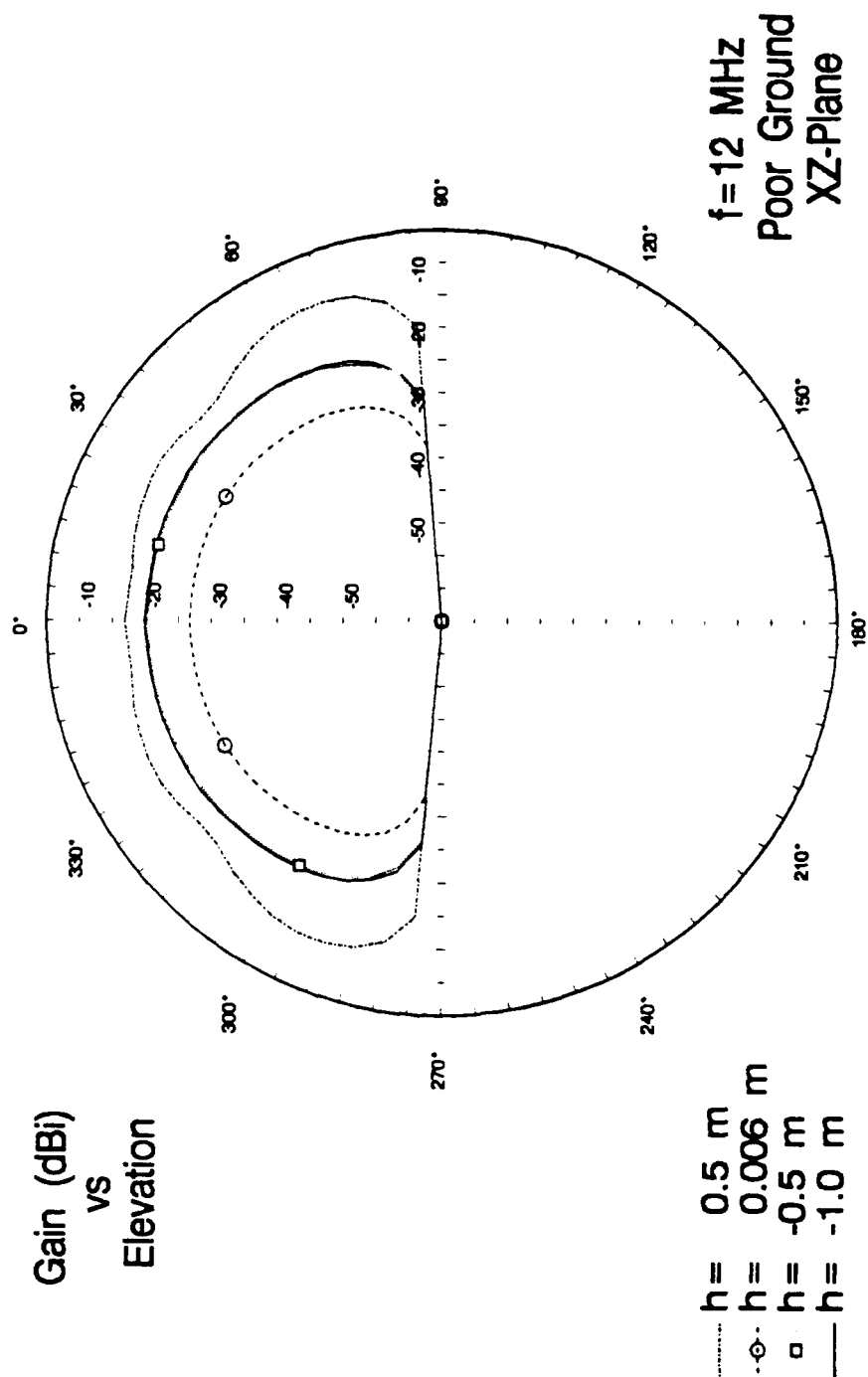


Figure 32. Elevation pattern for ELPA-302 for f=12 MHz over poor ground.

ELPA-302 Antenna

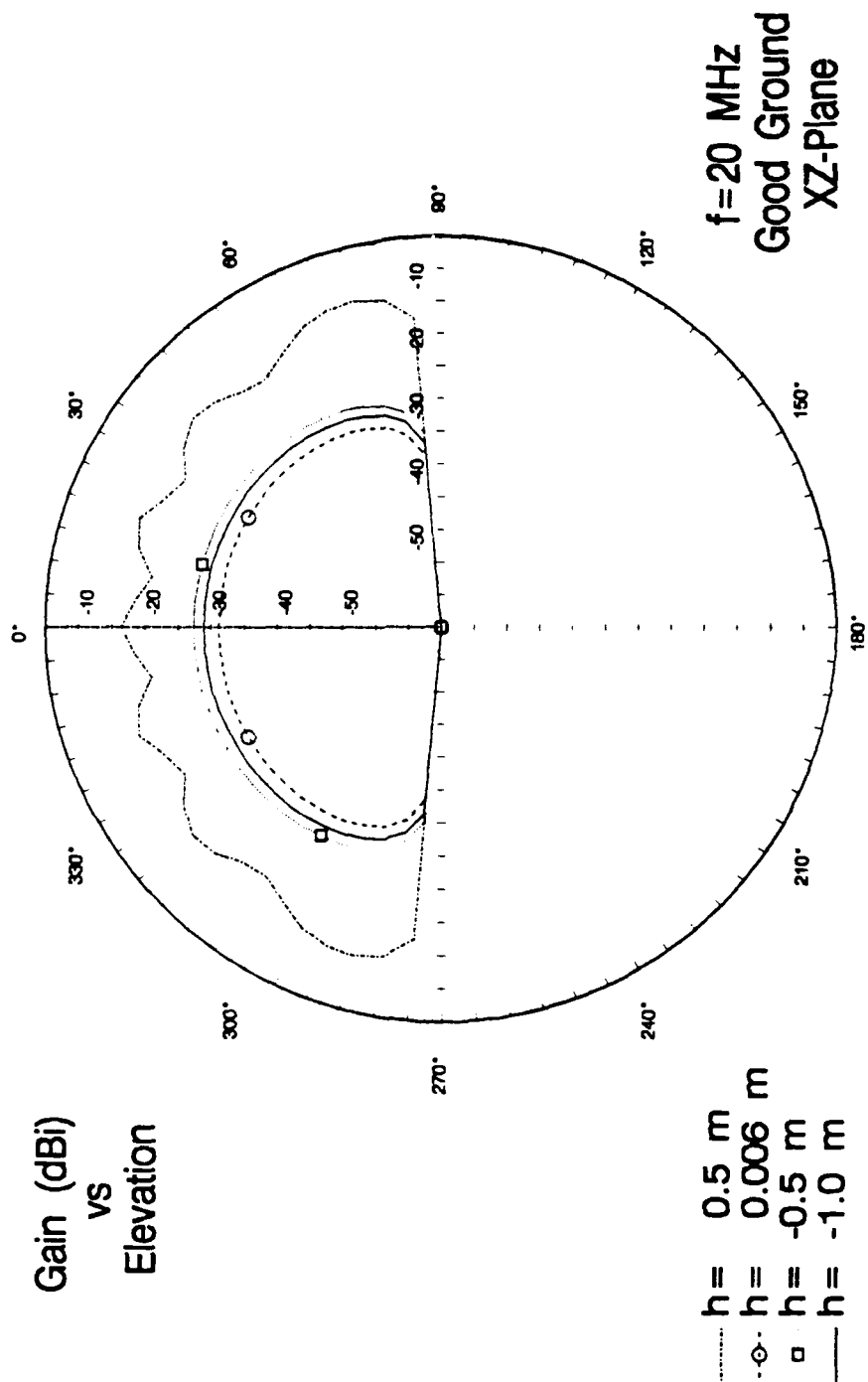


Figure 33. Elevation pattern for ELPA-302 for f=20 MHz over good ground.

ELPA-302 Antenna

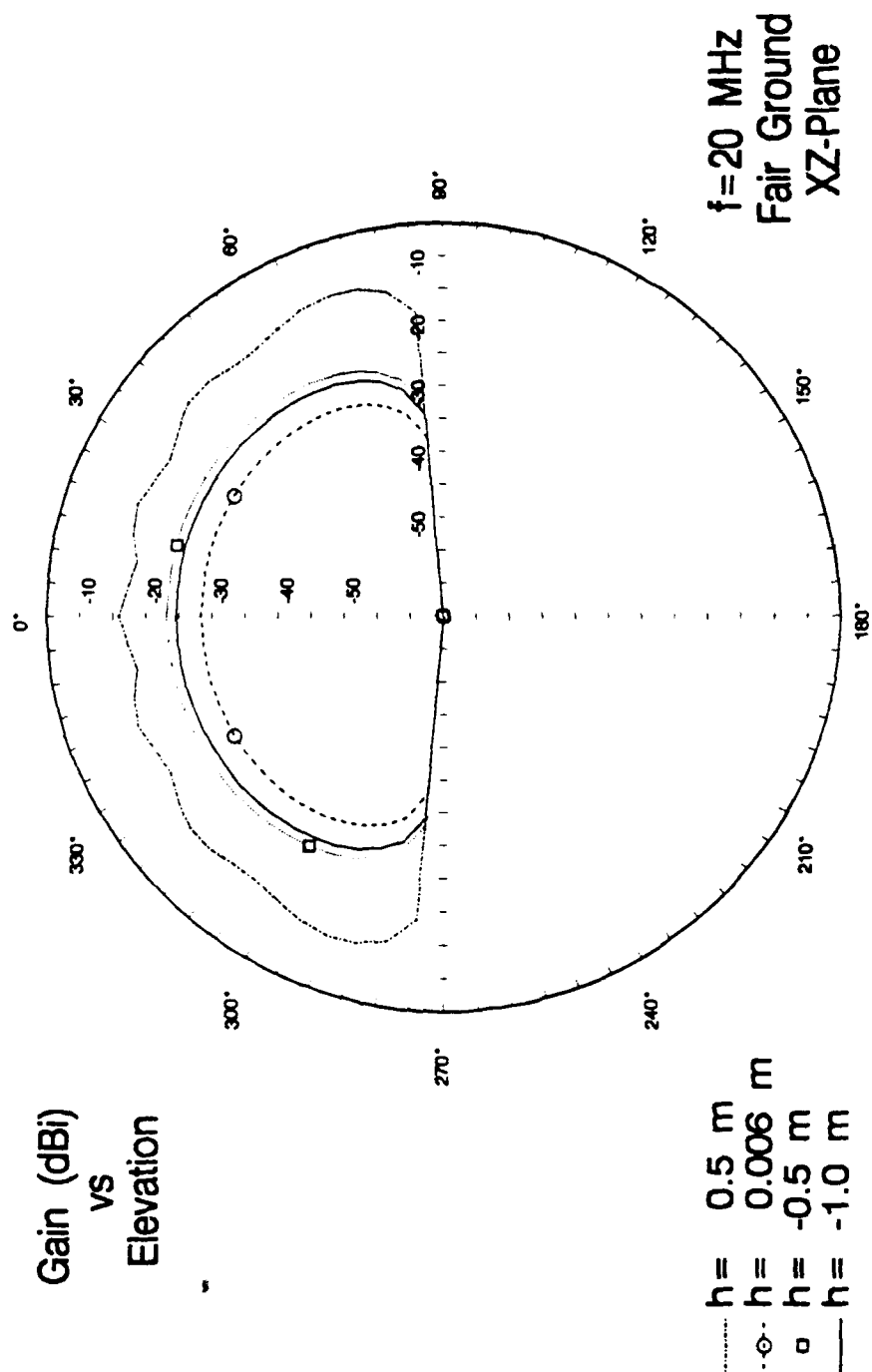


Figure 34. Elevation pattern for ELPA-302 for f=20 MHz over fair ground.

ELPA-302 Antenna

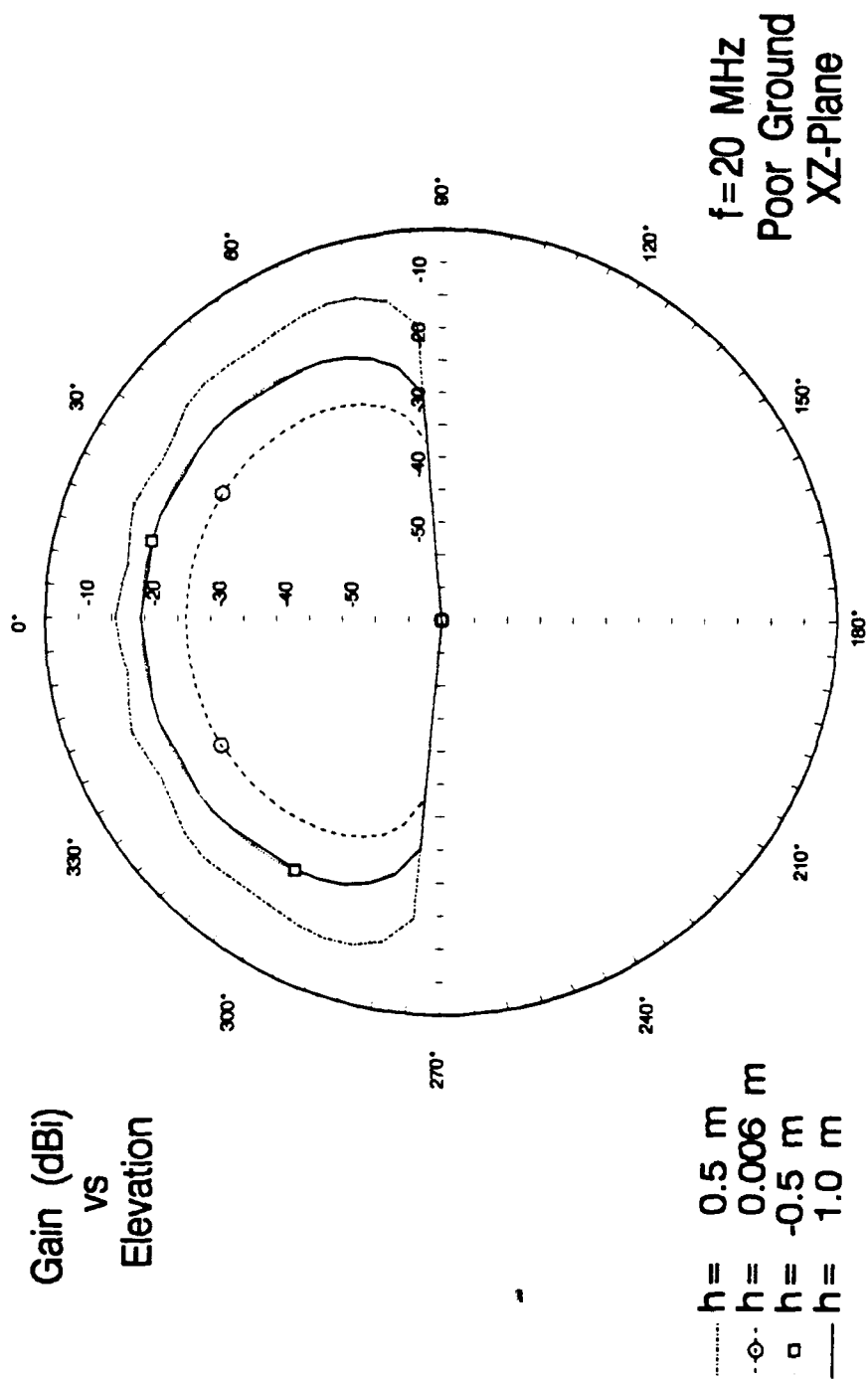


Figure 35. Elevation pattern for ELPA-302 for f=20 MHz over poor ground.

ELPA-302 Antenna

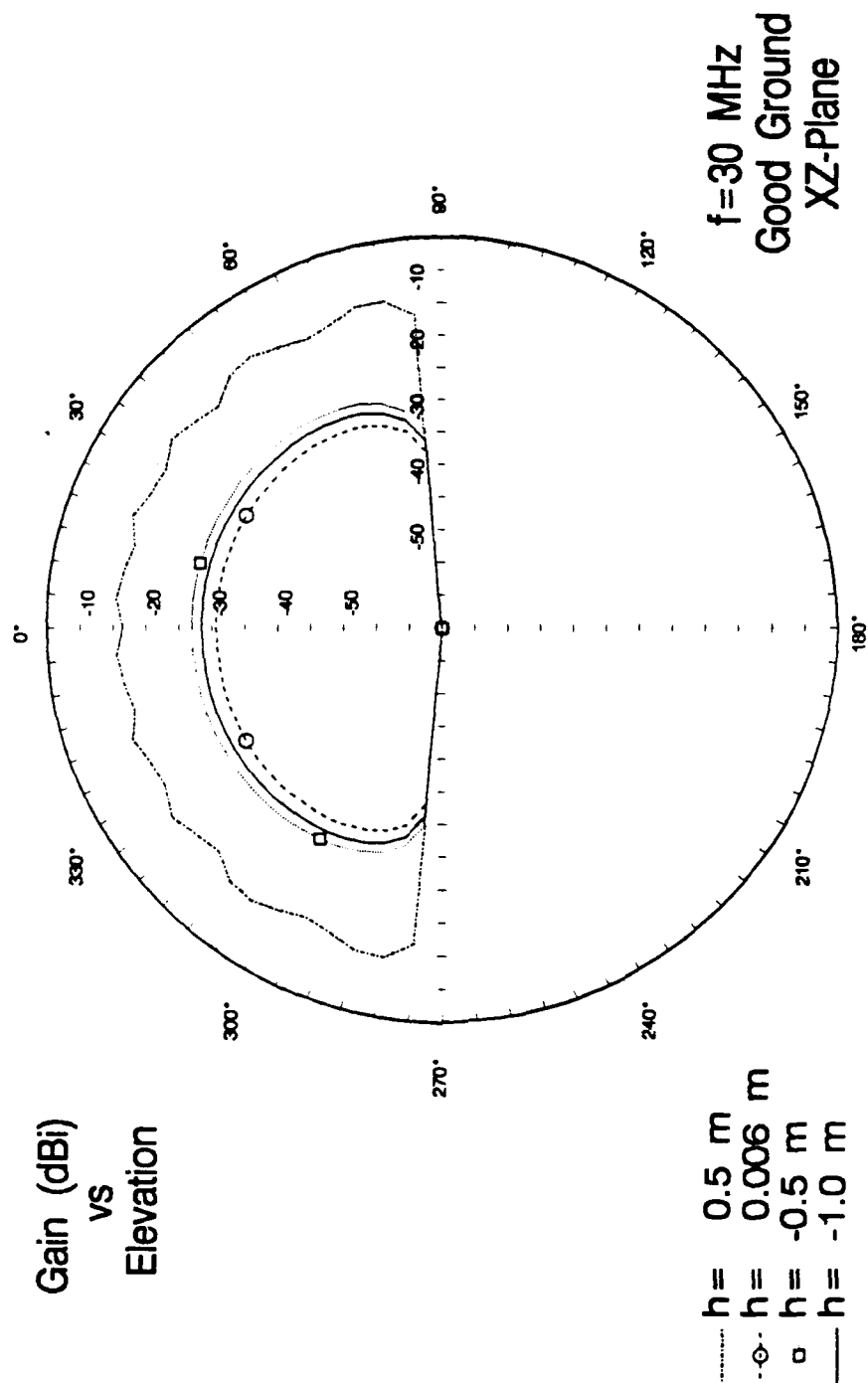


Figure 36. Elevation pattern for ELPA-302 for $f=30$ MHz over good ground.

ELPA-302 Antenna

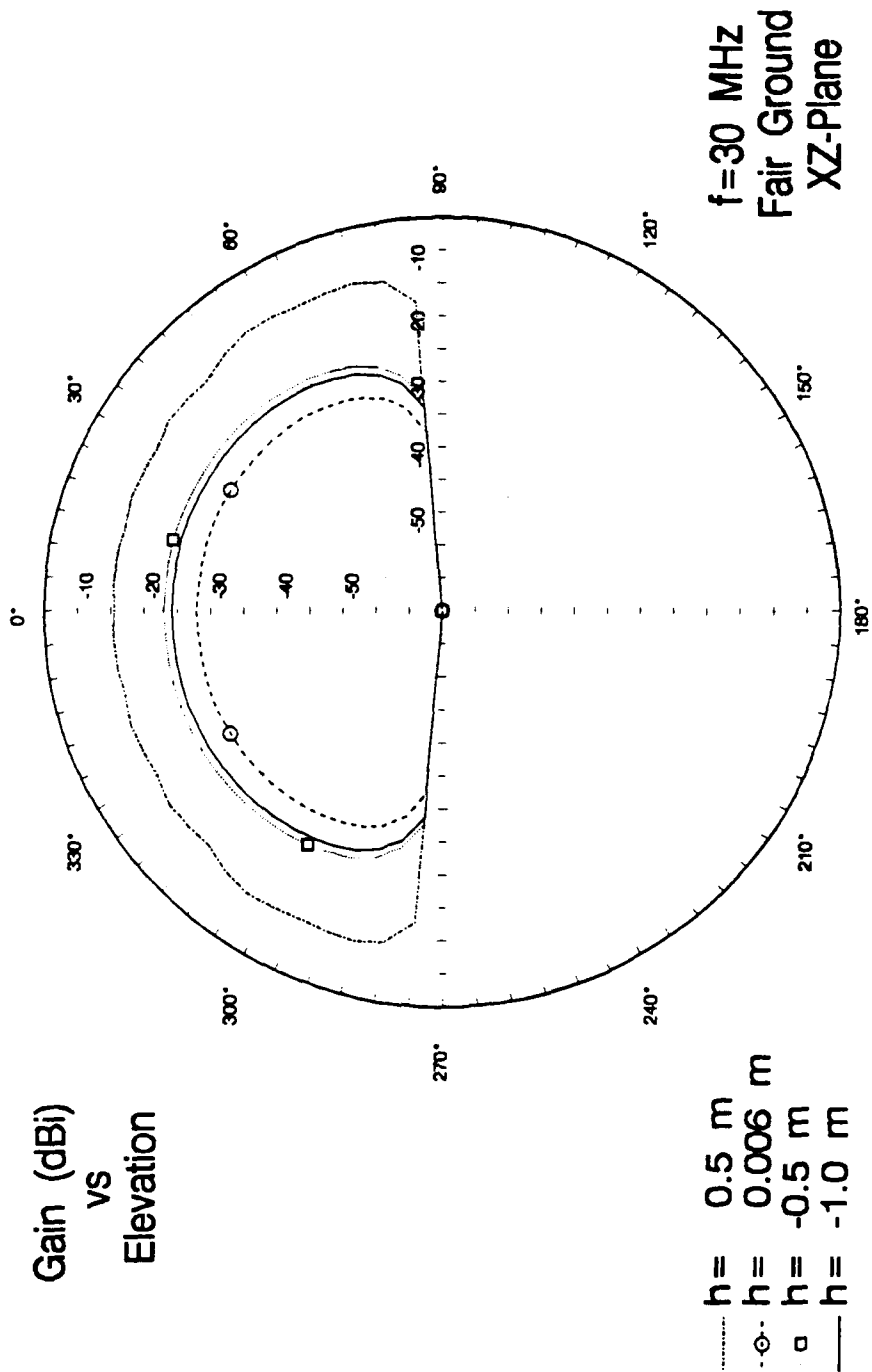


Figure 37. Elevation pattern for ELPA-302 for $f=30$ MHz over fair ground.

ELPA-302 Antenna

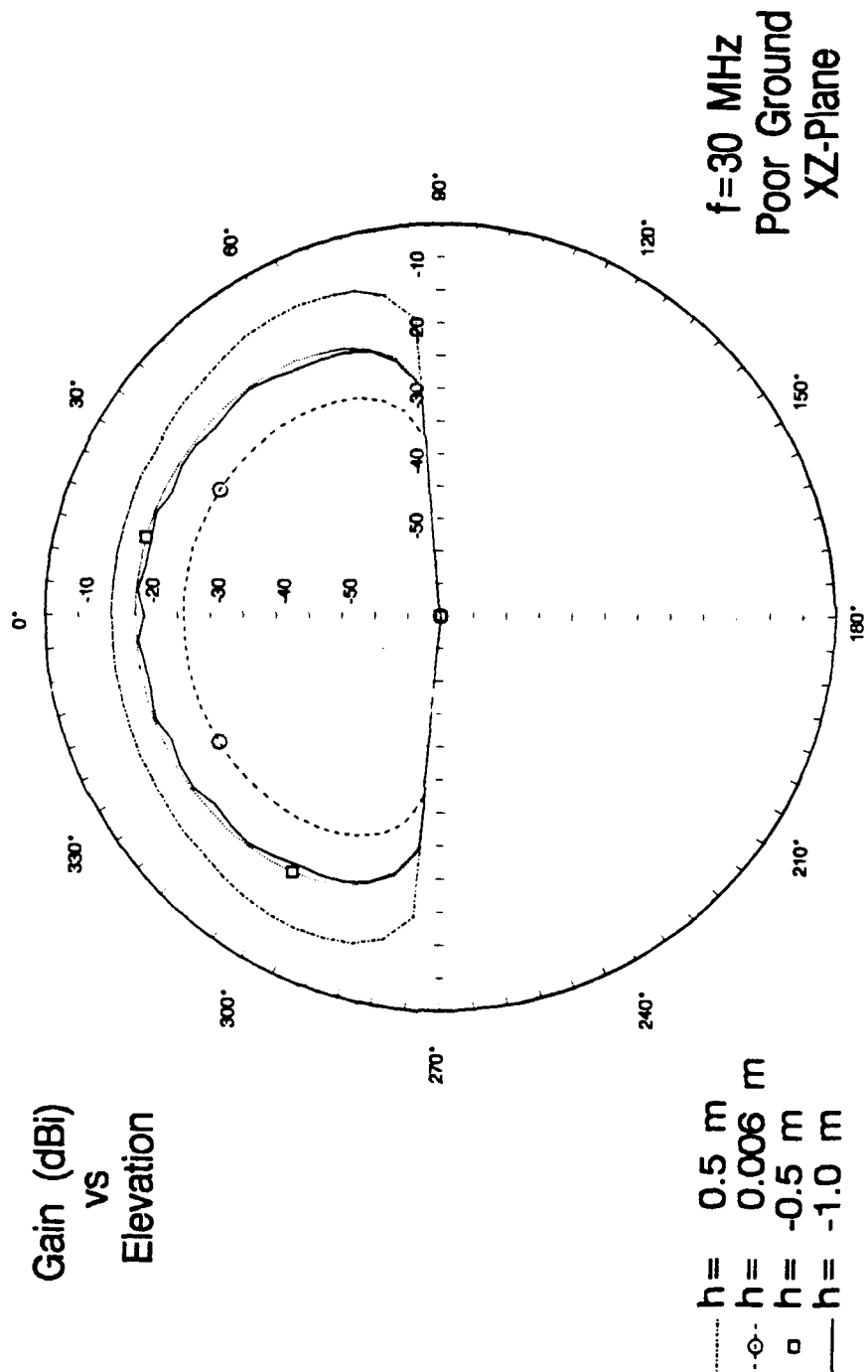


Figure 38. Elevation pattern for ELPA-302 for f=30 Mhz over poor ground.

ELPA-302 Antenna

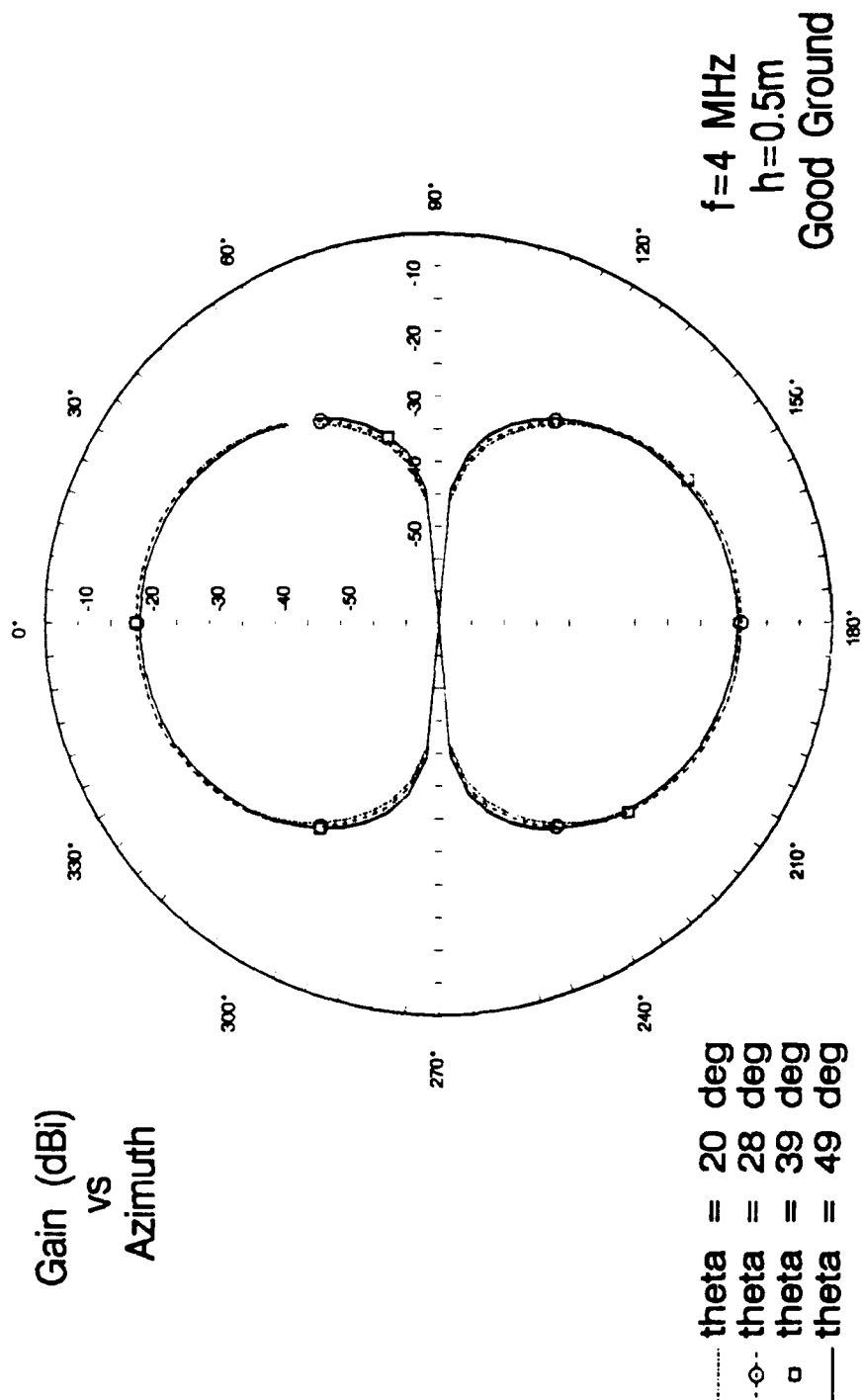


Figure 39. Azimuth pattern for ELPA-302 for f=4 MHz, h=0.5m, varying takeoff angle (theta).

ELPA-302 Antenna

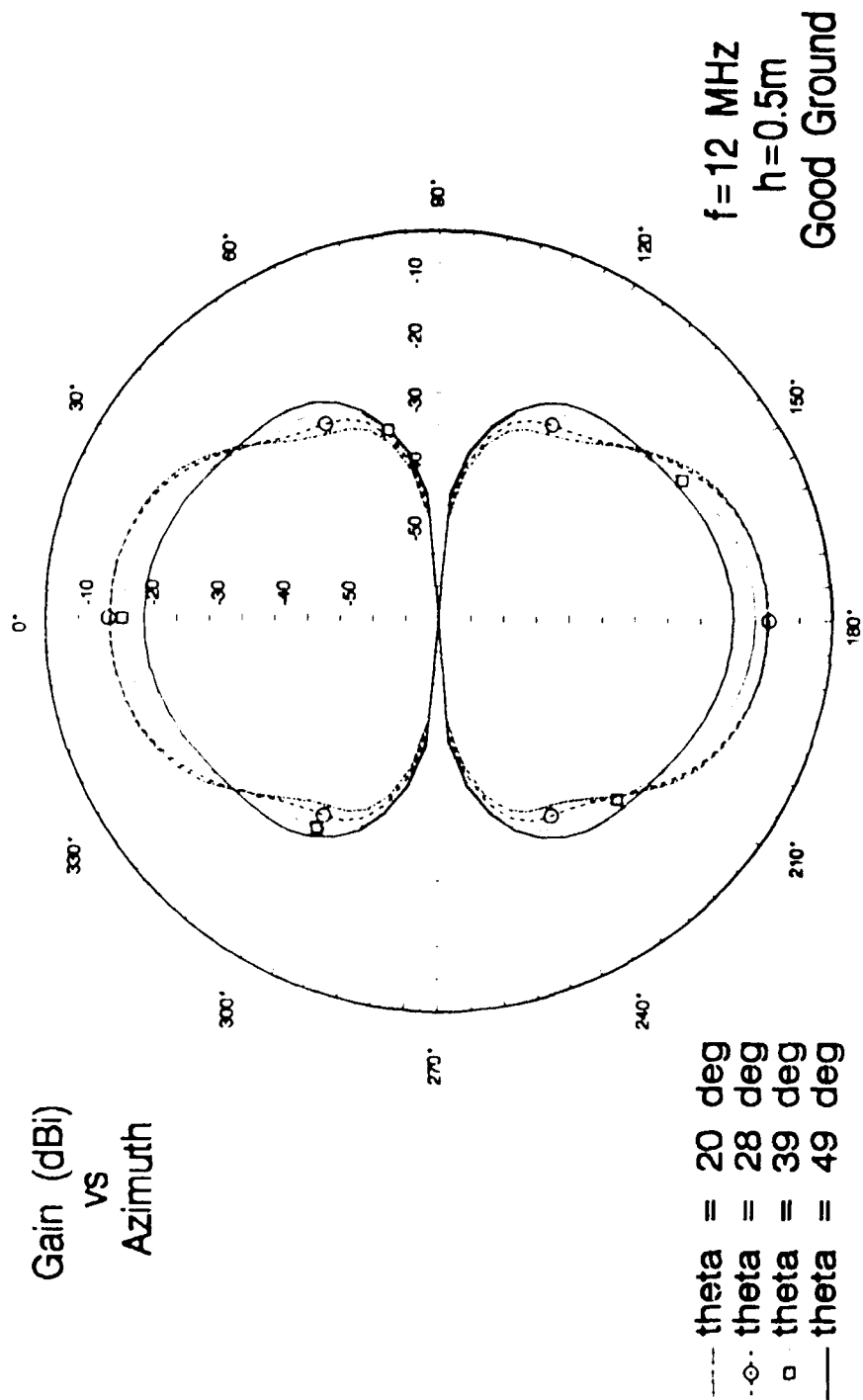


Figure 40. Azimuth pattern for ELPA-302 for $f=12\text{ MHz}$, $h=0.5\text{m}$, varying takeoff angle (θ).

ELPA-302 Antenna

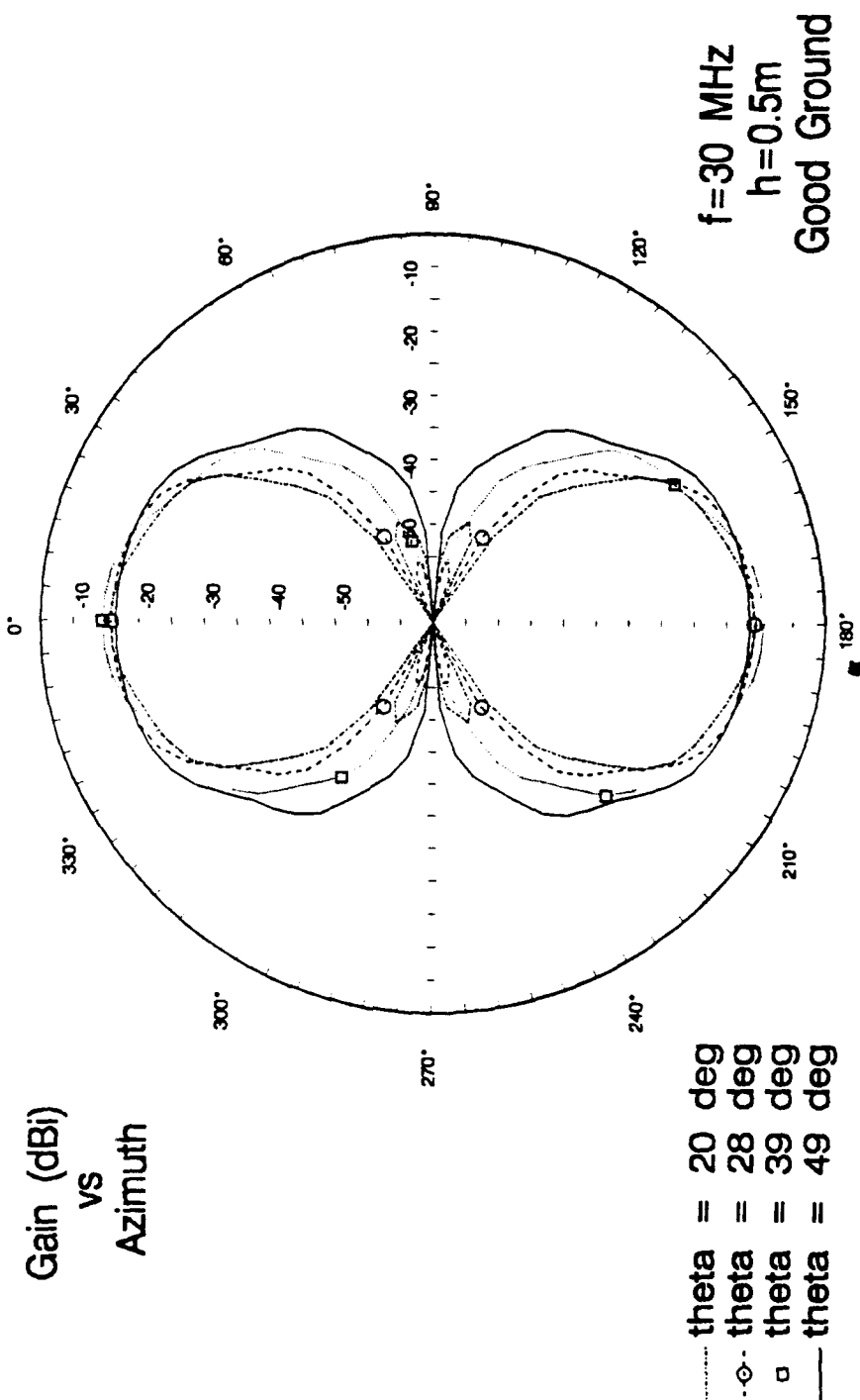


Figure 41. Azimuth pattern for ELPA-302 for f=30 MHz, h=0.5m, varying takeoff angle (theta).

ELPA-302 Antenna

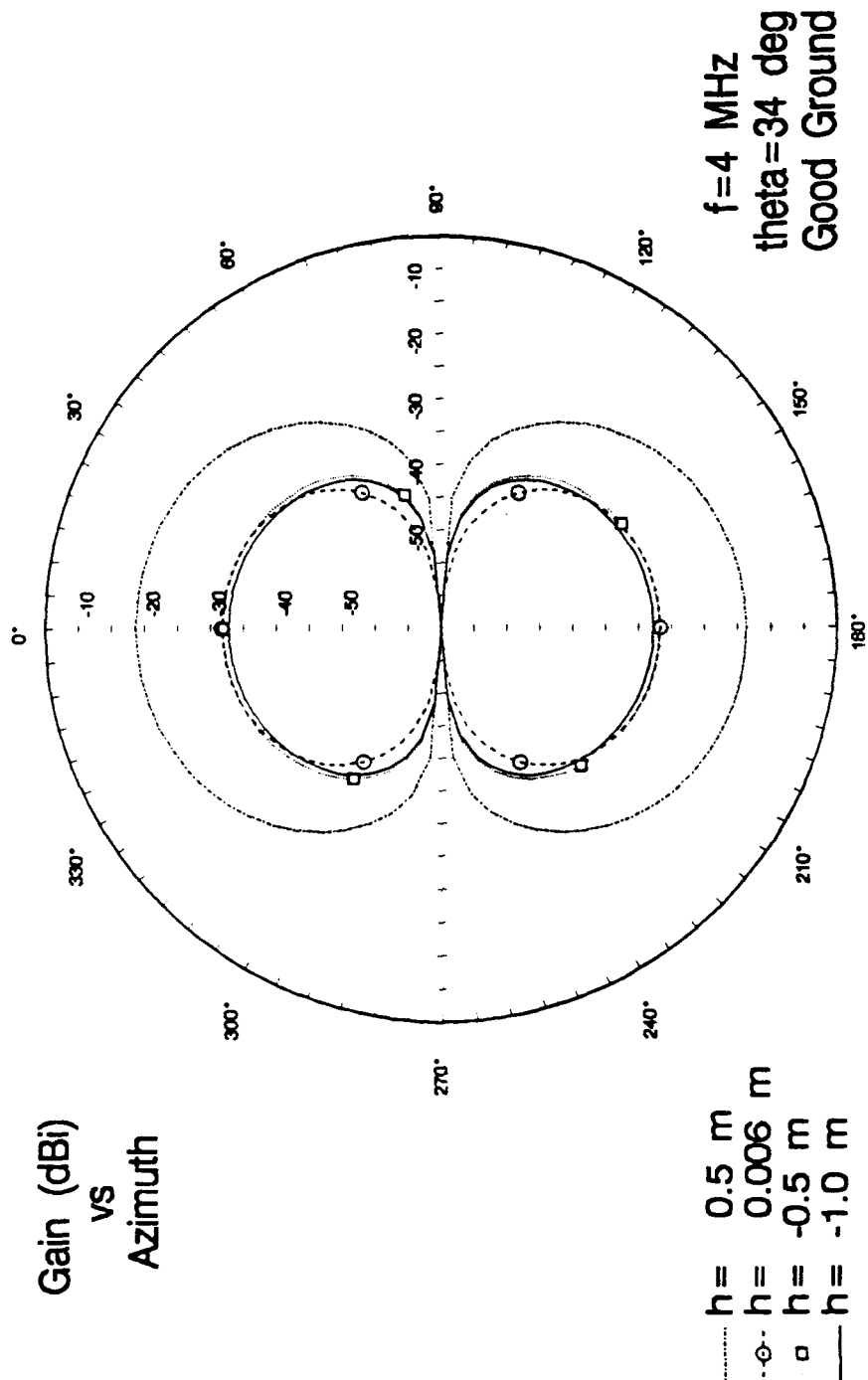


Figure 42. Azimuth pattern for ELPA-302 for $f=4$ MHz, constant takeoff angle (θ), varying heights.

ELPA-302 Antenna

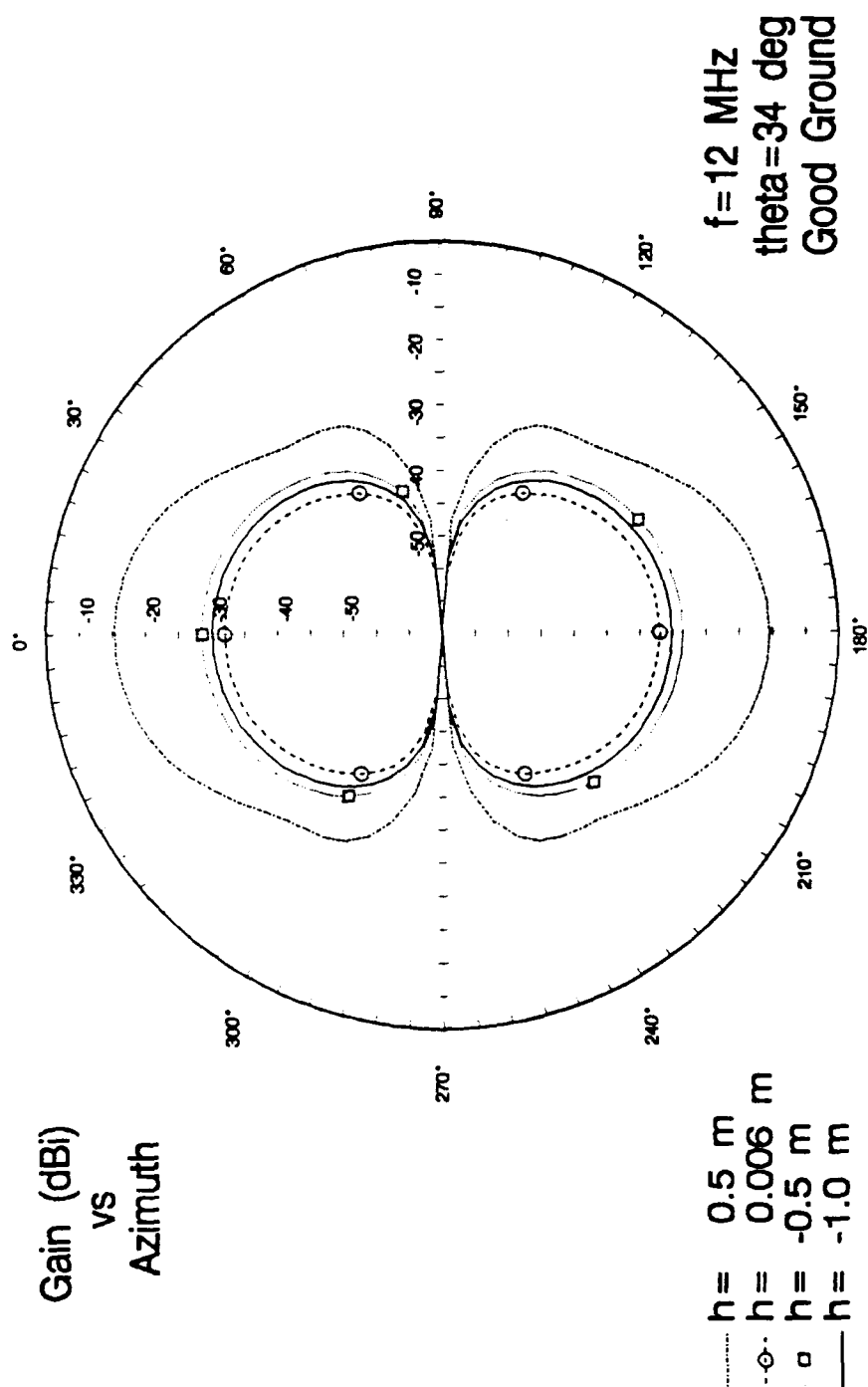


Figure 43. Azimuth pattern for ELPA-302 for $f=12$ MHz, constant takeoff angle (θ), varying heights.

ELPA-302 Antenna

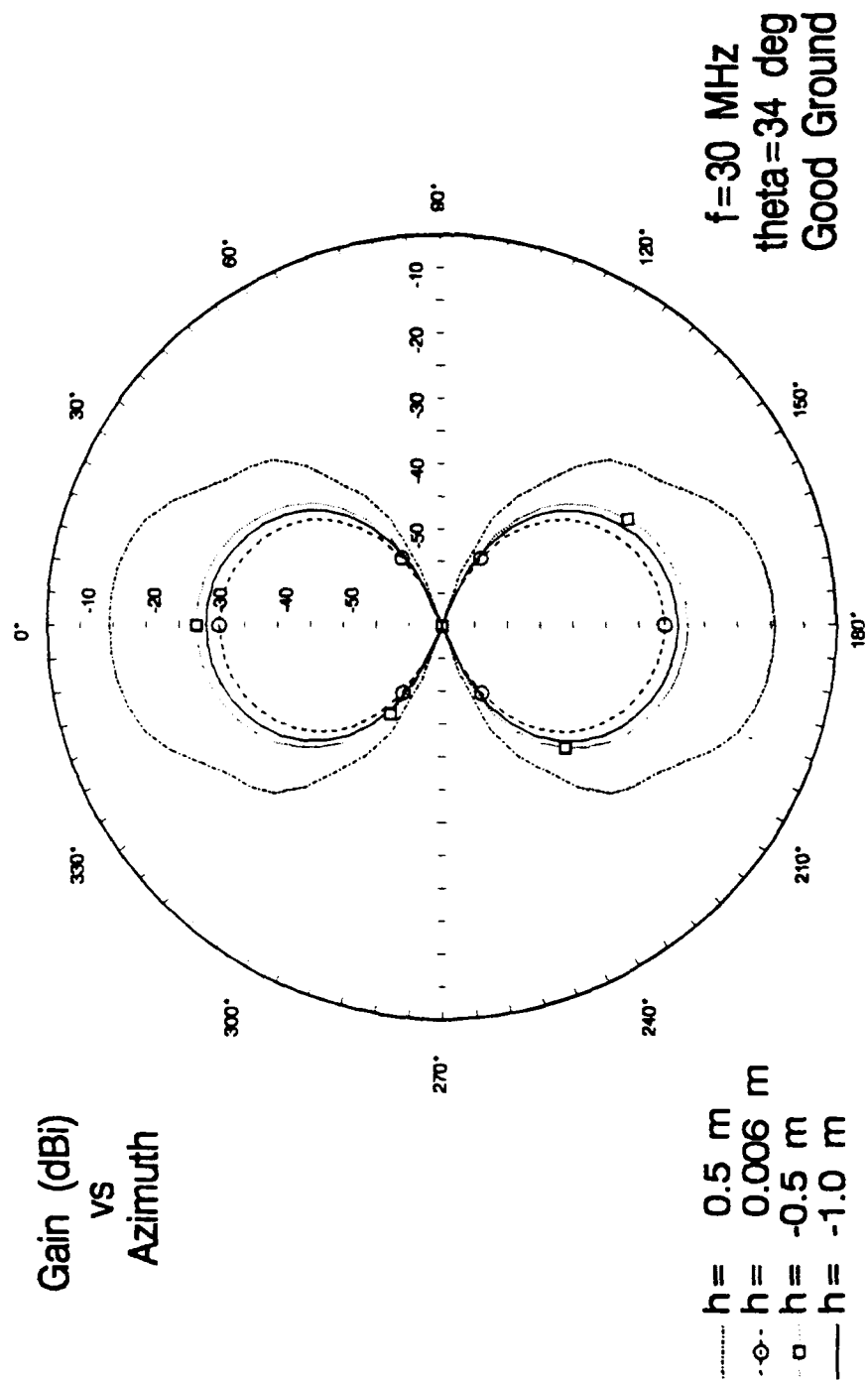


Figure 44. Azimuth pattern for ELPA-302 for $f=30$ MHz, constant takeoff angle (θ), varying heights.

show a maximum gain of -16 dB at 2 Mhz for $h = 0.5$ meters over poor ground. The patterns illustrate that changes in height and ground condition have a great effect on antenna gain.

For all ground conditions, a height of 0.5 meters provides optimal gain at the desired takeoff angles while the buried antennas have approximately 12 dB less gain. The buried antennas, however, have an increase in gain as ground conditions degrade. One explanation for this can be related to image theory. As the ground becomes more lossy, the distance between the image plane and the antenna increases. This allows for more constructive addition of the transmitted and reflected wave. If the image plane was exactly $\lambda/4$ distance from the antenna, then constructive interference would be at a maximum. In poor ground, the image plane to antenna distance is closer to $\lambda/4$ than in good ground. [Ref. 1] A height of 0.5 meters provides optimal gain at the desired takeoff angles.

Azimuth patterns for the ELPA-302, shown in Figures 35 through 41, were modeled in two ways. First, the height was kept constant at 0.5 m (the height which provided the highest gain) and the takeoff angle was varied to illustrate the change in azimuthal gain versus takeoff angle. Next, the takeoff angle was held constant at 34 degrees, a median value, and the height above ground was varied to illustrate the change in azimuthal gain versus height.

The VSWR and various radiation patterns agree with those

in Reference 2, which lends validity to the results obtained here.

D. HORIZONTAL DIPOLE MODEL

The horizontal dipole is an omni-directional antenna designed primarily for HF skywave propagation. It consists of two wires of equal length connected via a balun to a transmission line as illustrated in Figure 45. The horizontal dipole modeled is not terminated because, in some tactical environments, trimming and terminating antennas is not always practical. The overall characteristics of the horizontal dipole are similar to those of the ELPA-302, but with some exceptions that will be discussed later. PAT7 was used to model this antenna.

The VSWR for the horizontal dipole was taken for good and poor ground conditions at each height and is illustrated in Figures 46 and 47. For good ground, the VSWR is not significantly affected by changes in height. For poor ground, the VSWR is relatively constant for heights above ground but significantly lower for heights below ground. The comments on the ELPA-302 also apply to the horizontal dipole with respect to electrical effects of the ground.

Antenna radiation patterns for the horizontal dipole are illustrated in Figures 48 through 71. Each figure shows the pattern for fixed ground conditions for heights of 0.5 meters, 0.006 meters, -0.5 meters, and -1.0 meters. The patterns are

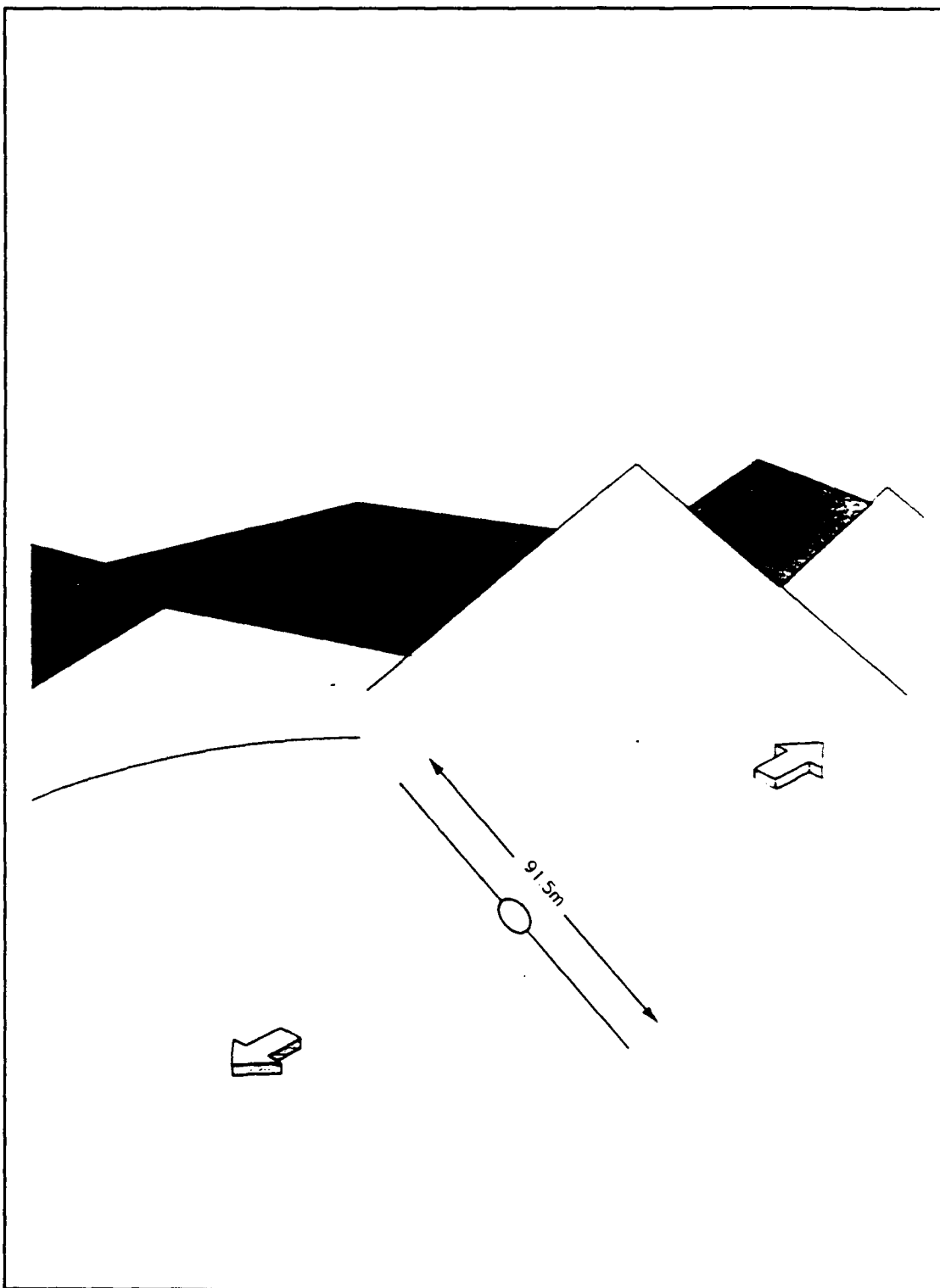


Figure 45. Horizontal Dipole.

Horizontal Dipole

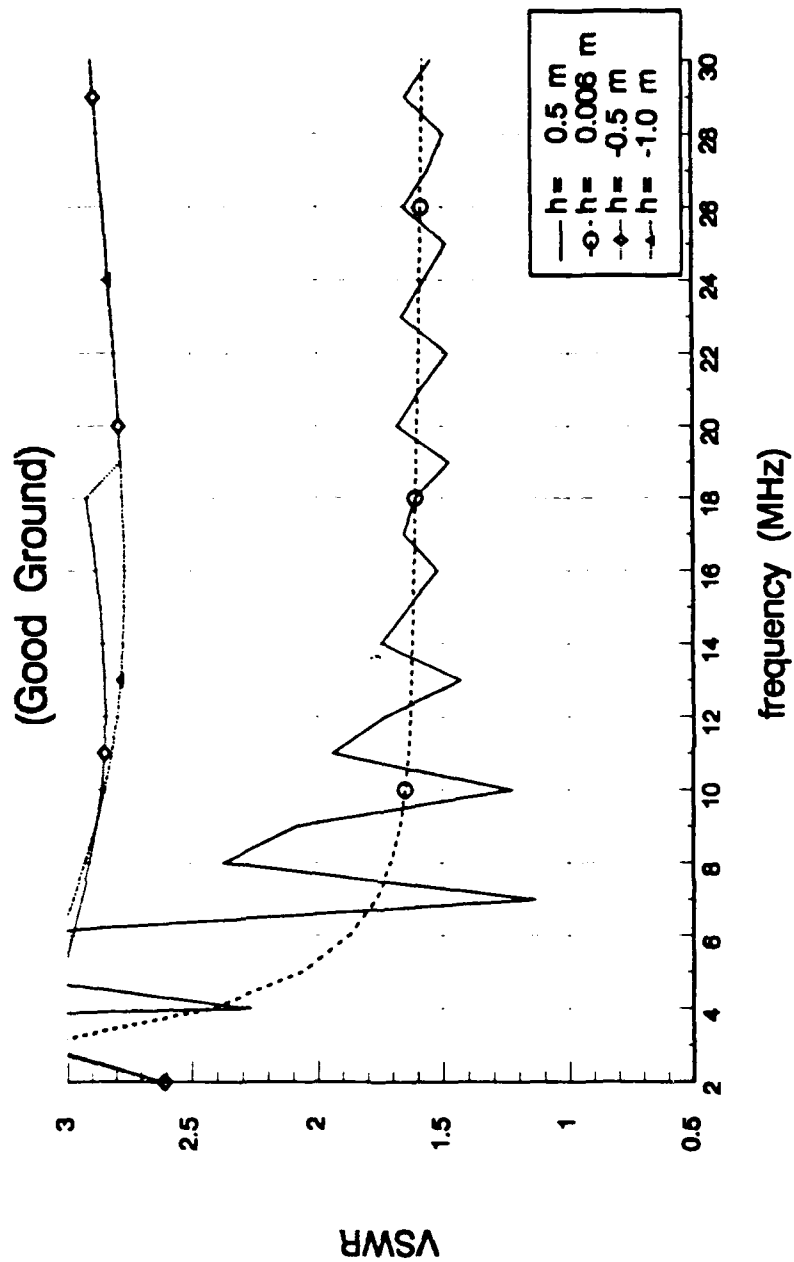


Figure 46. VSWR for horizontal dipole for varying heights over good ground.

Horizontal Dipole

(Poor Ground)

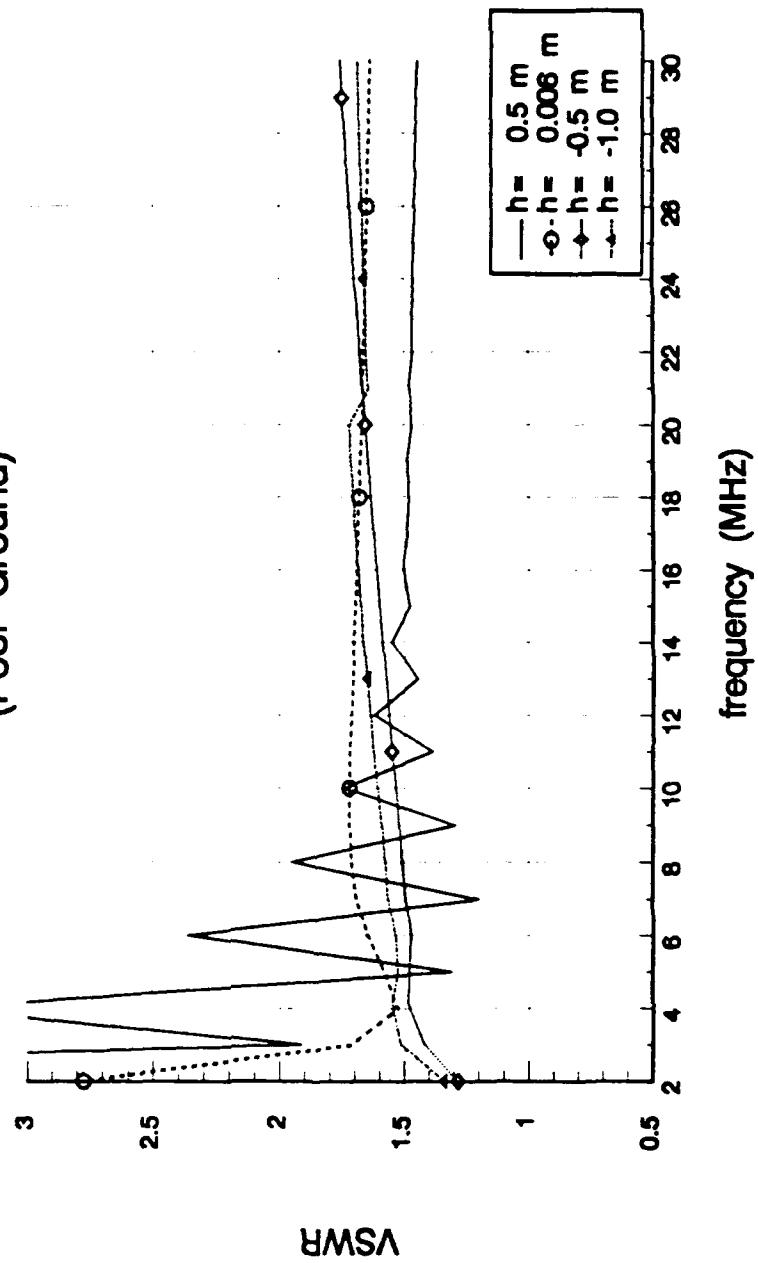


Figure 47. VSWR for horizontal dipole for varying heights over poor ground.

Horizontal Dipole

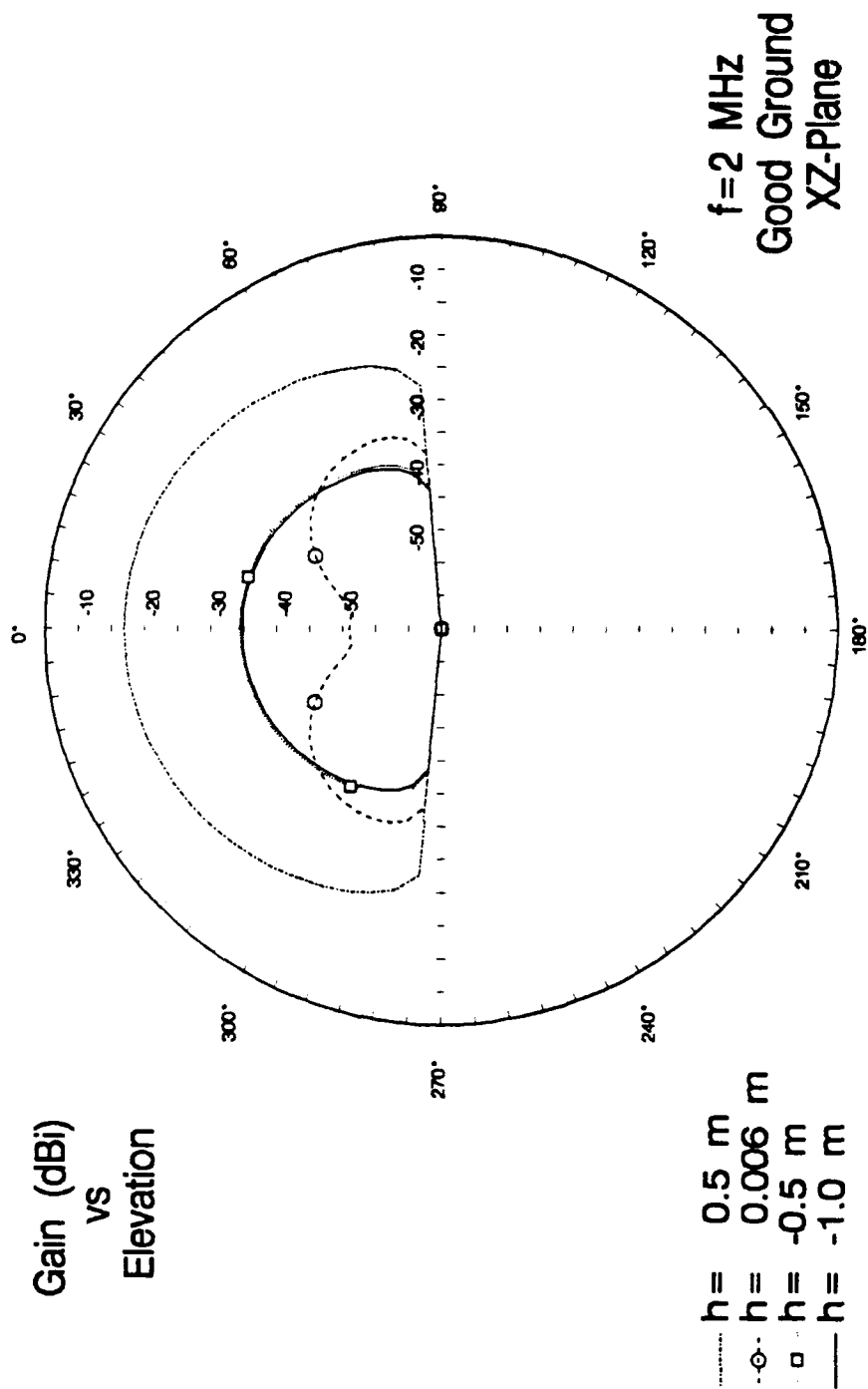


Figure 48. Elevation pattern for horizontal dipole for $f=2$ MHz over good ground.

Horizontal Dipole

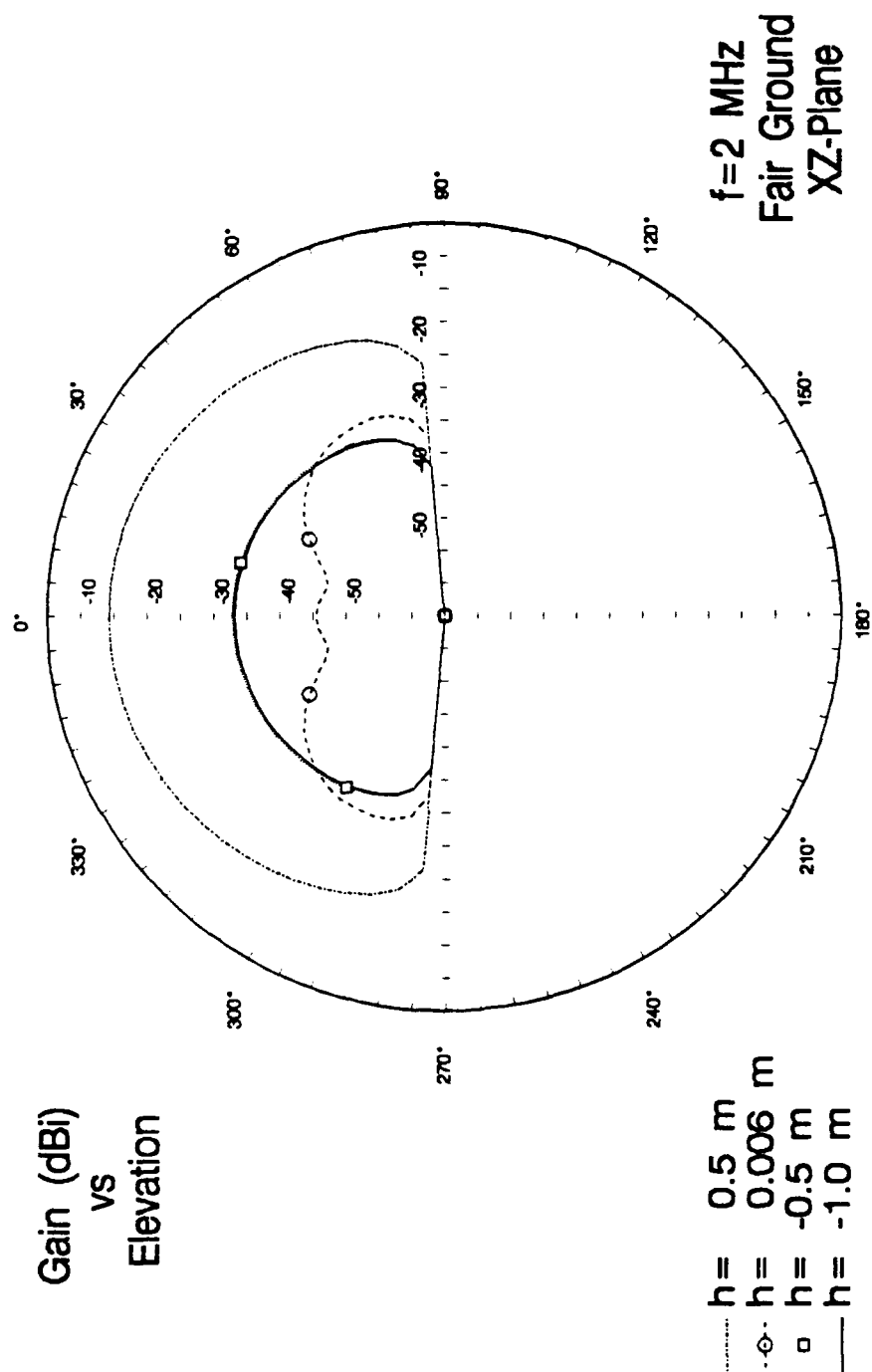


Figure 49. Elevation pattern for horizontal dipole fro $f=2$ MHz over fair ground.

Horizontal Dipole

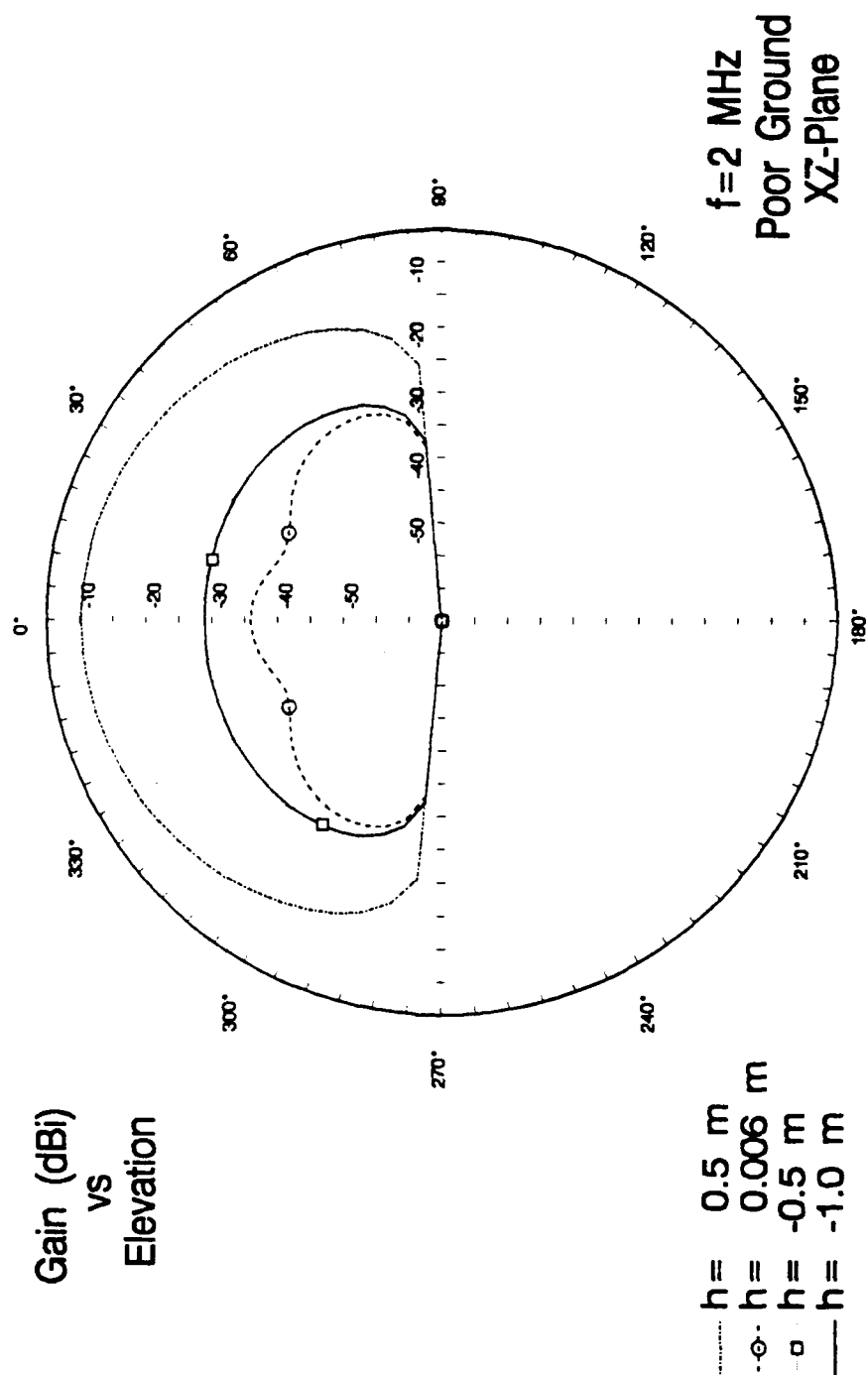


Figure 50. Elevation pattern for horizontal dipole for $f=2$ MHz over poor ground.

Horizontal Dipole

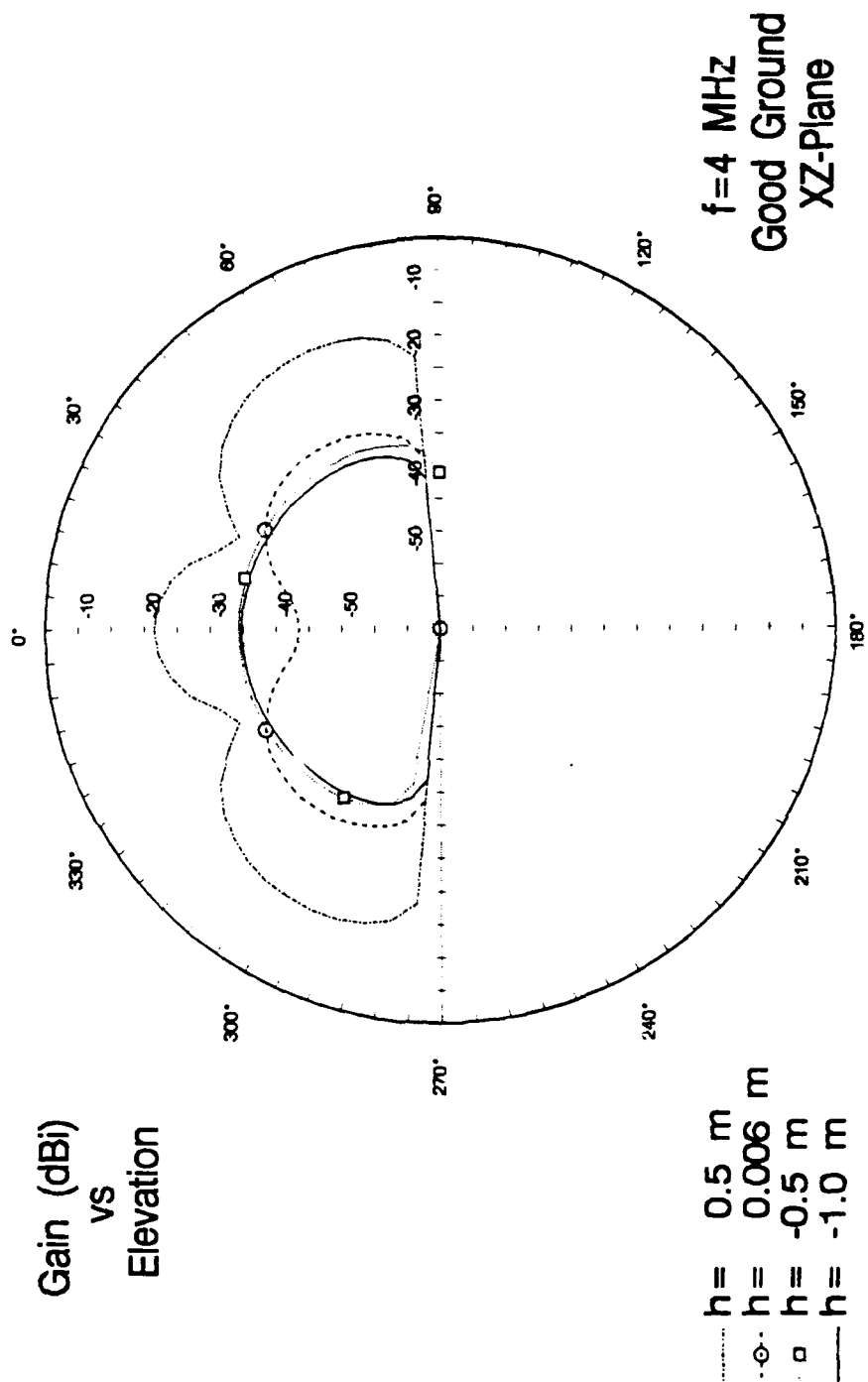


Figure 51. Elevation pattern for horizontal dipole for $f=4$ MHz over good ground.

Horizontal Dipole

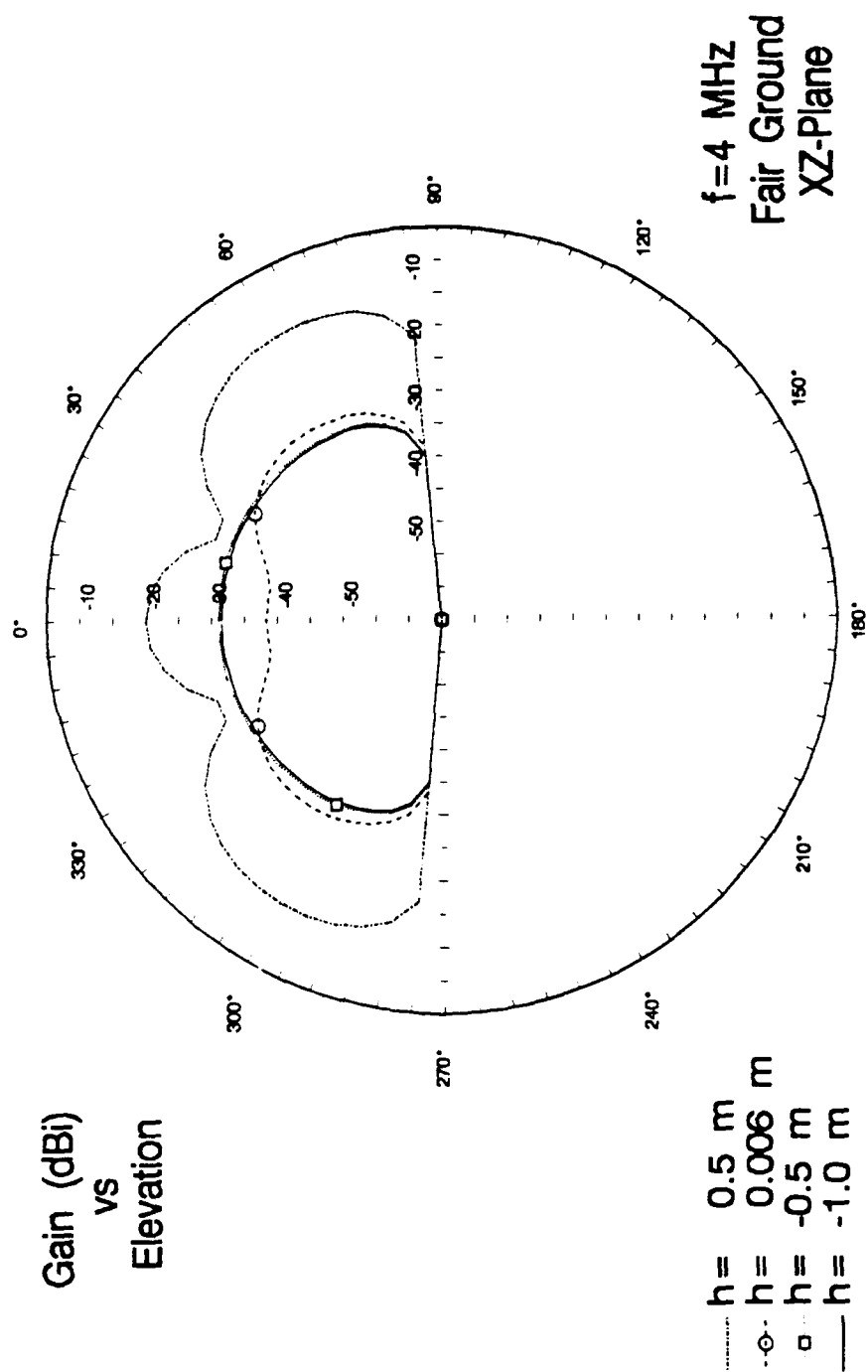


Figure 52. Elevation pattern for horizontal dipole for $f=4$ MHz over fair ground.

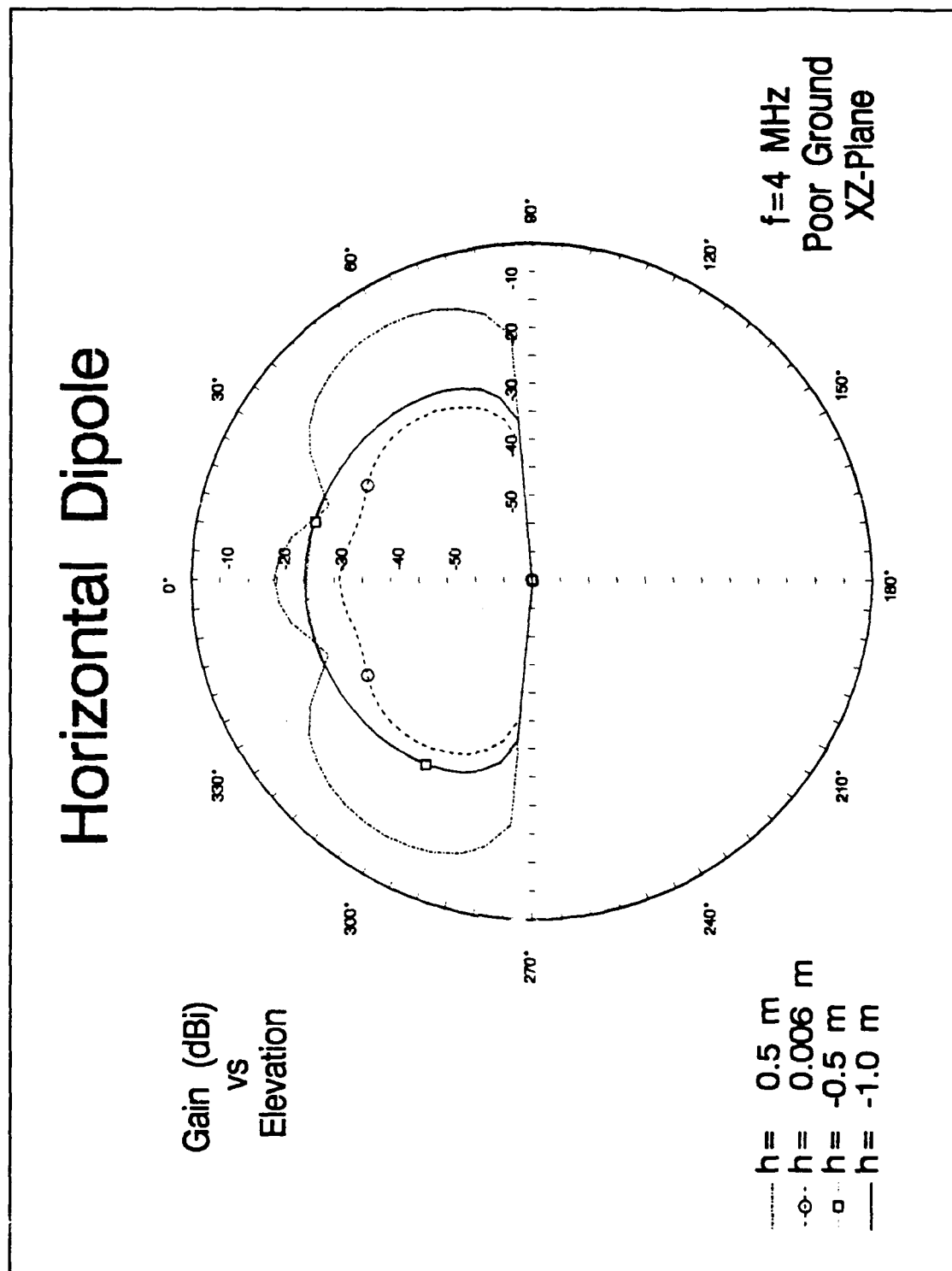


Figure 53. Elevation pattern for horizontal dipole for $f=4$ MHz over poor ground.

Horizontal Dipole

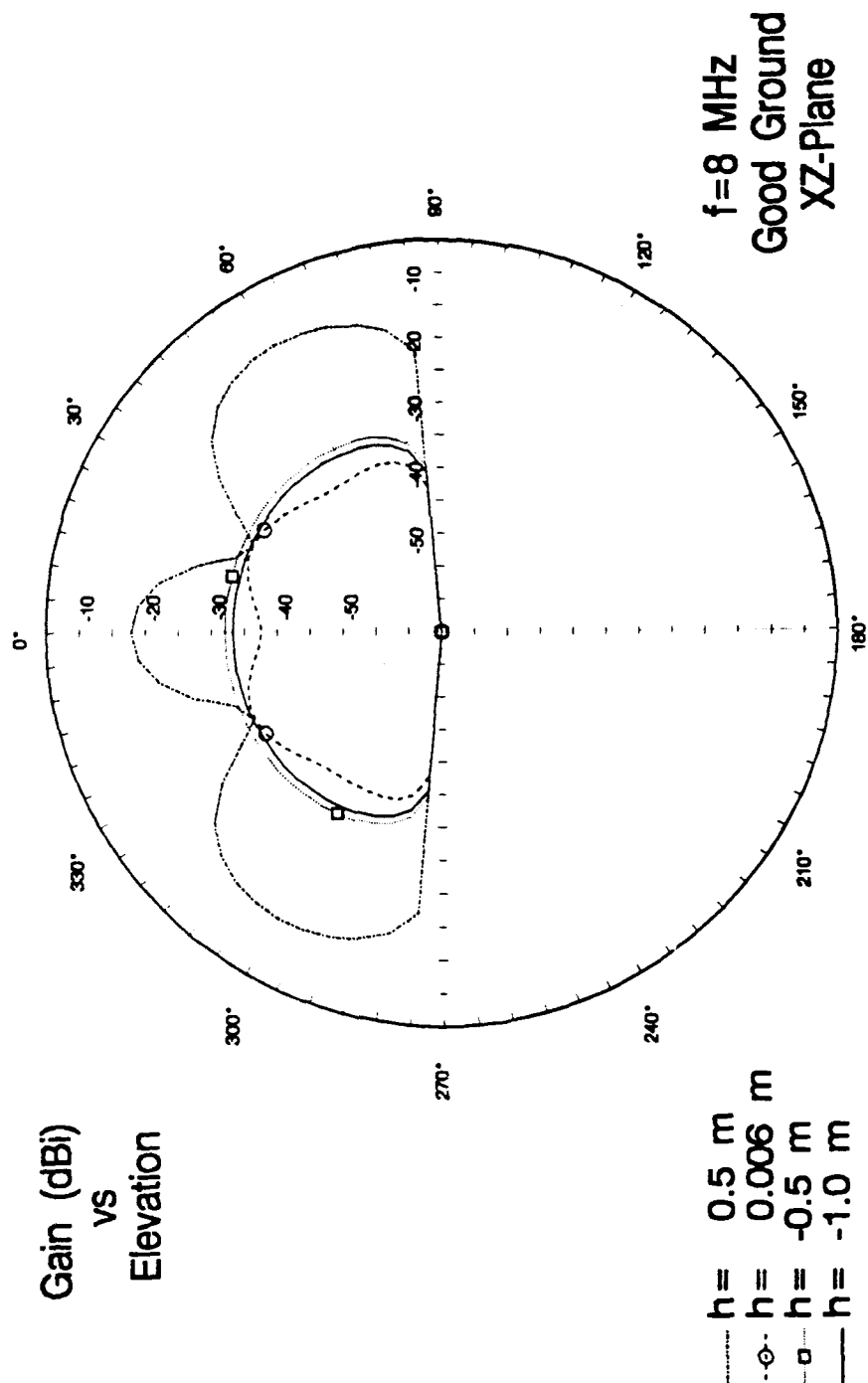


Figure 54. Elevation pattern for horizontal dipole for f=8 MHz over good ground.

Horizontal Dipole

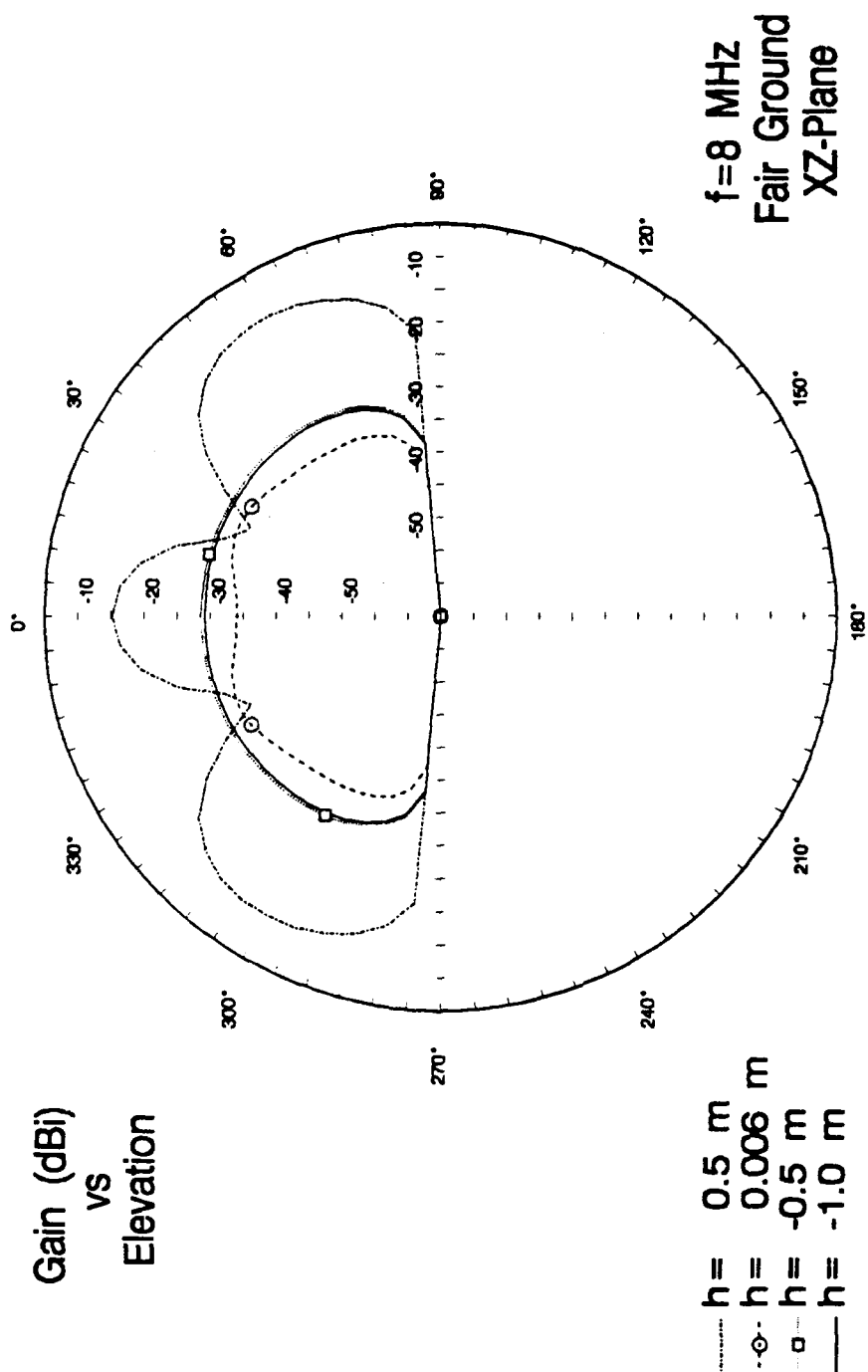


Figure 55. Elevation pattern for horizontal dipole for $f=8$ MHz over fair ground.

Horizontal Dipole

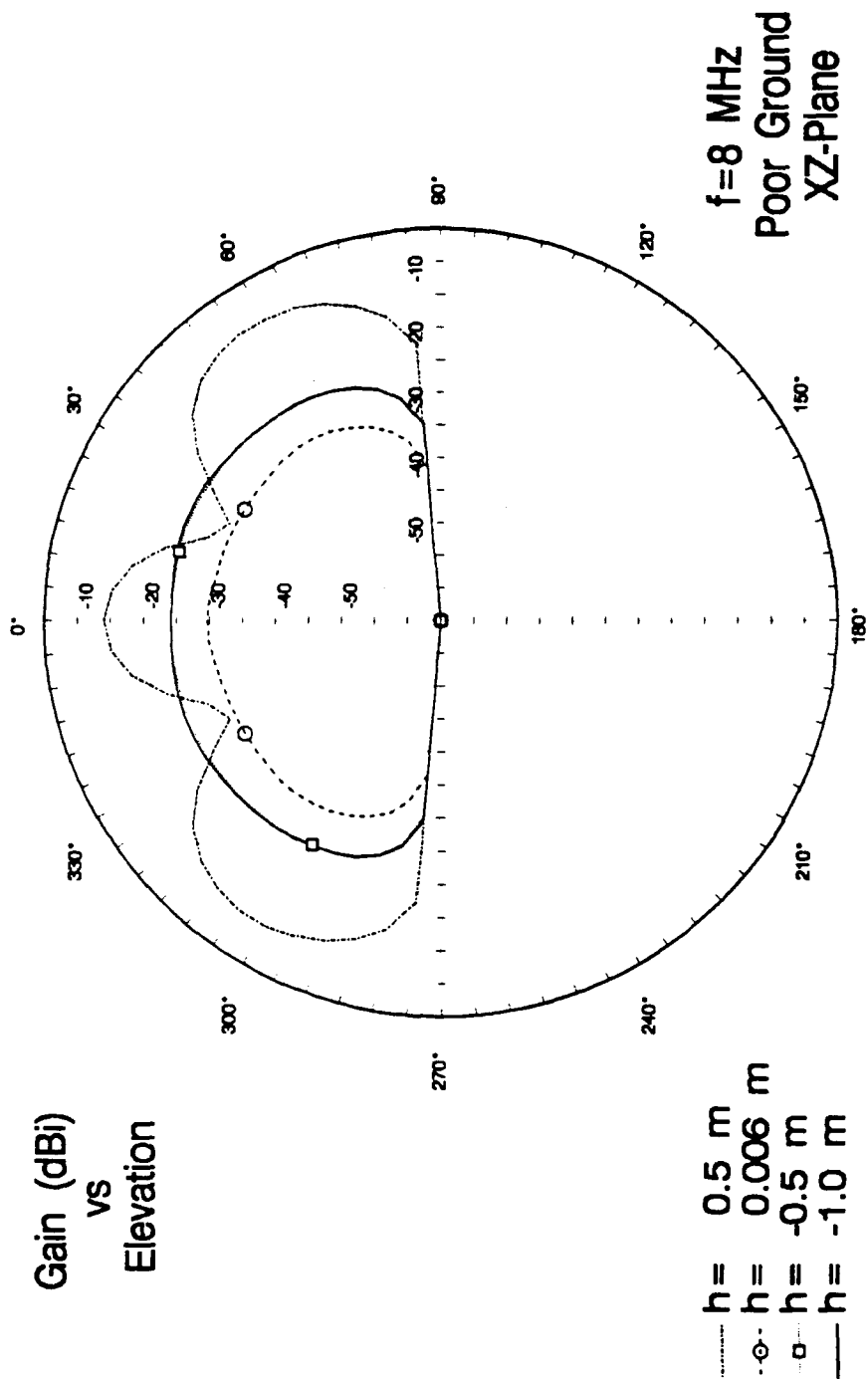


Figure 56. Elevation pattern for horizontal dipole for $f=8$ MHz over poor ground.

Horizontal Dipole

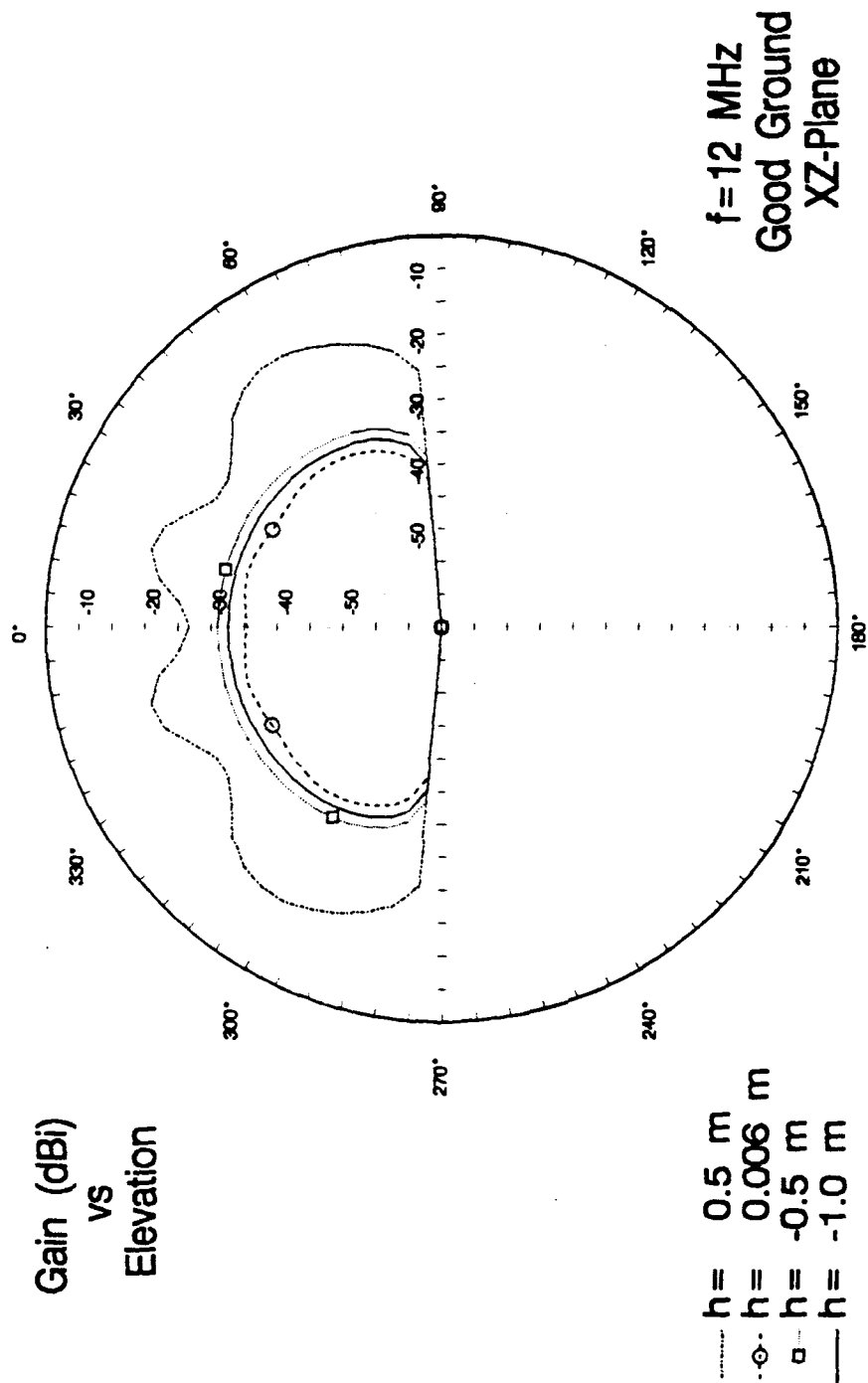


Figure 57. Elevation pattern for horizontal dipole for $f=12$ MHz over good ground.

Horizontal Dipole

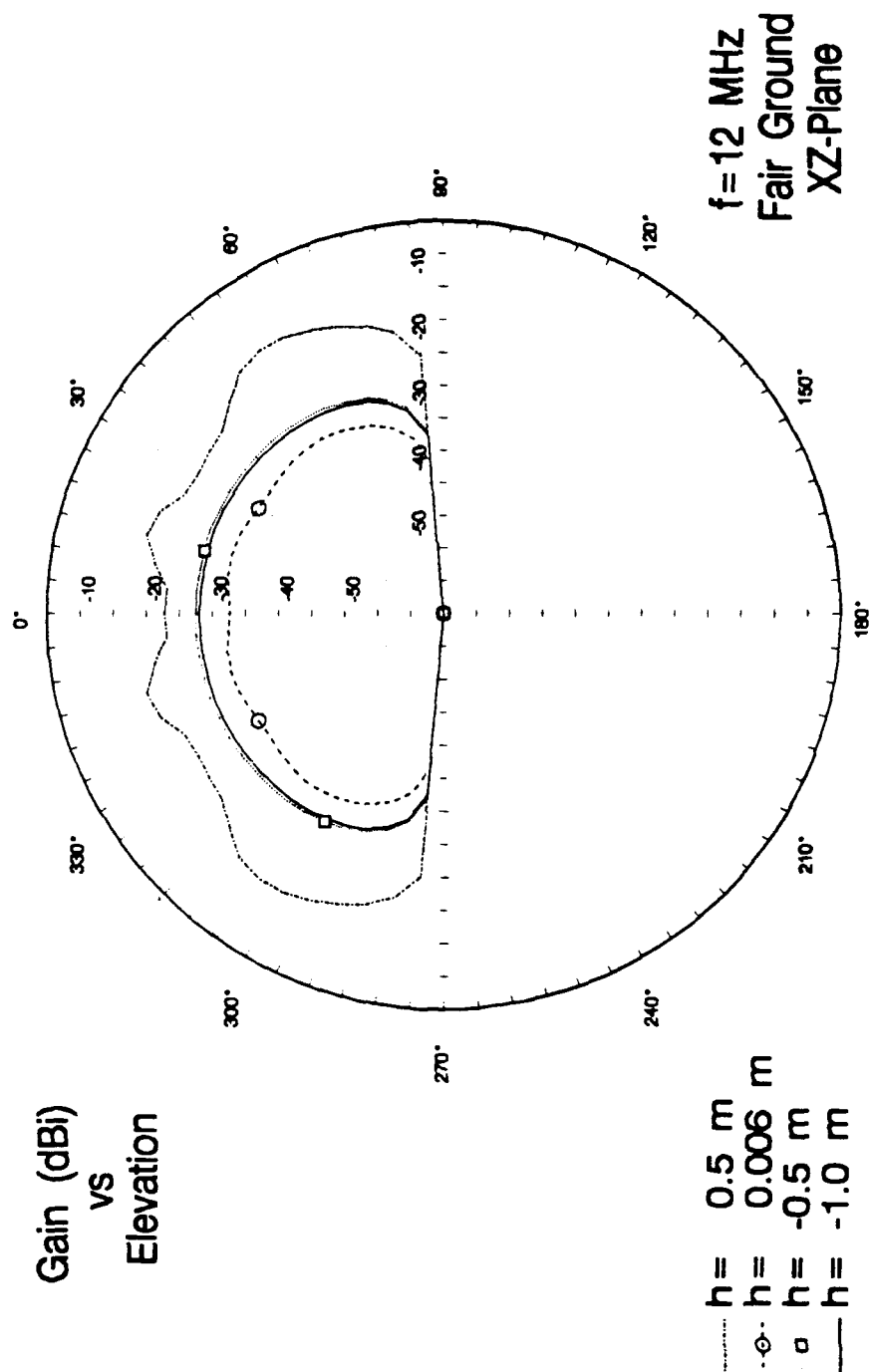


Figure 58. Elevation pattern for horizontal dipole for $f=12$ MHz over fair ground.

Horizontal Dipole

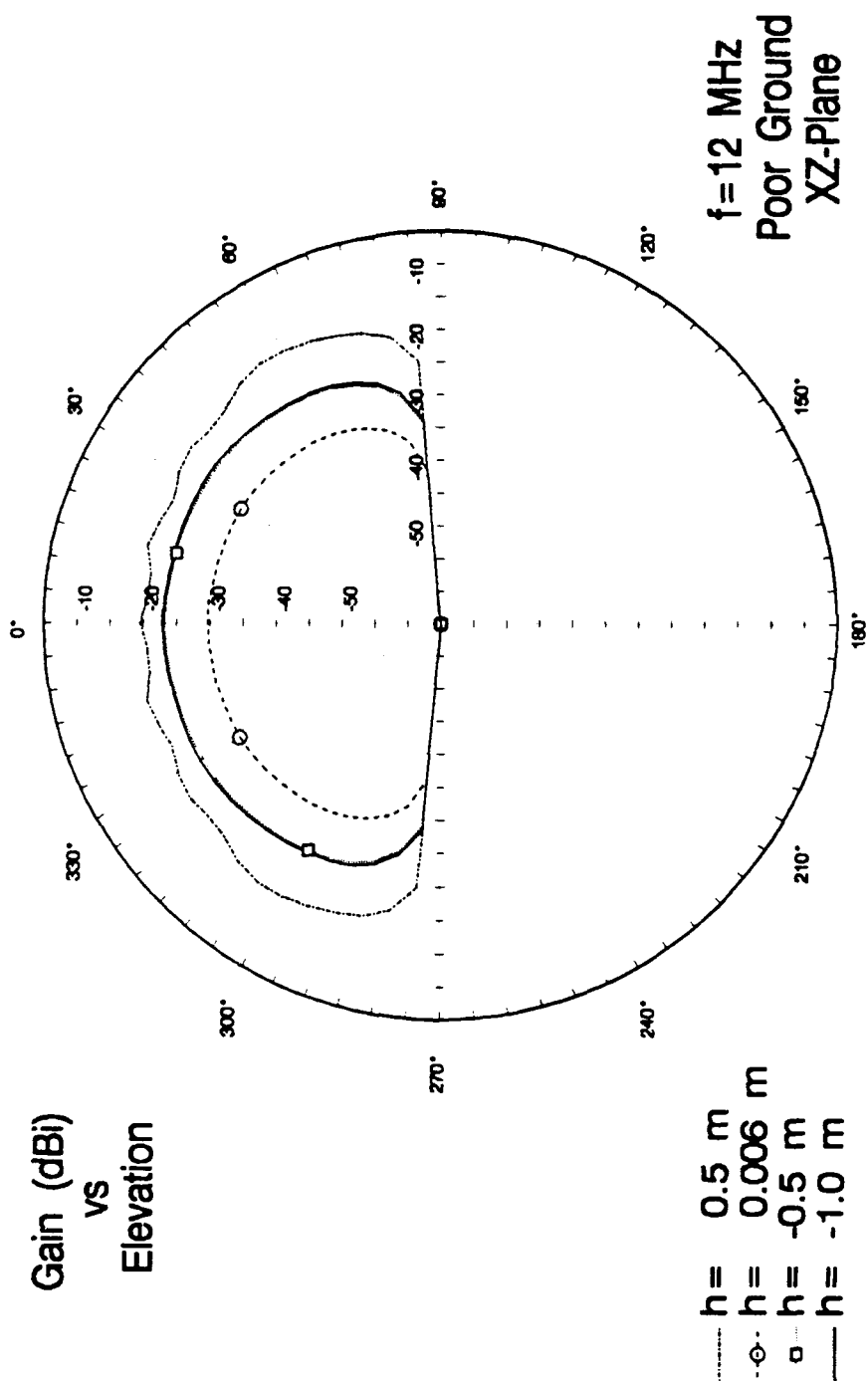
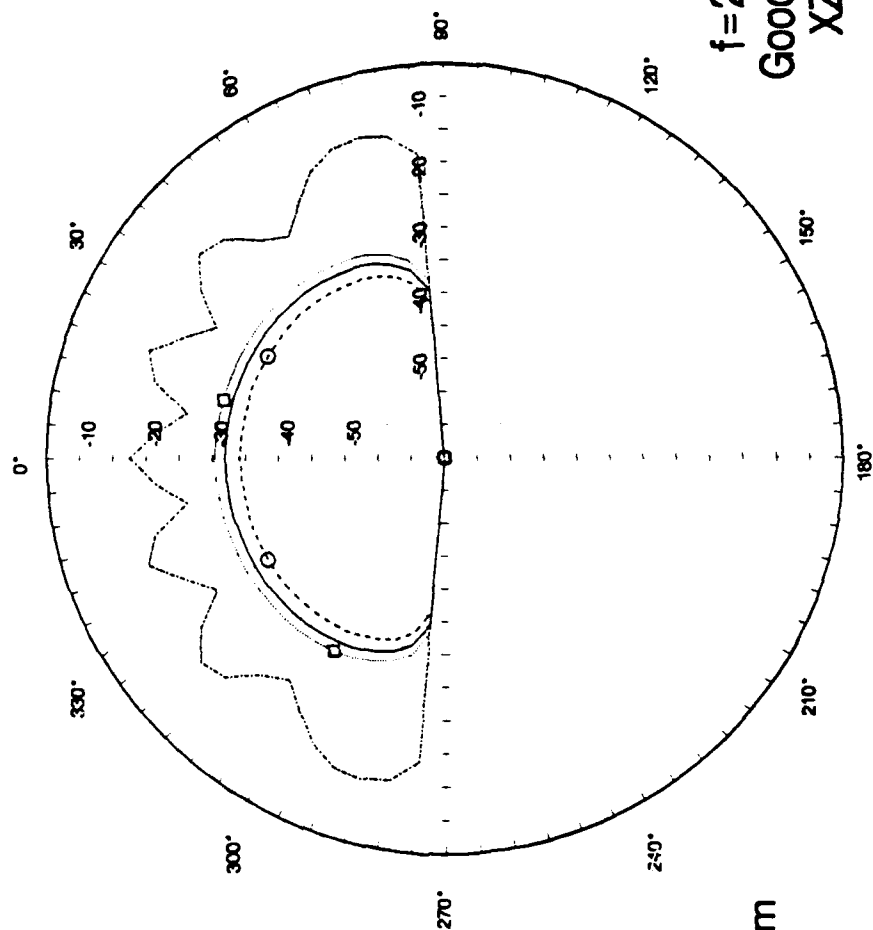


Figure 59. Elevation pattern for horizontal dipole for $f=12$ MHz over poor ground.

Horizontal Dipole

Gain (dBi)
vs
Elevation



$f = 20$ MHz
Good Ground
XZ-Plane

$h = 0.5$ m
 $h = 0.006$ m
 $h = -0.5$ m
 $h = -1.0$ m

Figure 60. Elevation pattern for horizontal dipole for $f=20$ MHz over good ground.

Horizontal Dipole

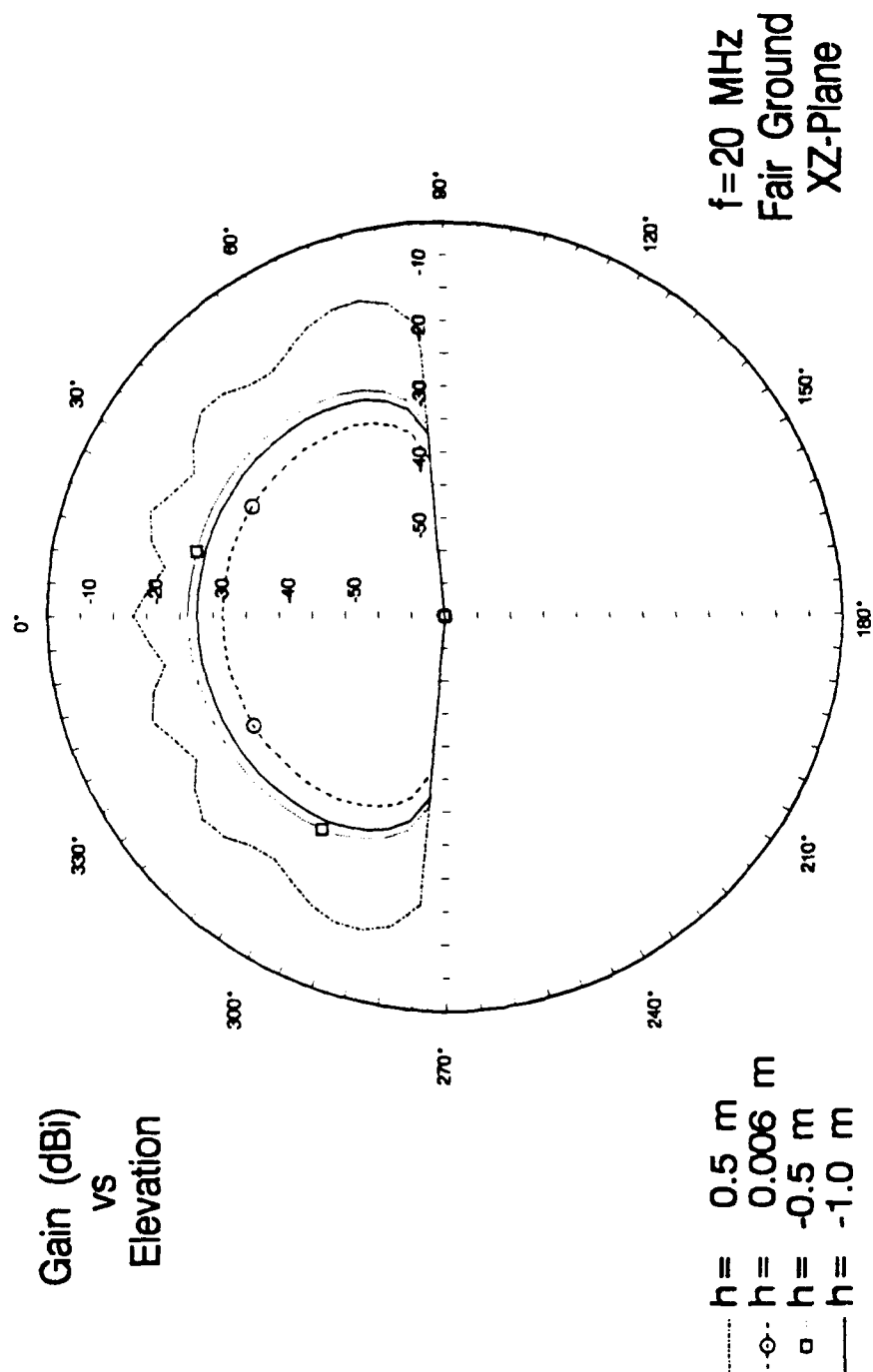


Figure 61. Elevation pattern for horizontal dipole for $f=20$ MHz over fair ground.

Horizontal Dipole

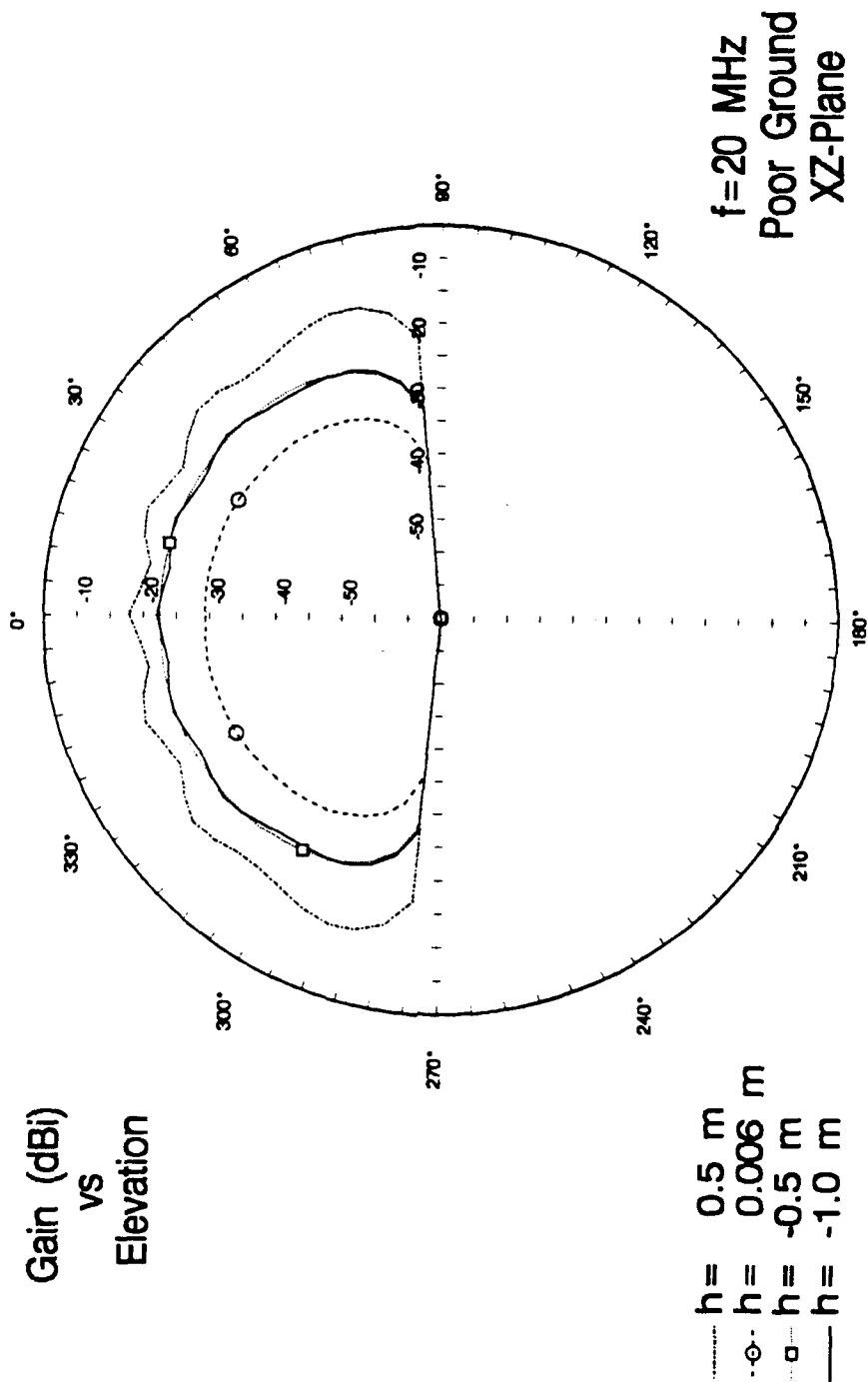


Figure 62. Elevation pattern for horizontal dipole for $f=20$ MHz over poor ground.

Horizontal Dipole

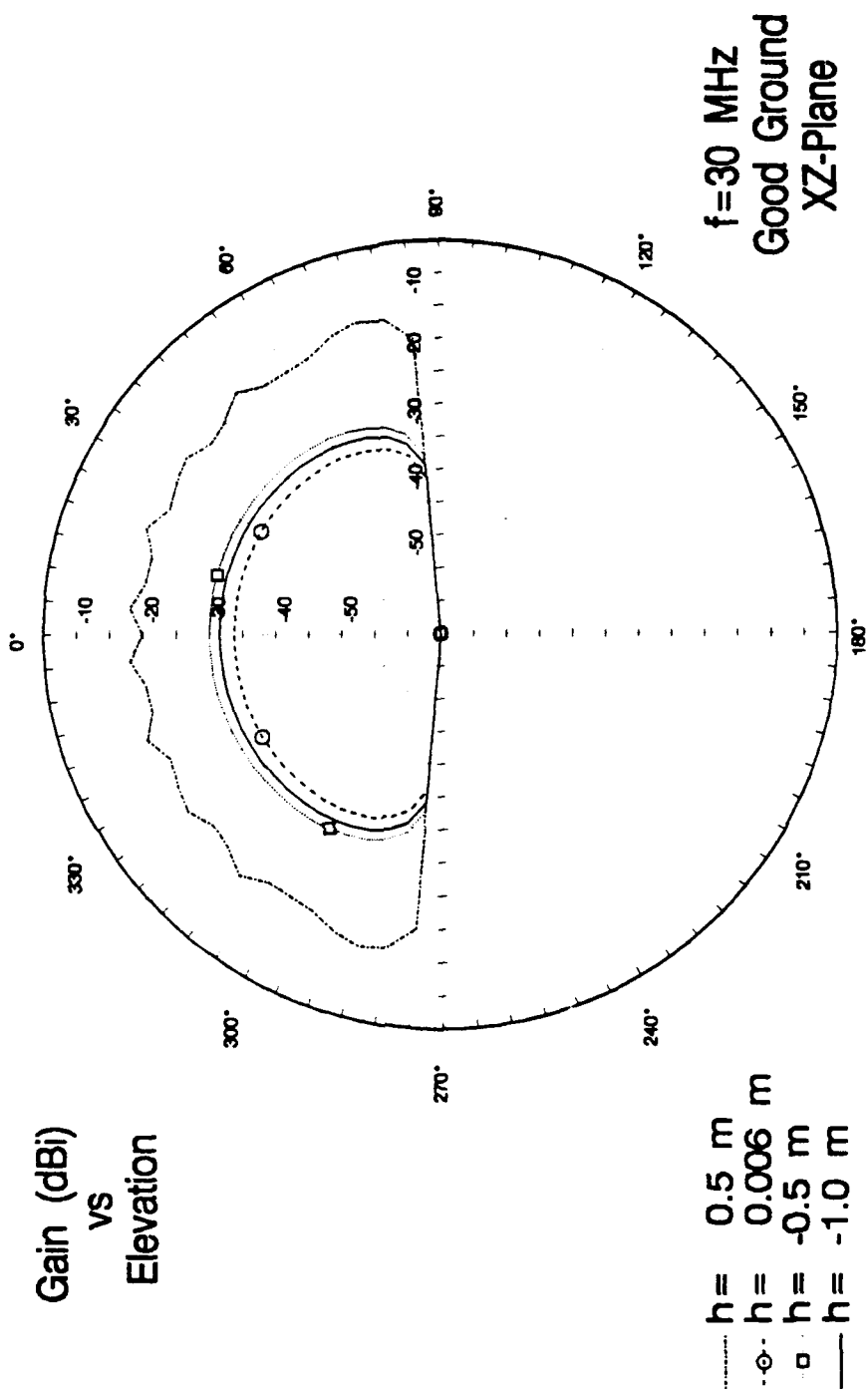


Figure 63. Elevation pattern for horizontal dipole for $f=30$ MHz over good ground.

Horizontal Dipole

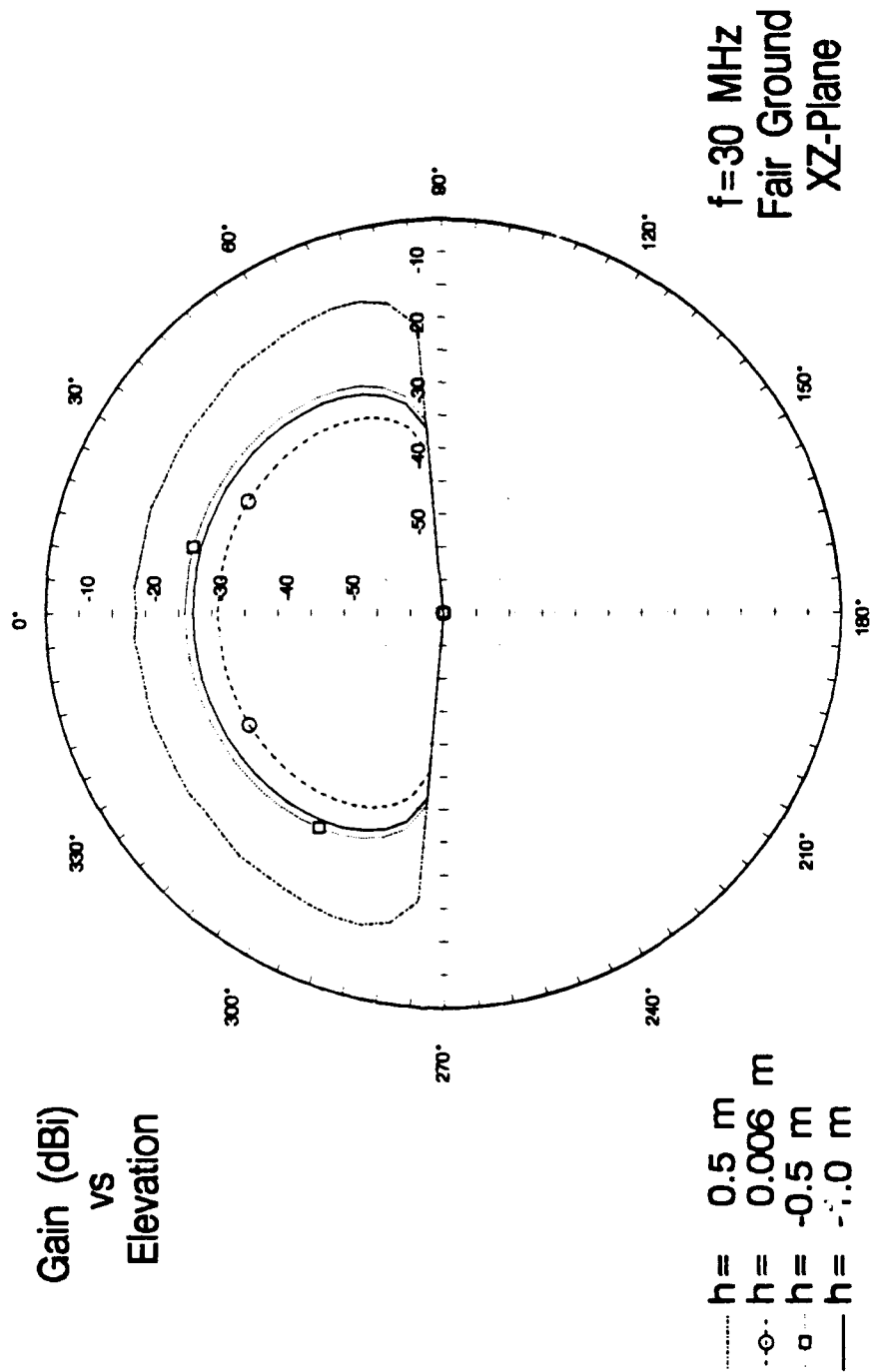


Figure 64. Elevation pattern for horizontal dipole for $f=30$ MHz over fair ground.

Horizontal Dipole

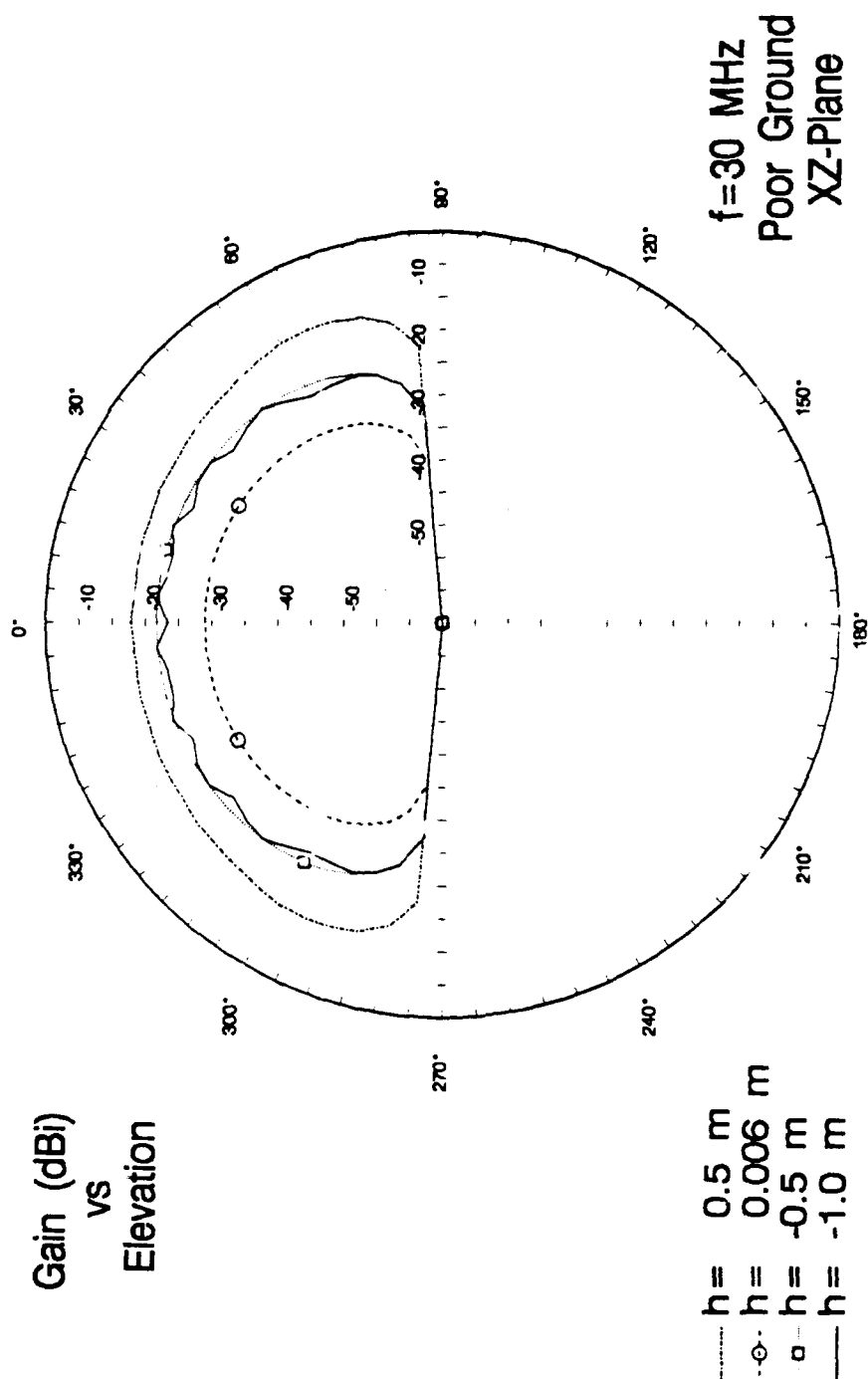


Figure 65. Elevation pattern for horizontal dipole for $f=30$ MHz over poor ground.

Horizontal Dipole

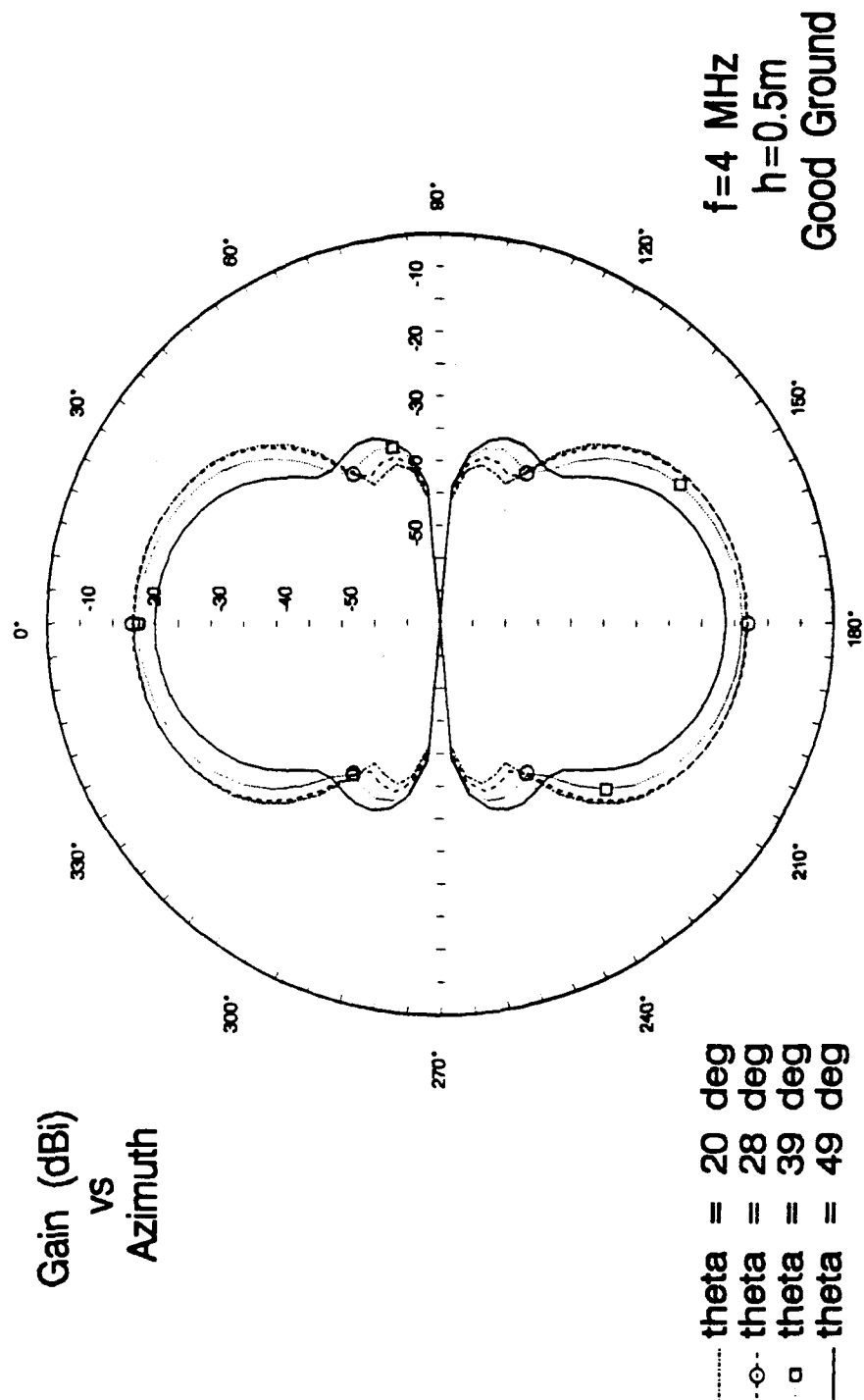


Figure 66. Azimuth pattern for horizontal dipole for f=4 MHz, h= 0.5m, varying takeoff angle (theta).

Horizontal Dipole

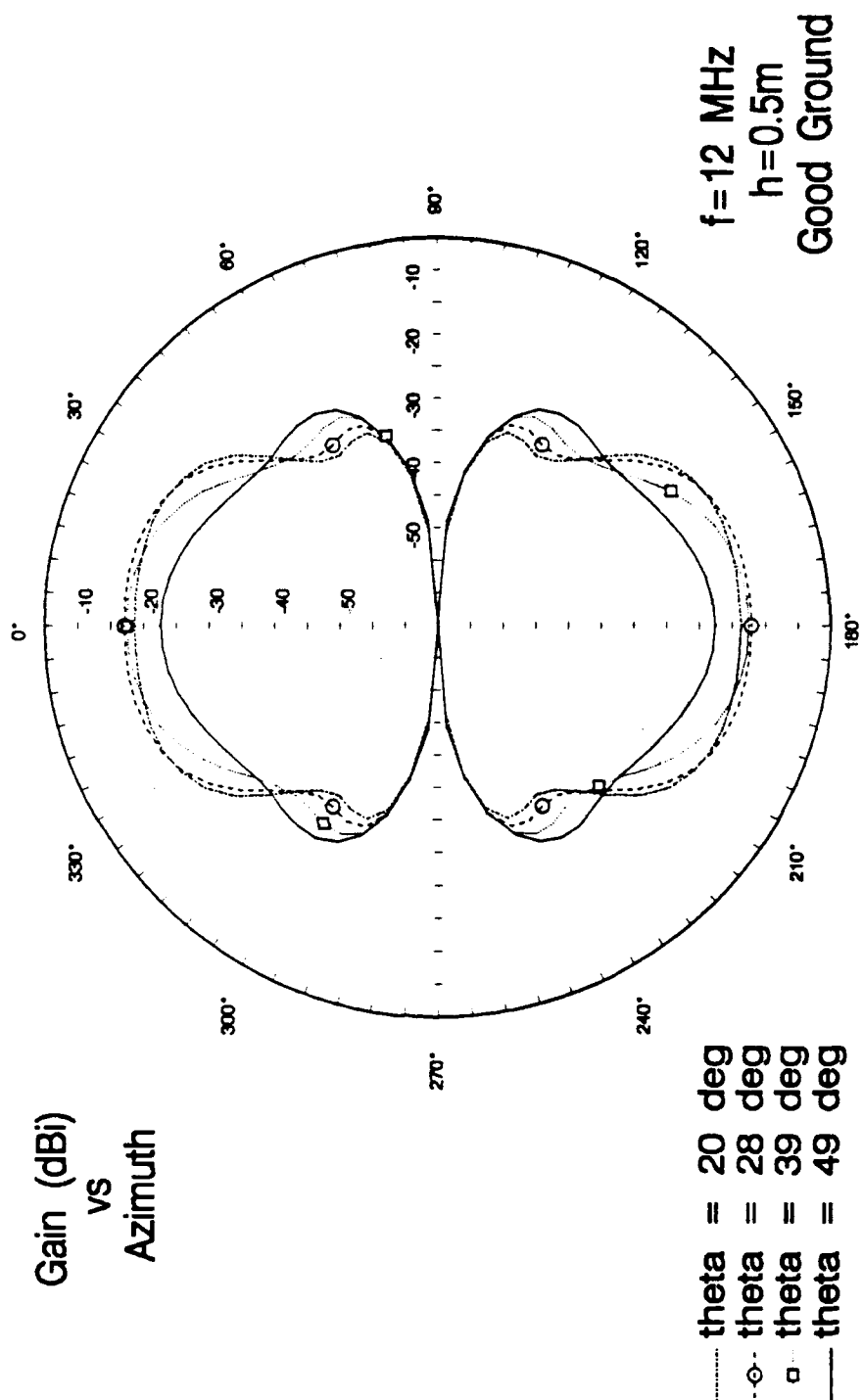


Figure 67. Azimuth pattern for horizontal dipole for $f=12$ MHz, $h= 0.5$ m, varying takeoff angle (θ).

Horizontal Dipole

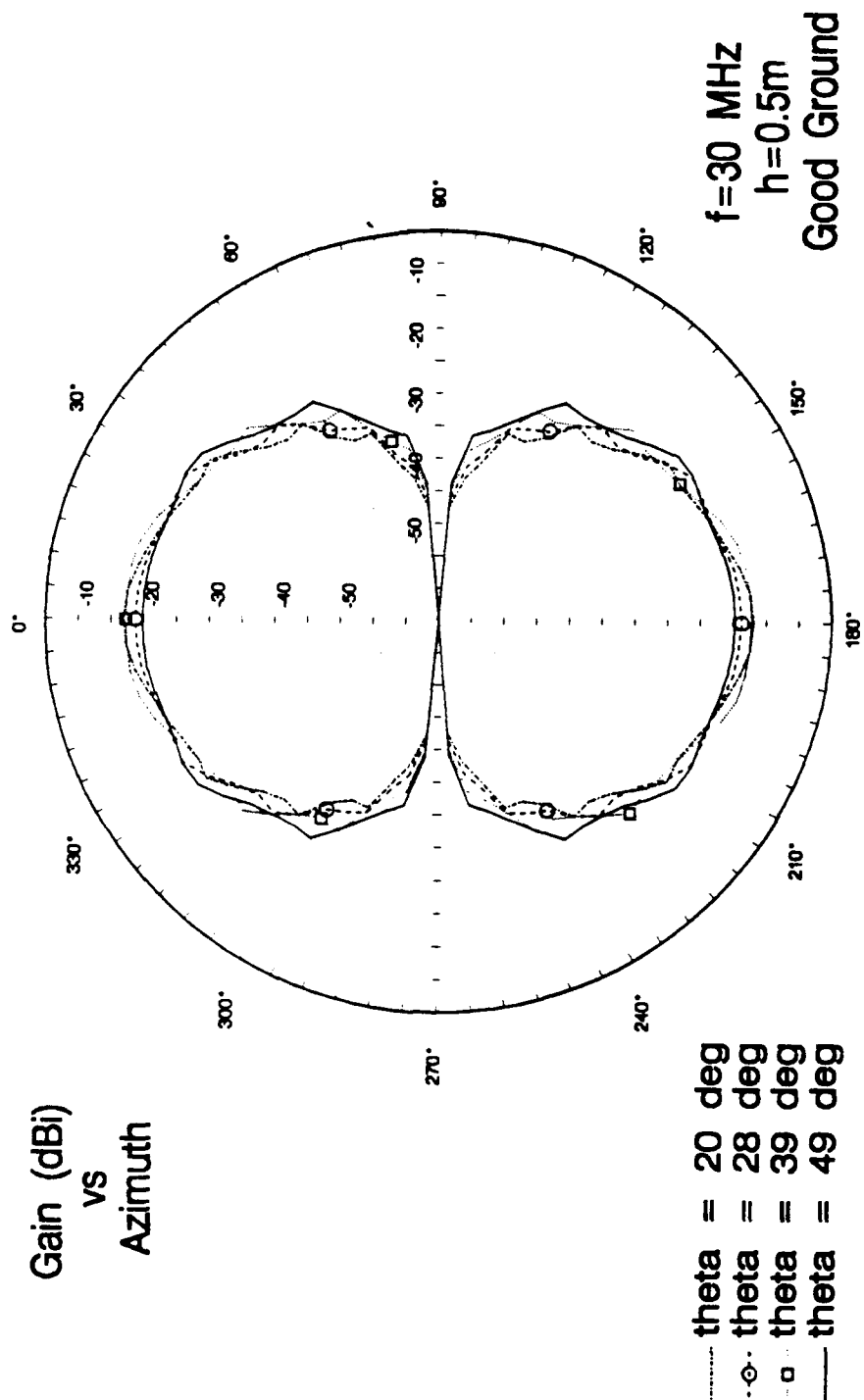


Figure 68. Azimuth pattern for horizontal dipole for $f=30$ Mhz, $h= 0.5\text{m}$, varying takeoff angle (θ).

Horizontal Dipole

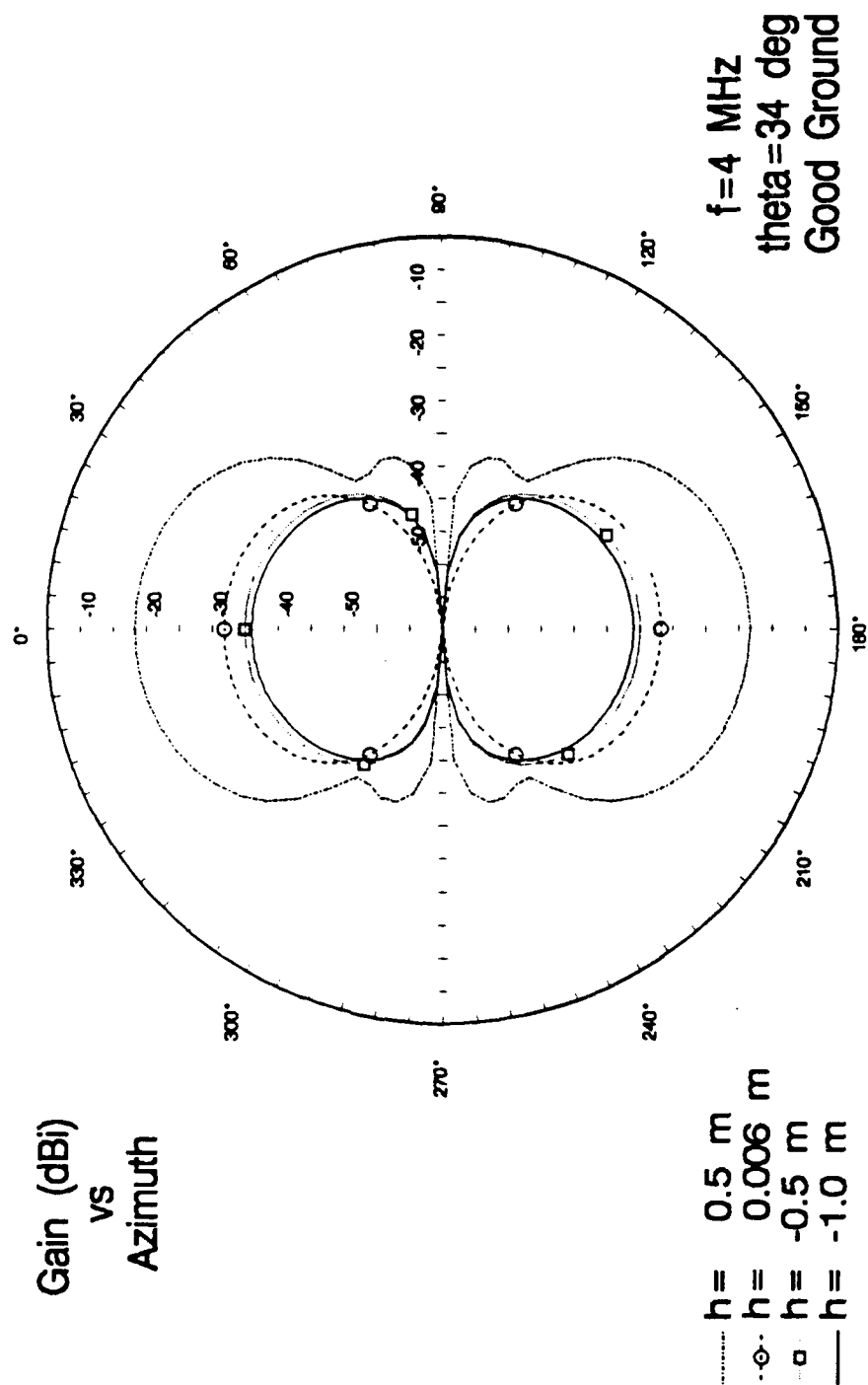


Figure 69. Azimuth pattern for horizontal dipole for $f=4$ MHz, constant takeoff angle (θ), varying heights.

Horizontal Dipole

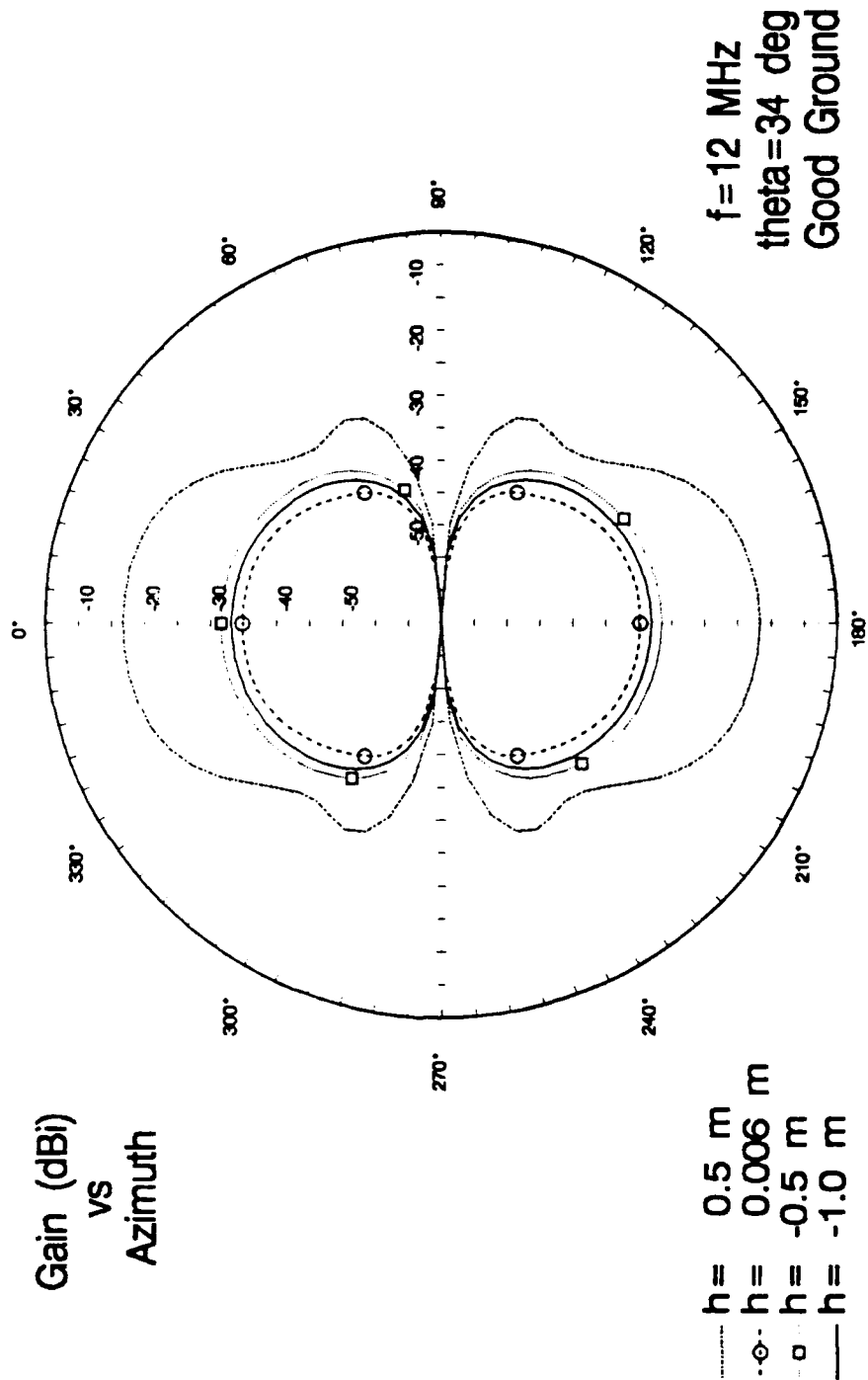


Figure 70. Azimuth pattern for horizontal dipole for $f=12$ MHz, constant takeoff angle (θ), varying heights.

Horizontal Dipole

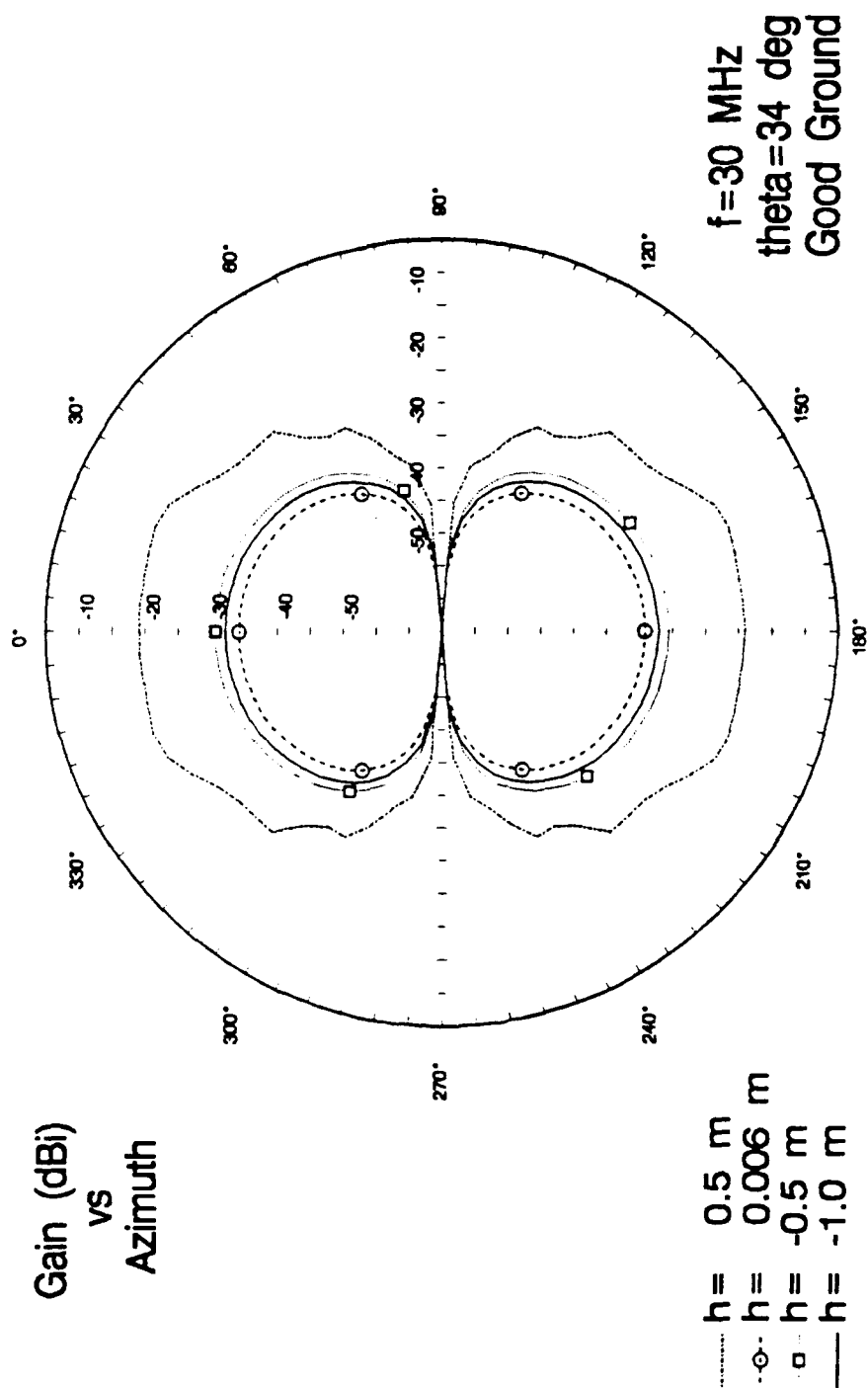


Figure 71. Azimuth pattern for horizontal dipole for $f=30$ MHz, constant takeoff angle (θ), varying heights.

oriented for transmission of the main beam along the positive and negative x-axis. The reference plane was from the xz-plane through the origin. The radiation patterns show a maximum gain of -5 dB at 2 MHz for $h = 0.5$ meters over poor ground. The patterns illustrate that change in height and ground conditions have a great effect on the radiation pattern. As ground conditions vary from good to poor, the peak gain actually increases a maximum of approximately 7 dB at 2 MHz.

When the antenna is buried, there is an increase in peak gain as ground conditions degrade. This can be explained using image theory as discussed for the ELPA-302. Also, as in the case of the ELPA-302, the height at 0.5 meters provides optimal gain at the desired takeoff angles for all ground conditions. The buried antenna's gain in the direction of the takeoff angle is 15 dB less than the gain of the antenna above ground.

Azimuth patterns for the horizontal dipole are shown in Figures 55 through 65 and were modeled to illustrate the change in azimuthal gain versus takeoff angle and the change in azimuthal gain versus height.

The results the various radiation patterns obtained are similar in shape but not in gain to what would be expected of a dipole in free space. This allows a rough check of the model used here and suggests the results are within reason.

V. EXPERIMENTAL VERIFICATION

The results of this thesis should be verified by experiment before a final decision to procure a specific antenna is made. A proposed experiment is included for continuation of this thesis by another party. The experiment should contain five sites in the hub-spoke configuration discussed earlier to test the performance of the antennas. Each of the three antennas would be operated at the hub site with the four spoke sites located from 300 to 600 miles incrementally away in radius from the hub and 90 degrees apart. This will test the omni-directional capabilities and the short to medium skywave range of the antennas. Ground constants at the sites should be measured accurately and compared with model results. The antennas should operate for 24 hours per day to test frequency response for day and night communications. The test should continue from several days to a week to ensure that a fairly normal ionosphere activity period was used. The VSWR for each antenna should be measured over the entire spectrum. The antenna elevation and azimuth radiation patterns should be measured via a helicopter flyover.

The importance of accurate measurements under the identical conditions used for the models is paramount for a

valid comparison of results.

VI. CONCLUSIONS

A. MODEL COMPARISON

A direct comparison between the models discussed is dependent upon the user's criteria. All of the antennas demonstrate broadband characteristics and omni-directional azimuthal capability. The HT-20T has the highest gain at each of the required takeoff angles and the lowest VSWR when compared to the ELPA-302 and horizontal dipole. The ELPA-302 and horizontal dipole provide adequate gain at the required takeoff angles at heights above ground and for buried antennas under certain conditions. The VSWR for the ELPA-302 is practical for use with transmitters that require a VSWR of 2.5 or less. The VSWR for the horizontal dipole is too high for most frequencies below 7.0 MHz. The ELPA-302 and horizontal dipole are much easier to construct and erect than the HT-20T, and provide a much less visible battlefield target.

B. RECOMMENDATIONS

From the results of this thesis, the HT-20T antenna is recommended for use whenever there is adequate space, time, a minimum requirement on displacement, and when concealment is not a priority. An example of this type of employment would be for physically large communications systems, like the TDCC, that do not displace frequently. The ELPA-302 is recommended

when concealment is a priority, ground conditions are poor, and when deploying vehicle-mounted radios which move more frequently than the TDCC type systems, but are sometimes able to stay in position long enough so that burying the antenna would be practical. The horizontal dipole is recommended for limited use for manpack, mobile employment, and where mobility and ease of construction and concealment are a priority. It is important that, in this method of employment, the limited frequency range of the antenna is considered for frequency allocation and mission planning. A typical application would be a reconnaissance unit or an infantry unit which moves constantly but could stop in order to employ a simple, field expedient tactical antenna in a desert environment where poor ground prevails.

Each of these antennas have advantages and disadvantages as outlined in this thesis. Each antenna can optimize communications under certain conditions. The user must make the final decision on which antenna to use in order to maximize communications.

APPENDIX A. SAMPLE NEC-3 DATA SET

COMMENT CARDS

CM THIS IS AN HT-20T ANTENNA, f=2 MHZ OVER GOOD GROUND
CE

GEOMETRY CARDS

GW10,15,.5,0.25,9.2,26.4,12.95,1,.001
GW20,1,26.4,12.95,1.,26.4,12.95,0.,.001
GW30,6,26.4,12.95,0.,26.4,12.95,-2.,.001
GW5,10,-.5,0.25,9.2,-26.4,12.95,1,.001
GW15,1,-26.4,12.95,0.,26.4,12.95,0.,.001
GW25,6,-26.4,12.95,1.,-26.4,12.95,-2.,.001
GW2,1,-.5,0,9.2,-.5,0.25,9.2,.001
GW1,1,.5,0,9.2,.5,0.25,9.2,.001
GX0,010
GE-1,0,0

PROGRAM CONTROL CARDS

EX0,1,1,00,1.0,0,0
EX0,1,2,00,-1.0,0,0
EX0,2,1,00,1.0,0,0
EX0,2,2,00,-1.0,0,0
FR0,1,0,0,2.0,1
GN,2,0,0,0,30.0,.01
LD4,20,0,0,400,0.
LD4,15,0,0,400,0.
RP0,91,9,1501,0,0,1,10,0,0
PL3,2,0,4
RP0,4,181,1000,20.,0.,0.,2.,0.,0.
PL3,2,0,4
RP0,4,181,1000,28.,0.,0.,2.,0.,0.
PL3,2,0,4
RP0,4,181,1000,39.,0.,0.,2.,0.,0.
PL3,1,0,4
RP0,181,1,1000,-90,0,1,0,0,0

This is a sample data set for NEC-3 input to obtain data for elevation and azimuth patterns and input impedance.

APPENDIX B. SAMPLE PAT7 PROGRAM DATA SET

.	ELPA-302 ANTENNA	
T	Elevation (deg), Theta [0-180]	0
P	Azimuth (deg), Phi [0-360]	0
F	Frequency (MHz)	30
C	Conductivity of Soil (Siemens/m)	0.01
H	Permittivity of Soil (relative)	30
E	Permittivity of Insulation (relative)	5
X	Conductivity of Insulation (Siemens/m)	0
L	Length of Element (m)	46
Z	Height of Element (m)	0.5
A	Radius of Conductor (m)	0.001
B	Radius of Insulation (m)	0.005
N	Number of Elements	2
S	Spacing of Elements (m)	6.2
J	Azimuth Steering (deg)	0
K	Elevation Steering (deg)	90
M	Number of Subarrays	1
D	Distance between Subarrays (m)	0
I	Matching Impedance (ohms) [0=ignore]	0
W	Wave/Polarization/Symmetry/Termination	SVBO
G	Graph Gain (dBi) vs T = 0 to 180 by 5	

Enter symbol of variable to change, or;
O=Options, Q=Quit, R=Run:

This is a sample data set for the antenna radiation patterns used in the PAT7 program for the ELPA-302 antenna using good ground.

LIST OF REFERENCES

1. King, R.W.P. and Smith, G.S., Antennas in Matter, The MIT Press, 1981.
2. Eyring Inc., Operations Manual for the 302A Eyring Low Profile Antenna, 1990.
3. The Numerical Electromagnetic Engineering Design System, Version 3.0, The Applied Computational Electromagnetics Society, 1989.
4. King, M.B., Gilchrist, R.B., and Faust, D.L., Eyring Low Profile and Buried Antenna Modeling Program, Eyring Inc., 1991.
5. Boithias, L., Radio Wave Propagation, McGraw-Hill Book Company, 1987.
6. Antenna Products Corp., HT-20T Transportable HF Antenna, 1988.

INITIAL DISTRIBUTION LIST

	No. Copies
1. Commandant of the Marine Corps Code TE 06 Washington, D.C. 20380-0001	1
2. Defense Technical Information Center Cameron Station Alexandria, VA 22304-6145	2
3. Library, Code 52 Naval Postgraduate School Monterey, CA 93943-5002	2
4. Chairman, Code EC Department of Electrical and Computer Engineering Naval Postgraduate School Monterey, CA 93943-5000	1
5. Director, Research Administration Naval Postgraduate School Monterey, CA 93943-5000	1
6. Dr. Richard W. Adler, Code EC/Ab Department of Electrical and Computer Engineering Naval Postgraduate School Monterey, CA 93943-5000	5
7. Dr. David C. Jenn, Code EC/Jn Department of Electrical and Computer Engineering Naval Postgraduate School Monterey, CA 93943-5000	1
8. Mr. Wilbur R. Vincent, Code EC/Ab Department of Electrical and Computer Engineering Naval Postgraduate School Monterey, CA 93943-5000	5
9. Captain Bobby G. Gregory Jr., USMC P.O. Box 593 Frisco, CO 80443	5
10. Marine Corps Tactical Systems Support Activity Attn: Captain R. Smith, USMC Camp Pendleton, CA 92055	1